A CHARACTERIZATION OF DEFICITS ASSOCIATED WITH LOSS OF NCB5OR IN THE MOUSE BRAIN

By

Matthew Allen Stroh
B.S., University of Kansas, 2012

Submitted to the graduate degree program in Neuroscience and the Graduate Faculty of the University of Kansas in partial fulfillment of the requirements for the degree of Doctor of Philosophy.

_____
Co-Chair Dr. Hao Zhu

_____
Co-Chair Dr. Doug Wright

_____
Dr. Russell Swerdlow

_____
Dr. John Stanford

_____
Dr. Brian Ackley

Date Defended: 4/18/2016

The Dissertation Committee for Matthew A. Stroh
certifies that this is the approved version of the following dissertation:

A CHARACTERIZATION OF DEFICITS ASSOCIATED WITH LOSS OF NCB5OR

IN THE MOUSE BRAIN

_____

Co-Chair Hao Zhu, PhD

_____

Co-Chair Doug Wright, PhD

Date approved: 4/18/2016

ABSTRACT

The simplest approach to the study of an event is to first consider that of the simplest cause. When investigating the mechanisms governing idiopathic diseases, this generally takes the form of an *ab initio* genetic approach, often in search of a single genetic culprit. To date, this genetic 'smoking gun' has remained elusive for many affected by diabetes mellitus and a number of neurodegenerative diseases. With no single gene, or even subset of genes, found to be causative in all cases, other approaches to studying the etiology and treatment of these diseases seem reasonable. One such approach is considering trends consistently observed in diseases closely correlated with one another. In the cases of diabetes mellitus and neurodegenerative diseases, overlapping themes of mitochondrial influence or dysfunction and iron dyshomeostasis are apparent and relatively consistent. This might suggest that gene networks involved in the maintenance of mitochondrial and iron related pathways are etiologically important. Thus, this dissertation focuses on a reductase, NCB5OR, whose absence has been shown to result in diabetes mellitus, mitochondrial dysfunction, and altered iron metabolism in mice. Specifically, we focus on the effects of NCB5OR deficiency on mouse neural tissue as a means of exploring genes and pathways known to result in these overlapping trends.

In order to study the effects of NCB5OR deficiency on neural tissue and pathways we used mice globally deficient for NCB5OR (GKO) and also developed a conditional knockout mouse that inactivates NCB5OR in the cerebellum and midbrain (CKO). Using either of these models, three questions were addressed: What effect does NCB5OR deficiency in the mouse cerebellum and midbrain have on iron homeostasis and locomotor behavior? What effect does loss of NCB5OR in cerebellohypothalamic circuitry have on feeding behavior and metabolism? Does

loss of NCB5OR affect major neurotransmitters in the brains of mice globally deficient for NCB5OR?

Chapter 1 details background information on the MIND (mitochondria, iron, neurodegeneration, and diabetes) paradigm, which provides the context in which these studies were conducted. Although over 100 neurodegenerative diseases have been classified, the majority of the background presented will use Alzheimer's disease (AD) as the model complex, idiopathic neurodegenerative disease, providing a focused example of the MIND paradigm framework. Also discussed is the incidence of diabetes accompanied by neuropathy and neurodegeneration along with neurodegenerative disorders prone to development of diabetes. Mouse models containing multiple facets of this overlap are also described alongside current molecular trends attributed to both diseases. A detailed background pertaining to NCB5OR as well as known phenotypes and preliminary observations associated with its absence are presented. Finally, a review of the cerebellum and its contribution to motor and higher order cognitive processes is presented so as to help better understand why the cerebellum was chosen as the primary model system for the study of NCB5OR in neural tissue.

Chapters 2-4 address the above three questions with studies aimed at initial characterization of the effects of NCB5OR deficiency. Briefly, results from Chapter 2 demonstrate an altered state of iron homeostasis in the mouse cerebellum devoid of NCB5OR. Additionally, analysis of locomotor behavior revealed altered locomotor activity, proprioception, and sensitivity to harmaline-induced tremor in CKO mice. Chapter 3 explores metabolic and behavioral changes in CKO mice which reveal the complex nature of NCB5OR deficiency on neural pathways that participate in feeding behavior and neural regulation of metabolism. Finally, Chapter 4 presents data that suggest that the absence of NCB5OR does not affect levels of serotonin (5-HT),

dopamine (DA), γ-aminobutyric acid (GABA), or glutamate (Glut) in the cerebellum but does increase levels of DA in the frontal cortex of mice globally deficient for NCB5OR.

The primary purpose of this work is to contribute to the understanding of the complex nature and etiology of idiopathic neurological disease by providing evidence emphasizing the importance of genes whose function influences iron and metabolic homeostasis. It is hoped that the data presented here helps to shed light on pathways and genetic networks whose composite function could provide insight into the development of complex neurological disease.

ACKNOWLEDGEMENTS

To....

Anna,

Put simply, you inspire me to be a better person every single day. Your intellect, kindness, support, and caring are traits to be admired and have changed my view not only of myself, but of the world around me. Your encouragement and confidence in me provide momentum in everything I do. You are an outstanding person and scientist and I look forward to the years I get to spend with you. Thank you for being you.

My Parents: Kelli, Lindsay, Arthur, and Robyn,

"Life can only be understood backwards; but it must be lived forwards." – Kierkegaard We have all had to decide and we have all had to endure. Without you, I would not be where I am today. Each one of you is responsible for shaping, driving, and supporting me through my struggles and triumphs. In my case, a village really was the only way to raise the child. Thank you.

My Siblings: Krysten, Amanda, Seth, and Dominic,

I could not ask for better siblings. We have had our spats, disagreements, high times, and lows, but regardless of what happens, you will always be a part of who I am and I could not be more proud of that fact. Thank you for your support and encouragement throughout this process. It has been a blast growing up with you and I look forward to the many years to come.

Dr. Hao Zhu,

Your patience, kindness, and understanding have been unfaltering when guiding me through these past 4 years. I am not the easiest person to teach or to understand, yet you always

found a way. You believed in my potential when others wrote me off, and now I am able to pursue a career of passion and a fulfilled life because of your resolve. I am forever grateful.

My Committee,

I extend my most sincere thanks to each of you for taking the time and putting forth the effort to shape me for the path ahead. Your patience and tolerance speaks volumes and makes it possible for individuals like myself to pursue their passion. Thank you for giving me the tools to push forward.

The Fallen,

You did not make it back and I did. I am doing my best to make that worth something. Til Valhalla.

Aut cum scuto aut in scuto

LIST OF ABBREVIATIONS

2-DoG	-	2-deoxyglucose
5-HT	-	serotonin
AD	-	Alzheimer's Disease
ANOVA	-	analysis of variance
APP	-	amyloid precursor protein
CKO	-	conditional knockout (cerebellum and midbrain)
COX	-	cytochrome c oxidase
CP	-	ceruloplasmin
Cp-GPI	-	GPI-linked ceruloplasmin
D2R	-	dopamine receptor 2
DA	-	dopamine
DAO	-	dorsal accessory olive
DHBA	-	3,4-dihydroxybenzylamine
DMT1	-	divalent metal transporter 1
ELISA	-	enzyme linked immunosorbent assay
ETC	-	Electron transport chain
FA	-	Friedreich's ataxia
FAD	-	familial Alzheimer's disease
Fe	-	iron
FPN1	-	ferroportin 1
FtH	-	ferritin heavy chain
FtL	-	ferritin light chain
FXN	-	frataxin
GABA	-	γ-Aminobutyric acid

GKO	-	global knockout
Glut	-	glutamate
HILIC	-	hydrophilic interaction liquid chromatography
HMOX	-	heme oxygenase
HPA	-	hypothalamic-pituitary-adrenal
HPT	-	hypothalamic-pituitary-thyroid
IAPP	-	islet amyloid polypeptide
IRP1/2	-	iron regulator protein ½
IS	-	internal standard
ISC	-	iron-sulfur cluster
LOAD	-	late onset Alzheimer's disease
LOD	-	limit of detection
LOQ	-	limit of quantitation
MAO	-	medial accessory olive
MIDD	-	maternally inherited diabetes and deafness
MIND	-	Mitochondria, Iron, Neurodegeneration, and Diabetes
MitoFN2	-	mitoferrin 2
MODY	-	Maturity-onset diabetes of the young
MPP	-	motion power percentage
MT2	-	metallothionein 2
MT3	-	metallothionein 3
NCB5OR	-	NADH cytochrome b5 oxidoreductase
NFT	-	neurofibrillary tangle
PD	-	Parkinson's Disease
ROS	-	reactive oxygen species

T1D	-	type 1 diabetes
T2D	-	type 2 diabetes
Tf	-	transferrin
TfR1	-	Transferrin receptor 1
TKO	-	islet transplanted global knockout mice
UPLC-MS/MS-		ultra performance liquid chromatography tandem mass spectrometry
VTA	-	ventral tegmental area
WT	-	wild-type

TABLE OF CONTENTS

LIST OF FIGURES AND TABLES

Chapter 1: INTRODUCTION AND BACKGROUND

Chapter 2: LOSS OF NCB5OR IN THE CEREBELLUM DISTURBS IRON PATHWAYS, POTENTIATES BEHAVIORAL ABNORMALITIES, AND EXACERBATES HARMALINE-INDUCED TREMOR IN MICE

CHAPTER 1

INTRODUCTION AND BACKGROUND

1.1 Mitochondria and Iron in Neurodegeneration and Diabetes (MIND)

1.1.1 Borrowed Evolution: β-cells and neurons. Elements influencing the development of diabetes mellitus and a number of neurodegenerative and neurological disorders have been well established (see reviews (Swerdlow, 2009, 2011a)), however, given their complexity, a succinct analysis of major underlying themes spanning them has yet to be presented. Approximately 60–70% of the 25.8 million Americans with diabetes develop neurological symptoms and damage (Prevention, 2011). Moreover, more than 20 neurodegenerative syndromes among the 100 characterized so far are associated with diabetes mellitus (Ristow, 2004). In Alzheimer's disease (AD) there is an approximately 35% diabetes incidence (Janson et al., 2004). Likewise, the presence of diabetes mellitus results in a 65% increased risk of AD (Arvanitakis, Wilson, Bienias, Evans, & Bennett, 2004) and Parkinson's disease (PD) (Hu, Jousilahti, Bidel, Antikainen, & Tuomilehto, 2007). In order to explore these trends and the polygenic networks potentially governing these diseases we are considering two common areas linking them: mitochondria and iron. We will start by making note of the inherent similarities between the neurological and endocrine systems.

In 1869 Paul Langerhans identified and described the endocrine, or hormone secreting, cells of the pancreas (Langerhans, 1869). These clusters of cells have since been named the Islets of Langerhans and been described in detail. Islets are composed of 5 known cell types, each playing an independent role in endocrine regulation. In diabetes mellitus the insulin producing and secreting β-cells are of particular interest since these cells are generally dysfunctional or altogether destroyed in events preceding the onset of diabetes. Interestingly, β-cell dysfunction in diabetes might provide a unique opportunity when considering different etiological approaches to diseases like AD and PD. This is due, in part, to an evolving realization that β-cells and

neurons possess striking similarities, both functionally and in genetic profile. In 2011, Arntfield and van der Kooy summarized the similarities between neurons and β-cells and suggested that in an instance of convergent evolution, β-cells ‘‘borrowed from the brain’’ (Table 1.1) (Arntfield & van der Kooy, 2011; Fujita, Kobayashi, & Yui, 1980; Pearse & Polak, 1971)). Basically, neurons and β-cells are derived from different tissue layers (ectoderm and endoderm, respectively) but are very similar in the way that they store, respond to, and transmit signaling molecules. Knowledge of the similarities between β-cells and neurons has existed for some time (Atouf, Czernichow, & Scharfmann, 1997). As early as the 1970’s, it was discovered that the pancreas actually synthesizes, stores, and secretes γ-aminobutyric acid (GABA), a major inhibitory neurotransmitter (Thomas-Reetz & De Camilli, 1994). Further investigation revealed that β-cells store and release GABA through synaptic-like microvesicles (Reetz et al., 1991). In fact, glucose mediated secretion of GABA by β-cells inhibits glucagon release from alpha-cells (Rorsman et al., 1989). Conversely, acetylcholine, another major neurotransmitter, is released from alpha-cells resulting in β-cells that are primed for adequate insulin response (Rodriguez-Diaz et al., 2011). Similar to neurotransmitter release in neurons, insulin secretion in β-cells is accomplished via membrane depolarization as a result of external cues. In diabetes, primary metabolic processes governing glucose mediated insulin secretion are impaired. Comparatively, metabolic processes governing synaptic plasticity and transmission are dysfunctional or impaired in AD. It seems evident that diabetes mellitus and neurodegenerative diseases like AD and PD could be the result of similarly perturbed mechanisms that ultimately govern their pathology. Thus closer analysis of shared changes and defects between these two diseases could prove beneficial in identifying key networks involved in their pathology.

In essence, diabetes, AD, and PD are simply complex and result in consistently broad and inconclusive etiological studies. For this reason we are proposing that idiopathic cases arise through each system's predisposed sensitivity to metabolic influence determined not by a single gene but rather by genetic networks whose composite function determines susceptibility. More accurately, we posit that changes in bioenergetic homeostasis, influenced largely by mitochondrial and iron related pathways, lie at the nexus of neurodegeneration and diabetes (Figure 1.1).

As a way of approaching the idiopathic and complex nature of these diseases we are proposing the consideration of a MIND (mitochondria, iron, neurodegeneration, and diabetes) paradigm in which systemic metabolic influence, iron homeostasis, and respective genetic backgrounds play a central role in the development of disease.

1.1.2 Forming the MIND Paradigm: Frataxin and the monogenic contributors

Friedreich's ataxia (FA) is a monogenic disease that provides a particularly elegant demonstration of the link between mitochondria and iron in the processes and pathways governing neurodegeneration and diabetes. Friedreich's ataxia patients experience peripheral nerve and dorsal root ganglia atrophy, ataxia in all four limbs, dysarthria, cardiac abnormalities including arrhythmia, and diabetes mellitus. The primary cause of FA is a significant reduction in the availability of the mitochondria-localized protein frataxin as a result of a large GAA trinucleotide repeat expansion in the first intron of FXN (Campuzano et al., 1996; Durr et al., 1996; Koutnikova et al., 1997). As is the case in other trinucleotide repeat disorders, it is postulated that this expansion results in either delayed transcription, altered transcript processing (E. Kim, Napierala, & Dent, 2011), or altered protein folding and translational efficiency like that observed in Huntington's disease (Bauer & Nukina, 2009; Polling, Hill, & Hatters, 2012;

Robertson & Bottomley, 2012). Various studies suggest that frataxin is a key component in iron–sulfur processing in the mitochondrial matrix (Adinolfi et al., 2009; Schmucker et al., 2011). Iron-sulfur clusters are key components to catalytically active subunits in the mitochondrial electron transport chain (ETC). A number of models for Friedreich's ataxia have been developed, ranging from transgenic mice to immortalized and induced pluripotent stem cell cell lines (Perdomini, Hick, Puccio, & Pook, 2013; Puccio et al., 2001; Ristow et al., 2003).

Other monogenic instances in diabetes and Alzheimer's disease have been documented in the forms of subtypes and models, representing a small percentage of the population for which a single contributing factor can be identified (Andersen et al., 2004; Florez, Hirschhorn, & Altshuler, 2003; Haass et al., 1995; Hutton & Hardy, 1997; Shulman, De Jager, & Feany, 2011; W. Wang et al., 2011). Further examination reveals that many of these monogenic causes lie in major pathways contributing to metabolic flux, mitochondrial function, and regulation of iron metabolism and homeostasis (Duce et al., 2010; Hsu et al., 2000; Protter, Lang, & Cooper, 2012; Rogers et al., 2008; W. Wang et al., 2011; Xie et al., 2004).

1.1.2a Monogenic events in diabetes

Maturity-onset diabetes of the young (MODY) and maternally inherited diabetes and deafness (MIDD) can be considered two major, albeit rare, monogenic forms of diabetes mellitus (Florez et al., 2003). In MIDD, a single A→G mutation in the mitochondrial-encoded gene for tRNA leucine results in diabetes and deafness (van den Ouweland et al., 1994). In parallel, more than half of the 6 genes attributed to the development of MODY (Florez et al., 2003) impact features and pathways critical to proper metabolic function (H. Y. Wang, Antinozzi, Hagenfeldt, Maechler, & Wollheim, 2000; H. Y. Wang, Maechler, Antinozzi, Hagenfeldt, & Wollheim, 2000). Monogenic cases of non-mitochondrial origin have been identified in patients with miss-

sense polymorphisms in $KCNJ_{11}$, a gene encoding a major subunit of the ATP-sensitive K^+ channel (Fischer et al., 2008). Other monogenic diabetes models include animals lacking TFAM and NCB5OR (Brehm, Powers, Shultz, & Greiner, 2012). In the latter case, no significant contribution has been assigned to mutations or variations within the diabetic population (Andersen et al., 2004), yet NCB5OR null mice develop lean diabetes at age 7 weeks as a result of β-cell demise and display gross mitochondrial morphological changes accompanied by altered lipid metabolism (Larade et al., 2008; W. Wang et al., 2011; Xie et al., 2004). Interestingly, naturally occurring missense mutations in human NCB5OR lead to improper folding and significantly reduced levels of intracellular NCB5OR (Kalman et al., 2013). Recent data also suggest that ablation of NCB5OR leads to iron dyshomeostasis (H. Zhu, Wang, & Wang, 2013). Preliminary findings indicate neuromuscular junction defects and behavioral changes associated with altered neurological function in NCB5OR null mice (Stroh et al., unpublished data). Such cell-specific phenotypes from an otherwise non-cell-specific gene provide evidence that particular cell and tissue types may be more susceptible to particular genetic insult over others. This is a useful framework to study correlation and causation in disease.

1.1.2b Monogenic events in neurological disease

Alzheimer's disease is the most prevalent neurodegenerative disorder, affecting 13% of the population over the age of 65 (Hebert, Scherr, Bienias, Bennett, & Evans, 2003). Mutations in the amyloid precursor protein (APP), the precursor to amyloid plaques which are ,at times, considered to be a possible cause of Alzheimer's disease, have been associated with early onset, familial Alzheimer's disease (FAD). The Swedish mutation in APP leads to premature and accelerated cleavage of APP by β-secretase resulting in accumulation of amyloid oligomers (β-amyloids) (Haass et al., 1995). The toxicity and function of β-amyloids has long been debated

but recent evidence suggests that APP possesses ferroxidase and iron export activity (Duce et al., 2010), which may indicate APP normally participates in iron homeostasis. Regulatory elements in the APP mRNA directly link its function to the cellular iron status (Rogers et al., 2008).

One of the best known genetic contributors to late onset Alzheimer's disease (LOAD) is that of the APOEe4 allele. Patients who possess APOEe4 have a significantly elevated risk of developing LOAD, and account for approximately 40% of the LOAD population (Liu, Kanekiyo, Xu, & Bu, 2013). Carriers of the APOEe4 allele also demonstrate a reduced ability to clear Aβ42 amyloid deposits when compared to those possessing the e2 and e3 alleles (Castellano et al., 2011). Interestingly, evidence outlining metabolic brain abnormalities in young and old APOEe4 carriers alike suggests that metabolic decline, mitochondrial dysfunction, and eventual hypometabolism are critical risk factors in the development of APOEe4 associated LOAD (Alexander, Chen, Pietrini, Rapoport, & Reiman, 2002; Liang et al., 2008; Minoshima, Foster, & Kuhl, 1994; Reiman et al., 2001; Reiman et al., 1996; Reiman et al., 2004; Valla, Berndt, & Gonzalez-Lima, 2001; Valla et al., 2010). Less robust cognitive test performance in individuals harboring the allele can be observed in middle adulthood (Bloss, Delis, Salmon, & Bondi, 2008). These observations lend to the notion that changes in the metabolic environment occur much earlier than the development of the histological hallmarks of Alzheimer's disease, pointing to possible upstream pathologies.

1.1.3 Mitochondria and iron in sporadic neurological disease

Neurodegeneration is a generalized term used to describe loss of neuronal mass, locally or globally, as well as systemic malfunction and eventual loss of efficient neural transduction and communication. In either case, these events can result from changes in extra-neuronal networks by which the ideal neural environment is maintained, as is the case in multiple sclerosis

(Makris, Piperopoulos, & Karmaniolou, 2013), to changes in individual neuronal environments directly impacting their function. While it is obvious that genetic background plays a significant role in both mechanisms, contemplating the impact of compounded genetic variability (variable genetic networks) on disease susceptibility is not so trivial. Changes in metabolic function and iron regulation are observed in a number of neurological diseases yet the diseases remain pathologically distinct (Ponka, 2004). For this reason, variables governing mitochondrial function and iron regulation warrant further investigation. While many neurodegenerative diseases possess abnormalities in mitochondria and iron homeostasis, our focus will largely remain on changes in Alzheimer's disease.

In AD, the complexity of the disease is unmistakable with progressive cognitive decline consistently out of sync with historical pathological mechanisms like altered APP processing and amyloid fibril formation. In fact, significant amyloid plaque burden can be detected in elderly, but cognitively normal, individuals (Vlassenko et al., 2011). Even so, the most current and popular approaches to investigation and treatment are to simply analyze, understand, and eventually remove amyloid plaque deposits. So far this strategy has yielded negative or inconclusive results in clinical trials. Amyloid β oligomer deposition is a unique characteristic ascribed to Alzheimer's disease, however, inconsistencies in the effects of senile plaques call for reassessing the role of toxic amyloid species in AD etiology (Pimplikar, 2009). Not discounting the downstream role of APP processing in the pathogenesis of Alzheimer's disease, we would like to focus on pathways that are potential targets for therapeutic intervention prior to amyloid deposition and which aim to clarify susceptibility to the more common form of Alzheimer's disease, LOAD. With the aforementioned correlation between Alzheimer's disease and diabetes mellitus we will explore pathways that influence both diseases.

1.1.3a Mitochondrial and metabolic influence

Mitochondrial-derived metabolic dysfunction has been documented in multiple neurodegenerative disorders (A. C. Belin et al., 2007; Swerdlow, 2009; Trimmer et al., 2000). One of the most recognized of these disorders is Alzheimer's disease, for which a mitochondrial cascade hypothesis has been proposed (Swerdlow, Burns, & Khan, 2010, 2013; Swerdlow & Khan, 2004, 2009). Altered function in critical citric acid cycle components and ETC complexes as well as altered glucose metabolism and insulin resistance have all been observed in AD (Gibson et al., 1988; Perry, Perry, Tomlinson, Blessed, & Gibson, 1980; Sorbi, Bird, & Blass, 1983; Steen et al., 2005). It has even been suggested that Alzheimer's disease is in fact a form of type III diabetes (S. De La Monte, Wands JR. , 2008; S. M. de la Monte, 2014). This hypothesis is based on evidence of impaired insulin response pathways and insulin resistance in the Alzheimer's brain (Steen et al., 2005; Talbot et al., 2012). The most reported functional deficiencies in ETC complexes arise in complex IV (cytochrome c oxidase; COX) V_{max} activities, with complex I and III activities closely following suit. Reduced complex IV activity was first reported in mitochondria isolated from AD subject platelets (Parker, Filley, & Parks, 1990). Further investigations probing COX activity in the AD brain also showed decreased activity similar to that observed in platelet-derived mitochondria (Kish et al., 1992; Mutisya, Bowling, & Beal, 1994) . This raised questions as to whether mitochondrial dysfunction could influence neurofibrillary tangles and amyloid plaque deposition. Early studies provided evidence that altered metabolism impacted APP processing (Gabuzda, Busciglio, Chen, Matsudaira, & Yankner, 1994; Gasparini et al., 1997). Cytoplasmic hybrid (cybrid) studies, in which platelet mitochondria isolated from AD patients are transferred to mitochondria-deficient (ρ^0) neuronal

(neuroblastoma or teratocarcinoma) cells, have also reported changes in APP processing and amyloid species production (Khan et al., 2000; Swerdlow, 2007).

In addition, cybrid studies show a profound shift in overall cellular bioenergetic equilibrium with reductions in membrane potential and altered calcium homeostasis (Swerdlow, 2007). Changes in calcium homeostasis are consistent with changes in mitochondrial regulatory pathways and support observations that mice harboring presenilin 1 mutations, an established cause of familial AD (FAD), display mitochondrial dysfunction and altered cytosolic calcium homeostasis (Schneider, Zorzi, & Nardocci, 2013). Such observations also provide evidence for mitochondria as an upstream affecter in the production of β-amyloid since altered amyloid processing has been correlated with altered calcium homeostasis (Lee et al., 2013). Although there are conflicting accounts as to whether amyloid itself induces or alters the calcium changes observed in AD (Briggs, Schneider, Richardson, & Stutzmann, 2013), cybrid studies provide insight into mechanisms that may nurture β-amyloid production prior to its potential effects on intracellular calcium.

It is widely accepted that ETC activity naturally produces reactive oxygen species (ROS) (Grivennikova & Vinogradov, 2006; Tan, Sagara, Liu, Maher, & Schubert, 1998). Reactive oxygen species production and oxidative stress rapidly increases during times of cellular stress and mitochondrial dysfunction, leading to significant damage to cellular organelles and DNA. The frontal cortex of AD patients display oxidative stress (Ansari & Scheff, 2010) along with increased levels of 8-hydroxydeoxyguanosine and 8-hydroxyguanosine in DNA and RNA, respectively (Quinlan, Perevoshchikova, Hey-Mogensen, Orr, & Brand, 2013), which are also indicative of oxidative stress. Recently, investigators demonstrated that, while multiple components of the ETC are sites of ROS production, the contribution to total ROS production

from each site depends largely on the substrates being oxidized and not solely upon the protein function *per se* (Quinlan et al., 2013). This provides further insight into possible dietary and environmental factors that were not considered in previous studies.

Modes of inheritance for Alzheimer's disease and Parkinson's disease are sparsely Mendelian, lending to investigations of inheritance patterns in non-monogenic populations. These investigations have yielded ample data suggesting a maternal pattern of inheritance in Alzheimer's disease (Duara et al., 1993; Edland et al., 1996; Mosconi et al., 2010) [119–121], consistent with maternal inheritance of mitochondrial DNA (mt-DNA) (Giles, Blanc, Cann, & Wallace, 1980). These observations in whole support a mitochondrial cascade hypothesis in which mitochondria and cell bioenergetics lie at the forefront of AD pathology.

1.1.3b Iron dyshomeostasis in neurological disease

Iron metabolism and dyshomeostasis are implicated in a number of neurodegenerative disorders, including Parkinson's disease (PD), Alzheimer's disease (PD), neuroferritinopathy, aceruloplasminaemia, and neurodegeneration with brain iron accumulation (Ponka, 2004). Among them, AD and PD are the most prevalent forms without a single known cause. The role for iron in the pathogenesis of PD is being investigated but remains elusive with changes in iron and iron regulatory pathways consistently observed but spatially and temporally diffuse (Gotz, Double, Gerlach, Youdim, & Riederer, 2004). However, ample evidence supports consistent changes in redox-active metals in the brains of AD patients (Atwood, Huang, Moir, Tanzi, & Bush, 1999; X. D. Huang et al., 1999).

Early reports of iron accumulation in the AD brain (Goodman, 1953) have led to interest in the interaction and association of iron with the histological hallmarks of the disease: neurofibrillary tangles (NFTs) containing hyperphosphorylated tau and Aβ-containing senile

plaques. Iron accumulation in NFTs and amyloid plaques, as well as in the broader cortex, have been observed in AD patients and AD transgenic mouse models (M. A. Smith, P. L. Harris, L. M. Sayre, & G. Perry, 1997; Smith et al., 1998). Hyperphosphorylated tau-associated NFT formation has been shown to be induced and reversed by Fe^{3+} and Fe^{2+}, respectively (Yamamoto et al., 2002). In 2010, Duce et al. addressed questions surrounding the function of APP by demonstrating ferroxidase activity in ‘‘a conserved H-ferritin-like active site’’ within APP (Duce et al., 2010). It was concluded that APP loads oxidized iron into transferrin and demonstrates a significant interaction with ferroportin. These authors also reported the inhibition of APP mediated iron export by Zn^{2+}. Most relevant to observations in AD patients, APP knockout mice demonstrated insufficient iron export capacity and significant retention of iron in cortical neurons (Behl, Davis, Lesley, & Schubert, 1994; Harris, Hensley, Butterfield, Leedle, & Carney, 1995; X. D. Huang et al., 1999). The intracellular retention of iron likely potentiates a toxic cascade since Aβ-mediated reduction of iron has been shown to generate ROS, which in turn leads to increases in both APP and Aβ production (Behl et al., 1994; Harris et al., 1995; X. D. Huang et al., 1999). Recently, it was discovered that increased iron content from brain microbleeds enhanced the neurotoxic effects of Aβ (L. Wang, Xi, Keep, & Hua, 2012). Also, changes in serum iron and copper homeostasis were found to correlate and accurately predict cognitive decline (Mueller et al., 2012). It seems evident that iron’s role in the pathogenesis of AD lies either upstream or in tandem with Aβ accumulation. In comparison, the latter seems less likely as over expression of APP in trisomy 21 does not result in early life fibrillary amyloid accumulation (Arai, Suzuki, Mizuguchi, & Takashima, 1997). Instead, it is more likely that the effect of iron accumulation on Aβ-induced toxicity is the result of progressive insult to cellular iron processing.

Iron–sulfur clusters (ISCs) and heme are iron-containing prosthetic groups at the catalytic centers of many critical metabolic enzymes, including all four of the mitochondrial ETC complexes, and are essential to enzymes responsible for H_2O_2 removal and maintaining general cellular homeostasis. Mitochondria serve as the center stage for synthesis of ISCs and heme (Furuyama, Kaneko, & Vargas, 2007). As discussed earlier, mitochondrial and metabolic dysfunction are observed early in AD (Horowitz & Greenamyre, 2010). Normally, aging is accompanied by increased mt-DNA copy number, which is likely a compensatory mechanism for an aged and dysfunctional mitochondrial population (Barrientos et al., 1997) (Corral-Debrinski et al., 1992). However, in the late stages of AD, amplifiable levels of intact mt-DNA are reduced, possibly through down regulation of PGC1α and mitophagy-induced degradation of mitochondria (Swerdlow & Kish, 2002). Given the relationship between iron, APP, and senile plaques, it seems likely that the intracellular recycling of large amounts of iron containing mitochondrial protein coupled with reduced APP, and thus reduced or impaired iron export capability, may compound bioenergetic decline in Alzheimer's disease.

1.1.4 Mitochondria and iron in idiopathic diabetes

Diabetes mellitus can be characterized as a metabolic disorder for which three major types are known: Type 1 (T1D), Type 2 (T2D), and gestational diabetes mellitus. Type 1 diabetes (or insulin dependent diabetes mellitus) manifests as the result of autoimmune targeted destruction of insulin-producing β-cells in the pancreatic islets, leading to progressive loss of insulin secretion and resulting in absolute insulin deficiency. Type 2 diabetes (most often associated with obesity) is characterized as hyperglycemia in the context of insulin resistance and relative insulin deficiency. Gestational diabetes results in hyperglycemia and insulin resistance during the term of pregnancy in formerly non-diabetic women. Type 2 diabetes

accounts for 90% of diabetes mellitus cases, whereas Type 1 diabetes, gestational diabetes, and monogenic diabetes comprise the remaining 10%.

Insulin is a 5.8 kDa hormone produced by pancreatic β-cells and in the brain whose production and release is in response to elevated blood glucose levels. Insulin stimulation results in multiple complex, dynamic changes and cascades within a cell, ranging from changes in metabolic pathways and bioenergetic flux to targeted transcriptional changes in the nucleus (for review see (Saltiel & Kahn, 2001)). A primary defect in diabetes mellitus is that of glucose intolerance due to changes in insulin response. Many different, and often opposing, theories have arisen in an attempt to target the cause of insulin resistance. However, due to the complexity and variation within the disease, limited progress has been made. Diabetes mellitus results in dramatic changes to global metabolic regulation and substrate utilization for reasons that are undetermined, however evidence suggests that disturbed mitochondrial function and iron homeostasis play an important role.

1.1.4a Mitochondrial and metabolic influence

Type 2 diabetes is characterized by relative insulin resistance and impaired insulin secretion in the presence of glucose. Changes in insulin secretion and response suggest attempts to compensate for or regulate potentially harmful changes in metabolism. Mitochondria play a significant role in regulating insulin secretion in β-cells through regulating the ATP levels responsible for facilitating membrane depolarization and insulin granule, as well as anaplerosis coupled, exocytosis (for reviews see (Jitrapakdee, Wutthisathapornchai, Wallace, & MacDonald, 2010; Maechler, 2013)). Rapid, dramatic changes in mitochondrial morphology upon glucose stimulated insulin secretion have been observed as well as GTP modulated insulin secretion via changes in mitochondrial metabolism and calcium homeostasis (Jhun, Lee, Jin, & Yoon, 2013)

(Kibbey et al., 2007). Changes in mitochondrial and metabolic status in events preceding the onset of diabetes have been recognized for some time and have led to multiple theories proposing different roles for the observed mitochondrial dysfunction. Interestingly, changes in lipid oxidation and fatty acid storage occur just prior to disease onset with increased lipolysis accompanied by changes in circulating free fatty acids (Lewis, Carpentier, Adeli, & Giacca, 2002). It is debated whether this change constitutes a state of compensation or mitochondrial dysfunction. This mainly stems from inconsistent observations of the effects of fatty acid metabolism and altered mitochondrial function in different diabetic populations (i.e. obese vs. lean) (S. D. Martin & McGee, 2013) . Normally, glucose stimulated insulin secretion from β-cells increases in the presence of fatty acids; however this has been shown to decrease during prolonged fatty acid exposure (Sako & Grill, 1990). In contrast, some studies have found that increased fatty acid availability stimulates mitochondria-mediated fatty acid oxidation in muscle (Lewis et al., 2002). This suggests that insulin resistance in the periphery is not necessarily a product of mitochondrial dysfunction, but rather a non-canonical shift in primary bioenergetic pathways based on substrate availability. Still, mitochondria play a critical role in regulating pathways mediating insulin secretion and response, making them central to investigations of perturbed bioenergetic flux in diabetes.

In 1901 Eugene Opie discovered protein deposition in the pancreas of patients with hyperglycemia, describing ‘‘hyaline degeneration of the islands of Langerhans’’ (Opie, 1901). It was not until 1986 that islet amyloid polypeptide (IAPP) was identified and found to be a primary component of these deposits (Westermark, Wernstedt, Wilander, & Sletten, 1986). It has since been discovered that more than 90% of patients with T2D display IAPP associated protein deposition in the pancreas (Hoppener, Ahren, & Lips, 2000; Westermark, 1994). The human

form of IAPP (hIAPP) is secreted with insulin, although its exact function remains unknown. Interestingly, IAPP and brain-associated APP share 90% structural similarity (Ristow, 2004; Westermark, 1994), with hIAPP also possessing structural characteristics that allow it to form amyloid fibrils. Human IAPP has been shown to induce loss of β-cell mass through mitochondrial dysfunction induced activation of apoptotic pathways (Li et al., 2011). Results regarding the potential of an FDA approved treatment for T2D in a transgenic FAD mouse model were released in September of 2013. Liraglutide, a glucagon mimetic and GLP-1 agonist used to stimulate insulin secretion in the presence of glucose, was shown to result in decreased tau phosphorylation, decreased neurofilament formation, and increased memory performance and ability in mice (Xiong et al., 2013). This is consistent with previous findings that demonstrated reduced plaque formation and oxidative stress in transgenic mice treated with GLP-1 (Holscher, 2013). It is not surprising that exendin-4, a GLP-1 agonist, protects β-cells from hIAPP-associated cell death through improved mitochondrial function and biogenesis (Fan, Li, Gu, Chan, & Xu, 2010). Exendin-4 also increases adult neurite outgrowth of sensory neurons (Kan, Guo, Singh, Singh, & Zochodne, 2012), a result important in addressing diabetic neuropathy (*vide infra*). To our knowledge, the effects of GLP-1 agonists on mitochondrial function and oxidative stress in the AD brain have yet to be studied, although these results provide reason to suspect altered and improved metabolic status as a result of GLP-1 receptor modulation.

1.1.4b Iron homeostasis in diabetes

The effects of iron overload and dyshomeostasis in the pathophysiology of diabetes is relatively understudied. However, an increased interest has been generated with multiple groups finding an increased risk of Type 2 diabetes and insulin resistance associated with alterations in

tissue iron content, iron metabolism, and iron overload (Mendler et al., 1999; Simcox & McClain, 2013; M. C. Thomas, MacIsaac, Tsalamandris, & Jerums, 2004). Increased serum ferritin concentration, an indicator of tissue iron status, was positively correlated with the risk of developing T2D (Ford & Cogswell, 1999). More studies have confirmed the increased risk of diabetes with high normal or above normal serum ferritin levels and suggested that iron deficiency may not provide protection against this risk (Aregbesola, Voutilainen, Virtanen, Mursu, & Tuomainen, 2013). A recent study evaluating ferritin and transferrin saturation in pre-diabetes concluded that high ferritin combined with low transferrin saturation was associated with a higher risk of developing prediabetes (Cheung, Cheung, Lam, & Cheung, 2012).

Hereditary hemochromatosis, or iron overload, is commonly caused by mutations in the HFE gene and provides the strongest evidence of systemic iron changes leading to T2D. An allelic variant of HFE linked to hemochromatosis, termed the 'D allele', was shown to increase the risk for diabetes (Rong et al., 2012). HFE-associated diabetes suggests that changes in systemic iron homeostasis, particularly iron overload is associated with diabetes incidence. This has been strengthened with observations that dietary intake of red meat, a significant source of heme iron, is positively correlated with an increased risk of T2D (Jiang et al., 2004). Also, frequent blood donations and iron chelation therapy are shown to improve diabetes in T2D patients (Fernandez-Real, Lopez-Bermejo, & Ricart, 2005).

With little indication as to the exact role of iron overload in the risk for diabetes it is difficult to say whether iron dyshomeostasis is a catalyst or artifact of the disease. Studies on frataxin and NCB5OR pathways will help to provide novel insights into roles for iron metabolism in diabetes.

1.1.5 Alzheimer's disease and diabetic neuropathy

Diabetic neuropathy is a generalized term describing changes and defects in the nervous system of patients diagnosed with diabetes mellitus. Diabetic neuropathy does not discriminate between T1D and T2D. Several forms exist and can be divided into two distinct groups: generalized symmetric polyneuropathies (acute sensory, chronic sensorimotor, autonomic), and focal and multifocal neuropathies (cranial, truncal, focal limb, proximal motor, chronic inflammatory demyelinating polyneuropathy) (Boulton et al., 2005). Numerous studies have observed changes in bioenergetic pathways and mitochondrial function in diabetic neuropathy-associated neurodegeneration for both T1D and T2D (for reviews see (Chowdhury, Dobrowsky, & Fernyhough, 2011; Chowdhury, Smith, & Fernyhough, 2013)). In fact, improving mitochondrial bioenergetics through NF-kβ activation prevents sensory neuropathy in mouse models of T1D (Saleh et al., 2013). The glycolytic byproduct methylglyoxal, a reactive form of pyruvate that plays a role in the development of advanced glycation endproducts, is of particular interest to diabetes and diabetic neuropathy (Singh, Barden, Mori, & Beilin, 2001). Advanced glycation end products have been positively correlated with diabetic nephropathy along with a number of different diabetes associated complications (Beisswenger et al., 2013; Singh et al., 2001). A recent investigation found that methylglyoxal mediated modification of the Nav1.8 sodium channel is associated with hyperalgesia in diabetic neuropathy (Bierhaus et al., 2012), implicating a direct role for methylglyoxal in diabetes-induced nociceptive pain. In addition, a novel neurotoxin known as ADTIQ (1-acetyl-6,7-dihydroxy-1,2,3,4-tetrahydroisoquinoline) discovered in the brains of PD patients has been found to be the result of methylglyoxal reacting with dopamine (Deng et al., 2012). It has been suggested that this neurotoxin, the result of

altered bioenergetic homeostasis and a specific neurotransmitter, might be a common pathogen between Parkinson's disease and diabetes.

Both T1D and T2D result in impaired memory and learning, however the distinctions between T1D and T2D have led to much debate as to the underlying cause. Traditionally, impaired insulin signaling was primarily attributed to T2D and thought to be a larger risk factor for developing AD compared to T1D. However, recent studies have demonstrated worsened AD associated phenotypes in the context of T1D (Currais et al., 2012; Jolivalt et al., 2010), blurring the lines between T1D and T2D in AD. Still, little is known of the effects of AD on peripheral neuropathy. Interest has been generated due to reports of the underrepresented population of dementia patients who experience pain (C. Belin & Gatt, 2006), but it is not immediately clear whether pain associated with dementia is the result of true neuropathy or that of altered pain perception. In 2012, Jolivalt *et al*. provided physiological evidence that APP transgenic mice demonstrated ''similar patterns of peripheral neuropathy'' when compared to insulin-deficient mouse models (Jolivalt, Calcutt, & Masliah, 2012). This was attributed to impaired or altered insulin signaling through lowered insulin receptor phosphorylation as well as altered GSK3β-mediated metabolic regulation. Changes in insulin signaling and regulation are found in both diabetes and AD (for review see (Sima & Li, 2006)). Deficiencies in metabolic processes and pathways are clearly identified in both diseases, thus the presence of peripheral neuropathy like phenotypes in AD mouse models suggests shared pathogenic mechanisms.

1.1.6 Genetic variation, disease susceptibility, and potential therapeutics

A variety of neurodegenerative diseases display characteristics of MIND paradigm-associated defects. Still, with all of the data presented and available, the polygenic nature of these diseases makes identifying viable therapeutic targets the rate limiting step in treatment.

Traditionally, successful treatment development relies on two inherent criteria: disease incidence/impact and identifiable therapeutic targets. In complex, sporadic diseases like Alzheimer's disease or Parkinson's disease, the incidence of the disease is profound and indisputable. However, progress falls short when treatment is focused on therapeutic targets which are not major contributors to the majority of the disease.

The popular belief that Aβ initiates AD pathogenesis set off a plethora of anti-amyloid based treatments (Janus et al., 2000; Morgan et al., 2000; Schenk et al., 1999). So far targeting senile plaques in clinical trials has failed to stop or even conclusively slow disease progression (Aisen & Vellas, 2013; Mangialasche, Solomon, Winblad, Mecocci, & Kivipelto, 2010; Rinne et al., 2010). This implies amyloid deposition may represent a consequence, as opposed to cause, of the disease. A recent study of microbleed events associated with β-amyloid immunization has concluded that immunization actually facilitates cerebral microbleeds and worsens iron deposits in the choroid plexus (Joseph-Mathurin et al., 2013).

In light of these failed treatments, new approaches are needed. This can likely be achieved through targeted manipulation of multiple pathways based on currently unidentified endophenotypes. In AD, mitochondria-associated endophenotypes have been considered due to the maternal inheritance associated with sporadic AD and correlative maternal mt-DNA inheritance (Swerdlow, 2011b). With enough evidence supporting a mitochondrial and metabolic role in disease, a novel approach to treatment strategy has been proposed. Termed ''bioenergetic medicine'', the rationale behind the approach involves the manipulation or support of those pathways that influence or are directly involved in bioenergetic flux (Swerdlow, 2013). This includes previously described mitochondrial medicine approaches in which mitochondria and mitochondrial regulated cellular processes are targeted. These approaches include manipulating

ETC components based on the functional state of mitochondria or cell energy status, influencing mitophagy events, changing mitochondrial mass, and even directing mitochondrial mediated apoptotic events (Swerdlow, 2011b). A recent study by Zhang et al demonstrated prevention of Aβ accumulation and protection against cognitive decline in triple transgenic AD mice by modulation of the mitochondrial ETC complex I using a novel compound known as CP2 ((Zhang et al., 2015). Targeting bioenergetic flux for treatment might be better understood in the context of AD pathology.

During the early stages of AD, prior to mild cognitive impairment syndrome, β-amyloid deposition is abundant. It is not until after senile plaque formation drastically slows that the disease manifests. It has been suggested that the early deposition of senile plaques is coupled with a state of compensated metabolic function (Swerdlow et al., 2013). That is, compensation for dysfunctional metabolic processes is responsible for β-amyloid production in the events preceding cognitive impairment, representing a form of compensated brain aging. At the point at which the framework supporting these compensatory actions is stressed to fracture, metabolic processes are down regulated and hypometabolism sets in. At this stage, plaque deposition halts and uncompensated brain aging occurs, resulting in the onset of the clinical symptoms of Alzheimer's disease (Figure 1.2).

The notion of compensated vs. uncompensated states of dysfunction can also be applied to patterns in diabetes, with changes in metabolic flux, β-cell mass, and global metabolic regulation differing from prediabetes to clinical onset (Greenbaum, Buckingham, Chase, Krischer, & Diabetes Prevention Trial, 2011; Sysi-Aho et al., 2011; Tsai, Sherry, Palmer, & Herold, 2006; Yoneda et al., 2013) (Beck-Nielsen & Groop, 1994). In addition, pre-diabetic NCB5OR knockout mice show a marked increase in metabolic rate prior to the onset of diabetes

(Xu et al., 2011). It is possible, and even probable, that mechanisms similar to those responsible for compensated brain aging play a role in the events preceding the development of diabetes mellitus. Therefore, investigating pathways contributing to metabolic flux and dysfunction in both AD and diabetes will provide novel therapeutic insights.

The mitochondrial cascade hypothesis has helped to provide a broad overarching perspective to evidence of altered brain bioenergetics and mitochondrial function in AD. However, identifying targets for therapeutic intervention is as complex as the disease itself. This is due, in part, to the infancy of risk estimation incorporating both familial history and genetic background in complex diseases (Aiyar et al., 2013). The identification of endophenotypes and eventually multiple and specific targets in complex diseases will require personalized approaches to treatment, complicating the issue further. In short, complex diseases will require complex treatment. So with the development of complex, personalized treatment on the seemingly distant horizon, progress toward effective therapy can likely be made through evaluating genetic networks in the context of the MIND paradigm.

1.2 NADH Cytochrome b5 oxidoreductase

1.2.1 NCB5OR; gene, protein, and function

First cloned in 1999 by Dr. Hao Zhu, NADH cytochrome-b5-oxidoreductase (NCB5OR) is a highly conserved, ubiquitously expressed, soluble, heme-containing reductase associated with the endoplasmic reticulum (H. Zhu et al., 2004b; H. Zhu, Qiu, Yoon, Huang, & Bunn, 1999). The complete, functional isoform on which the majority of studies have been conducted is encoded by 16 exons located on chromosomes 6 and 9 in humans and mice, respectively. The protein contains a cytochrome b5 and b5 reductase domain, joined by a unique, HSP20 like linker region (Figure 1.3). While an exact function and pathway for NCB5OR has yet to be

determined, evidence suggests that the protein is a potent reductase of Fe and heme proteins (e.g. cytochrome c) *in vitro* and plays a significant role in the maintenance of iron homeostasis and pathways critical to proper metabolic and mitochondrial function (H. Zhu et al., 2004b; H. Zhu, Wang, W.F., Wang H.P., Xu, M., E, L., and Swerdlow, R.H., 2013). Since NCB5OR was shown to be associated with the endoplasmic reticulum, early studies aimed to clarify whether NCB5OR was involved in ER stress response pathways. Investigators concluded that while the NCB5OR promoter does respond positively to acute oxidative stress due to the presence of an anti-oxidant response element, overall it does not respond to the induction of ER stress or associated pathways and thus is not involved in the ER stress response (Larade & Bunn, 2006). In addition, the loss of NCB5OR results in increased respiration, oxidative stress, and fatty acid catabolism (Xu et al., 2011). Interestingly, it seems that while NCB5OR might respond to oxidative stress and plays no role in ER stress response pathways, loss of its function results in significant amounts of oxidative and ER stress.

Due to the reductase activity and observed altered iron homeostasis with decreased levels of ferritin proteins (both heavy and light chains) in its absence, NCB5OR was proposed to facilitate management of the labile iron pool content and cellular iron storage by reducing ferritin heavy chain, a key component of cellular iron storage. However, recent experiments involving ferritin-caged iron demonstrated that addition of recombinant NCB5OR does not release stored iron by way of ferritin reduction *in vitro*[1].

1.2.2 NCB5OR and diabetes

Transgenic mice globally deficient in NCB5OR (GKO mice) exhibit low body weight (beginning at 2 weeks of age), petite skeletal structure/build, lipoatrophy and impaired lipid storage, and develop early onset lean diabetes due to necrotic loss of insulin producing β-cells in

[1] Rivera and Zhu, unpublished data.

the endocrine pancreas (Larade et al., 2008; Xie et al., 2004; Xu et al., 2011). There is a definitive and pronounced difference of diabetes onset between male and females, with males displaying an onset of approximately 7 weeks of age and females delaying to as late as 20 weeks of age (Xie et al., 2004). The reason for this delay is unknown however it has been suggested that this might be due to the inherent differences in basal metabolic rates between males and females. Since NCB5OR was shown to be associated with the endoplasmic reticulum, early studies aimed to clarify whether NCB5OR was involved in ER stress response pathways. B-cell injury in NCB5OR deficient mice is rapid and severe. Investigations into the cause of β cell injury revealed a large amount of oxidative stress along with significant ER distention and ER stress that differs from canonical pathway associated with the unfolded protein response (W. Wang et al., 2011).

1.2.3 NCB5OR and mitochondria and iron.

Diabetes, oxidative stress, fatty acid catabolism, and even crosstalk with the endoplasmic reticulum all converge at a common medium: mitochondria. During multiple studies mitochondrial function and morphology were assess in tissues lacking NCB5OR. Electron microscopy performed on pancreatic β-cells isolated from GKO mice revealed an increase in mitochondrial number and distended morphology with some evidence of electron dense granules present within the mitochondrial matrix, a finding commonly attributed to iron accumulation (Xie et al., 2004). These changes are possibly indicative of mitochondria undergoing a permeability transition which could trigger apoptosis; however assays evaluating apoptotic β-cell death were negative, indicating otherwise.

Further studies utilized islet transplants (TKO mice) to further explore the systemic effects of NCB5OR deficiency without the confounding factors introduced by insulin deficient diabetes

(Larade et al., 2008). A primary observation made in these studies was that of continued lipoatrophy in the context of sufficient insulin production. Further analysis resulted in evidence that NCB5OR plays a vital role in fatty acid desaturation, a process upstream of mitochondrial β-oxidation. Microarray data derived from mRNA from TKO livers showed a marked increase in PGC-1α, a stimulator of mitochondrial biogenesis (Larade et al., 2008). An investigation specifically targeting the effects of NCB5OR deficiency on mitochondria, fatty acid catabolism, and oxidative stress demonstrated an increased rate of mitochondria mediated fatty acid oxidation in KO hepatocytes, accompanying observations of increased mitochondrial proliferation and content in the liver of pre-diabetic GKO mice (Xu et al., 2011). Similar findings regarding mitochondrial proliferation and content were confirmed in β-cells (W. Wang et al., 2011).

In order to better understand the totality of changes that loss of NCB5OR induces at the cellular level, microarrays and quantitative PCR of mRNA were conducted on GKO and WT islets from mice 5 weeks of age. A number of iron related genes, including genes involved in iron import and regulation, were significantly up regulated in GKO mice compared to WT, and changes in a few iron related genes were observed in new born mice. Further investigation into the status of iron in global and tissue specific, conditional KO mice revealed that GKO mice presented with mild to moderate anemia and general iron deficiency in iron rich tissues such as the spleen and liver. In fact, GKO mice subjected only to overnight fasting displayed a sharp decrease in circulating iron levels and transferrin saturation. During fasting states, the livers of WT mice displayed an 8-fold increase in Hamp1 expression while GKO mice displayed a 130-fold increase in Hamp1 expression. Hamp1 is a key regulator of dietary iron absorption at the duodenum. Hepcidin, the protein for which Hamp1 codes, is a potent inhibitor of ferroportin, the

key transporter for dietary iron absorption in the duodenum and the sole transporter responsible for cellular iron export. Thus when hepcidin levels increase, iron absorption decreases. The drop in serum iron concentration coupled with the increase in hepcidin levels is consistent with previous observations made in WT mice during the fasting state. Experiments conducted using radioactive ^{59}Fe revealed an interesting change in brain iron uptake. Initial iron assays of the brains of GKO mice displayed little to no iron deficiency. However, when GKO mice are fasted and undergo oral gavage with ^{59}Fe a significant increase in uptake of circulating ^{59}Fe is observed. The drastic response in GKO mice indicates an increased sensitivity to the fasting state and an overcompensation of iron regulatory elements due to NCB5OR deficiency.[2]

Defects in mitochondrial function and iron metabolism may be at the heart of dysfunction in the context of NCB5OR deficiency. ETC function, mitochondrial function, iron metabolism, and heme synthesis are processes that are reliant upon one another. Since iron dyshomeostasis can alter proper mitochondrial function and vice versa, there exists a state of pseudo-quantum entanglement when addressing the onset of dysfunction due to NCB5OR deficiency. This is important when considering the design of future studies aimed at understanding the effects of NBC5OR deficiency on specific systems, largely due to the existence of gene expression profiles that are unique for certain cell types and tissues.

1.2.4 Preliminary behavior observations in NCB5OR deficiency

Since the brain is metabolically demanding and heavily reliant upon proper iron homeostasis, observations of altered iron homeostasis and mitochondrial function led to early questions about the effects of NCB5OR deficiency on behavior. A preliminary behavioral experiment using a y-maze and force-plate actimetry showed that non-diabetic mice globally

[2]All findings presented in the previous paragraph are derived from a publication in preparation.

deficient for NCB5OR are significantly hyperactive compared to WT counterparts (Figure 1.4)[3]. However, since mice globally deficient for NCB5OR have possible confounding factors such as altered metabolism and mild to moderate anemia, further experimentation is needed to determine if behavioral changes observed in GKO mice are the result of primary or secondary dysfunction.

1.3 The Cerebellum: A model system

The cerebellum (or 'little brain') is a highly organized, distinct structure that houses up to 50% of the total neurons in the brain. The cellular organization of the cerebellum is composed of three easily identifiable layers: the molecular layer, the Purkinje layer, and the granular layer (Figure 1.5). Beginning in the 19th century, the cerebellum was thought to solely modulate motor function and maintenance of posture, tonus, motor learning, balance, and coordination. However this view has been challenged over the past few decades with a broad range of behavioral, physiological, and anatomical evidence suggesting a role for the cerebellum in higher cognitive functions such as language, learning, social cognition, and emotional processes (D'Angelo et al., 2011; De Smet, Paquier, Verhoeven, & Marien, 2013; Hoche, Guell, Sherman, Vangel, & Schmahmann, 2015; Schmahmann, 2001). Major contributions to this contention have been made by Schmahmann et. al. who first described cerebellar cognitive affective syndrome in 1997 (Schmahmann & Sherman, 1997, 1998). Investigations have revealed cerebellar damage and dysfunction to result in language or language associated deficits such as syntax impairment, verbal fluency, dyslexia/alexia, agraphia, apraxia, and aphasia (De Smet et al., 2013; Marien, van Dun, & Verhoeven, 2015).

The cerebellum's involvement in higher cognitive and emotional processes has sparked an interest in its involvement in those diseases in which related processes might be affected,

[3] W.F. Wang, M. Winter, K. McCarson, and H.Zhu, unpublished data

including AD. Traditionally the cerebellum's involvement in the presentation and pathology of AD was ignored, likely due to lack of information regarding cerebellar function coupled with a strong pathological and histological presentation of abnormalities in other brain regions. However, in 1980 Pro. et al demonstrated the presence of amyloid plaques in a postmortem analysis of the cerebellum in what were then characterized as 'pre-senile' Alzheimer's patients (Pro, Smith, & Sumi, 1980). In addition, articles published by separate groups during the Summer of 1989 reported the presence of amyloid plaques in the cerebellum of 52-80% of a population of pre-senile, senile, familial, and 21 trisomy associated AD patients (Brucher, Gillain, & Baron, 1989; Cole, Williams, Alldryck, & Singharo, 1989). Interestingly, another study screened over 600 peptides from the cerebellum of AD patients and found that 15 peptides were elevated, 9 of which were fragments of hemoglobin (Slemmon, Hughes, Campbell, & Flood, 1994). However, the presence of plaques in the cerebellum does not necessarily infer pathological consequences. Further investigation demonstrated significantly reduced volumes of the molecular (24%) and granular layers (22%) and a 32% reduction in the number of Purkinje cells from the cerebellums of 11 patients who had reached severe, end-stage AD (Wegiel et al., 1999). Structural MRI has also demonstrated significantly smaller posterior cerebellar lobes and correlative lower cognitive performance in AD patients (Thomann et al., 2008). Even the standard practice of normalization using the cerebellum in perfusion studies has been called into question based on evidence of cerebellar changes in AD (Lacalle-Aurioles et al., 2013). Deficits in neuropsychological functions can be directly correlated to altered metabolism in the cerebellum of AD patients (Newberg et al., 2003) as well as a general reduction in cerebellar glucose metabolism in advanced AD (Ishii et al., 1997).

Finally, the expression of NCB5OR in the cerebellum has been confirmed by qPCR and a previous study which suggested NCB5OR's importance in Bergmann glia function during development (Koirala & Corfas, 2010). Interestingly, NCB5OR expression correlates temporally with observed iron accumulation in Bergmann glia during early postnatal development (J. Y. Kim et al., 2014). These findings along with the unique structure, cognitive and motor influence, diverse and unique cell types, and distinct properties of the cerebellum make it an ideal model system for studying effects on a broad range of behaviors while maintaining focus on a simple and uniform molecular and anatomical environment.

1.4 Statement of Hypothesis

The etiology of many neurodegenerative diseases is still undetermined. In the absence of explanation and amidst a significant amount of data, it has been suggested that metabolism and metabolic pathways contribute significantly to the pathology of many neurodegenerative diseases. However the complex nature of these diseases makes identifying contributing genes, pathways, and processes extremely difficult. In order to address this issue we have begun exploring the notion of metabolic influence over complex neurodegenerative diseases by first considering those diseases that share incidence as well as common pathways and defects; specifically diabetes and pathways relating to mitochondria and iron.

We aim to investigate how genes important for metabolic and iron related processes affect neural tissue, specifically in the cerebellum. One such gene, NCB5OR, is an oxidoreductase ubiquitously expressed in mammalian tissue (H. Zhu et al., 1999). A previous study found that during early postnatal development NCB5OR was one of a subset of genes whose expression increased 120-fold in Bergmann glia cells in the cerebellum (Koirala & Corfas, 2010). It is important to note that this increase in expression parallels previously observed iron deposition in

Bergmann glia beginning in early postnatal development. Interestingly, global ablation of NCB5OR results in monogenic diabetes as well as defects in mitochondria and iron related pathways and processes. To further investigate the influence of iron and metabolic homeostasis in the pathology of disease we are investigating the effects of NCB5OR deficiency on neural tissue and pathways in the cerebellum and midbrain. Our **central hypothesis** is that loss of NCB5OR in the mouse cerebellum and midbrain will alter tissue iron homeostasis and result in dysfunction in pathways and behaviors to which the cerebellum and midbrain contribute. This research was directed by three central aims.

1. **To characterize changes in iron homeostasis and locomotion associated with loss of NCB5OR in the mouse cerebellum and midbrain.**
2. **To evaluate whether loss of NCB5OR in the cerebellum alters feeding behavior and metabolic homeostasis.**
3. **To determine the effects of NCB5OR deficiency on 5HT, DA, GABA, and Glut levels in the cerebellum and cortex of mice globally deficient for NCB5OR.**

CHAPTER 1 – TABLES AND FIGURES

Category	Similarity	Description
Physiology & function	APUD phenotype & paraneuron concept	All endocrine cells have the ability to take up and decarboxylate amine precursors, as well as produce polypeptide hormones [23], features that they share with neurons [24].
	Neurotransmitters	β-Cells synthesise glutamate and use it for intracellular signalling in glucose-responsive insulin secretion [25].
	Neurotransmitter assembly proteins	β-Cells express glutamic acid decarboxylase, an enzyme found in gamma aminobutyric acid (GABA)-secreting neurons but not other cell types [26].
	Neurotransmitter receptors	β-Cells contain glutamate receptors, which are mainly found in the central nervous system [27].
	Secretory granules & microvesicles	β-Cells store insulin in secretory granules that are secreted from synaptic-like microvesicles [26].
	Action potentials	Pancreatic β-cells are capable of generating action potentials similar to those used by neurons to transmit signals along their axons. These action potentials may cause the release of insulin from b-cells in a manner akin to the release of neurotransmitters from neurons [28].
	Glucose response	Neurons in the hypothalamus can sense blood glucose levels and are stimulated by changes in the same way β-cells are [29].
	Schwann cells	Islets are surrounded and highly penetrated by Schwann cells, the major glial cell of the peripheral nervous system [30]. These Schwann cells may be functioning as support cells for both the islets and innervating neurons [30].
	Cell migration	Themigration of pancreatic precursors into the surrounding mesenchyme has been shown to be dependent on the axon guidance protein, netrin-1 [31].
	Adhesion molecules	Endocrine cells of adult mammalian islets associate partially by the expression of neural cell adhesion molecule (NCAM) [32].
Gene expression	Global gene expression	β-Cells are more similar in global mRNA expression and chromatin methylation pattern to neurons than any other cell type, including pancreatic acinar cells [33].
	Sodium channels	Islet cells express the alpha-1 subunit sodium channel mRNA which is primarily expressed in the brain [34].
	Neurofilaments	Dissociated b-cells have been found to synthesise neurofilaments in vitro which may be recapitulating their developmental migration [26].
	REST expression	β-Cells lack expression of repressor element 1 silencing transcription factor (REST) which is expressed in non-neuronal cells and suppresses the neuronal phenotype [35].
	Insulin & other pancreatic endocrine hormones	Insulin, glucagon and ghrelin are expressed in the brain during development and in adulthood [36, 37].
	Glucosetransporters	The β-cell specific glucose transporter, Glut-2, is expressed in certain regions of the brain, including the hypothalamus, one of the sites of insulin action [38].
	Isl-1	The homeodomain protein Isl-1 is expressed in mature pancreatic endocrine cells, calcitonin-producing thyroid cells and neurons of the peripheral and central nervous systems [39].
Development	Pax-6	Pax-6 is involved in development of a-cells of the pancreas and proper insulin secretion from b-cells [40], as well as neurogenesis in the developing central nervous system [41].
	Nkx6.1	Nkx6.1 is a transcription factor involved in the formation of b-cells in the pancreas [40] as well as maturation and migration of hindbrain motor neurons [42].
	Notch	Notch is a transmembrane signalling protein that has been implicated in maintaining pancreatic precursors in a proliferative state, as well as influencing cell fate decisions [40]. Notch has been shown to have similar functions in the developing nervous system [41].
	Neurogenin	The transcription factor neurogenin-3 is repressed by Notch and when activated it contributes to specification of endocrine cells in the pancreas [40]. Notch may also repress neurogenin-1 and 2 which are involved in the specification of neurons from neural progenitors [41].
	HB9	HB9 is expressed in the embryonic gut and initiates formation of the pancreatic bud and is later expressed in mature b-cells[40]. BHB9 is also expressed in embryonic and adult motor neurons [43].
	PDX1	The pancreatic specific transcription factor PDX1 is turned on in the brain during development [44].

Table 1.1 Similarities between β-cells and neurons as described by Arntfield *et. al* (Arntfield & van der Kooy, 2011). Adapted with permission from John Wiley and Sons, Inc.

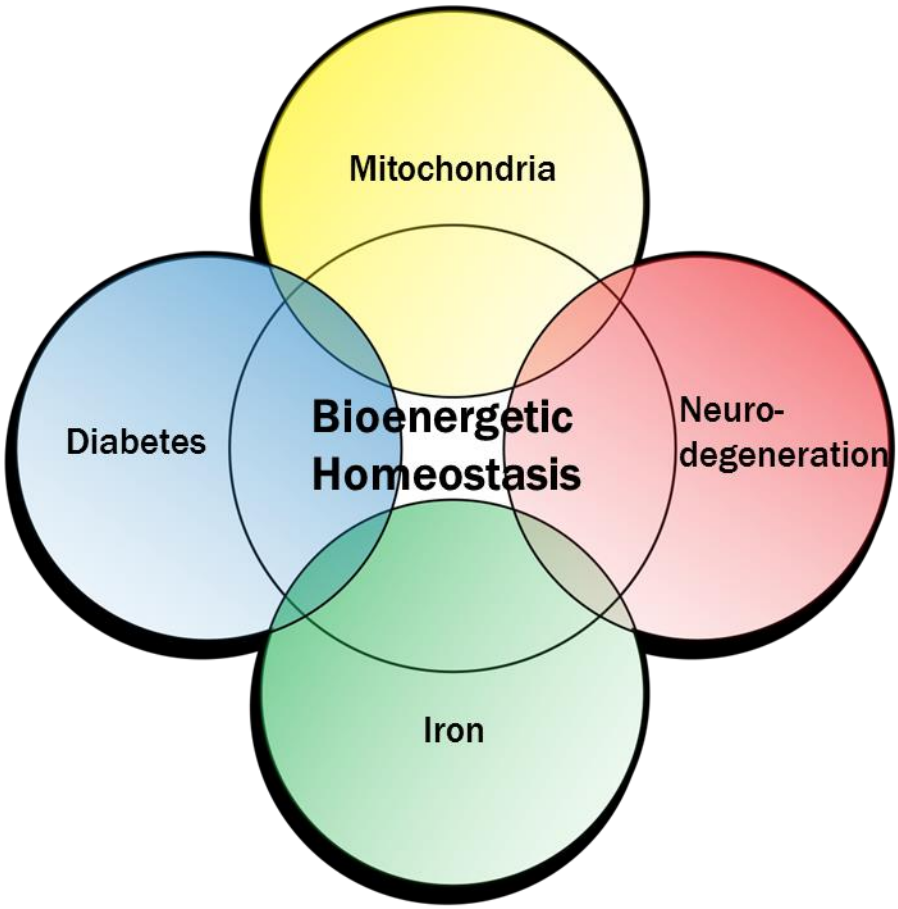

Figure 1.1 The MIND paradigm. Bioenergetic homeostasis lies at the nexus between common defects found in neurodegenerative disease and diabetes mellitus. Mitochondria and iron play a critical role in bioenergetic homeostasis, suggesting that disturbances in proper mitochondrial function and iron metabolism result in dysfunction common to both diabetes and neurodegeneration.

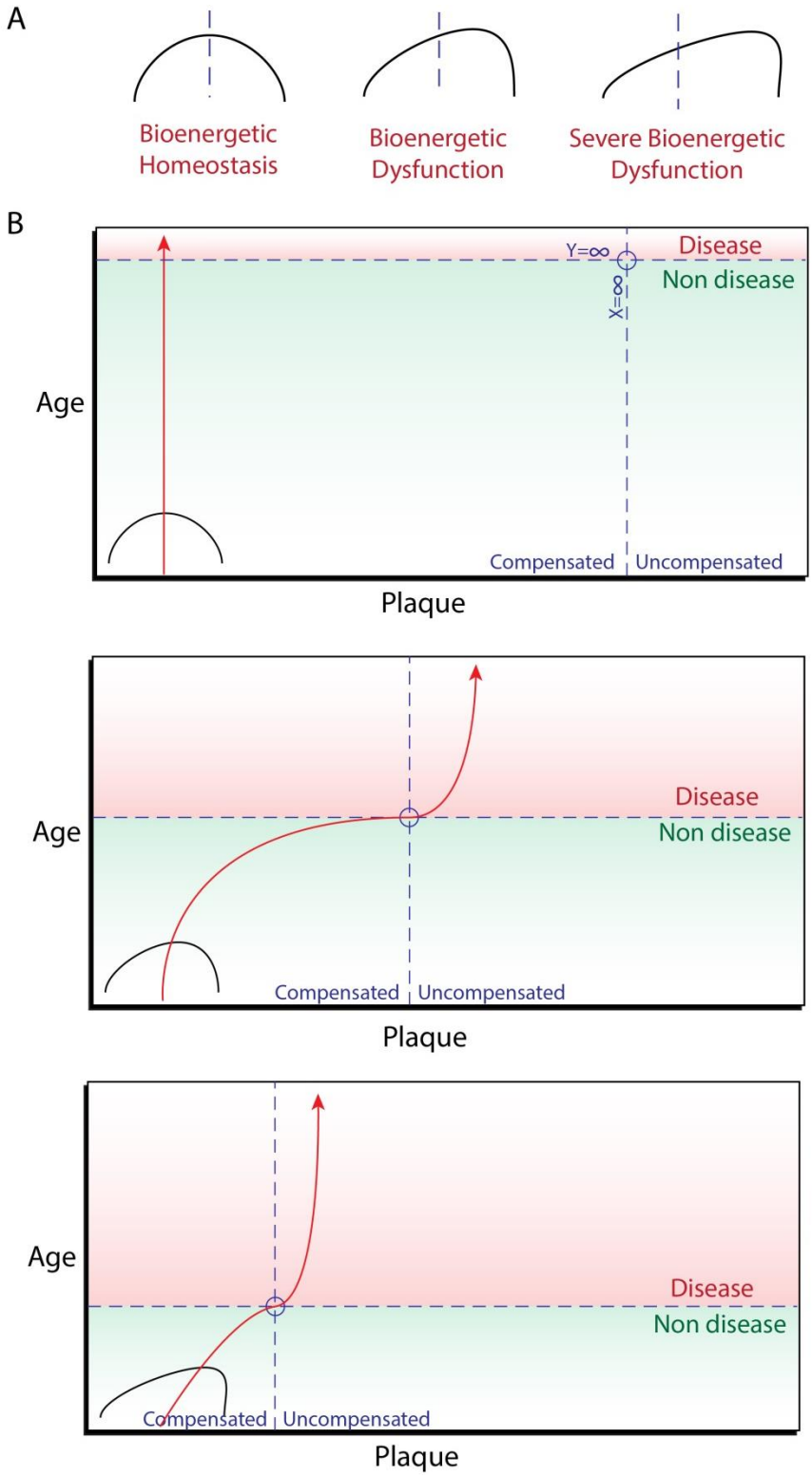

Figure 1.2 Bioenergetic homeostasis in disease. A.) Visual representation of bioenergetic homeostasis, with the midline indicating an ideal flux/balance in bioenergetic pathways.

Distorted mitochondrial function and iron metabolism result in bioenergetic dysfunction, shifting away from ideal bioenergetic homeostasis. B.) Graphical representation of compensated versus uncompensated states of bioenergetics in AD. Ideally, bioenergetic homeostasis results in compensated aging and no plaque deposition. However, in instances of bioenergetic dysfunction plaque deposition occurs during compensated brain aging. At the point at which compensatory mechanisms fail, plaque deposition slows or stops and disease manifests. Severe bioenergetic dysfunction results in the same trend, however this occurs at a much earlier age.

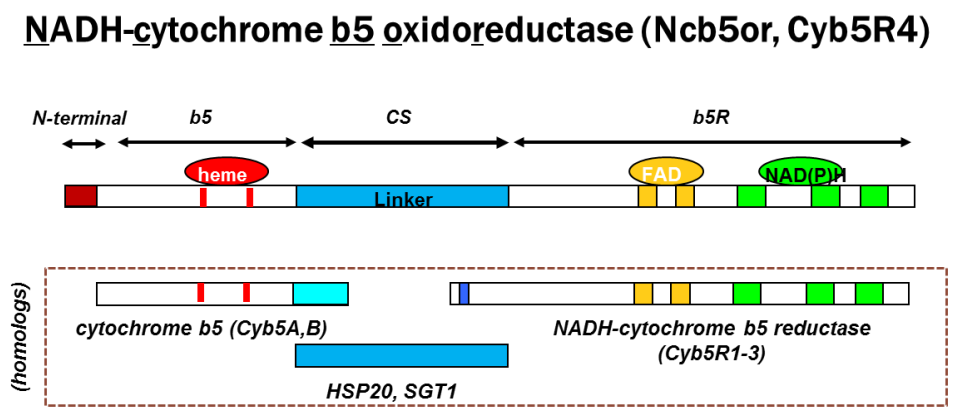

Figure 1.3 Structure and domains of the NCB5OR gene and protein. NCB5OR, also named Cyb5R4 (cytochrome b5 reductase 4), contains 3 homologous domains to protein-coding genes that exist separately in the genome. The protein is composed of an N-terminal cytochrome b5 domain linked to a C-terminal NADH-cytochrome b5 reductase domain by an HSP20-like linker region.

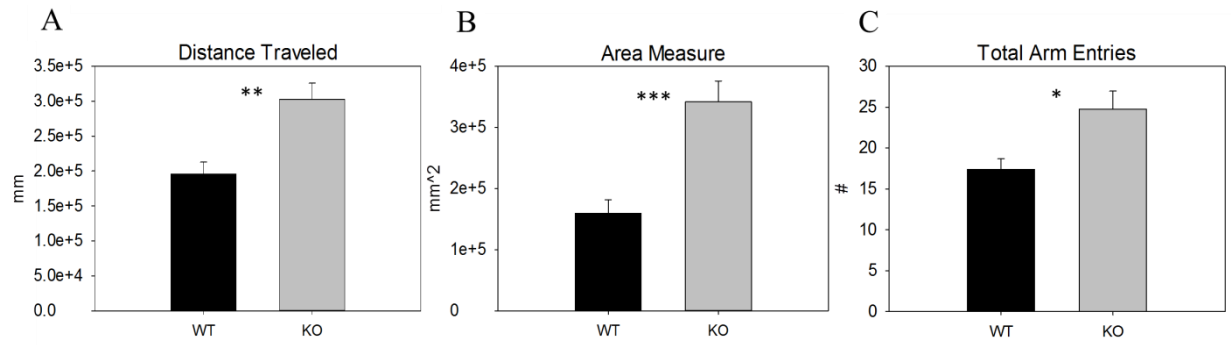

Figure 1.4 Preliminary observations of hyperactivity in female, non-diabetic GKO mice. (A&B) Force plate actimeter data reveals increased distance traveled and area measure in GKO mice. (C) GKO mice challenged with a y-maze experiment show significantly increased arm entries relative to WT mice, indicating increased exploratory locomotor activity in a confined space. Values are presented as mean +/- SEM (standard error of mean). n=5 WT n=9 GKO at 10 weeks of age.*, $p<0.05$; **, $p<0.01$; ***, $p<0.005$.

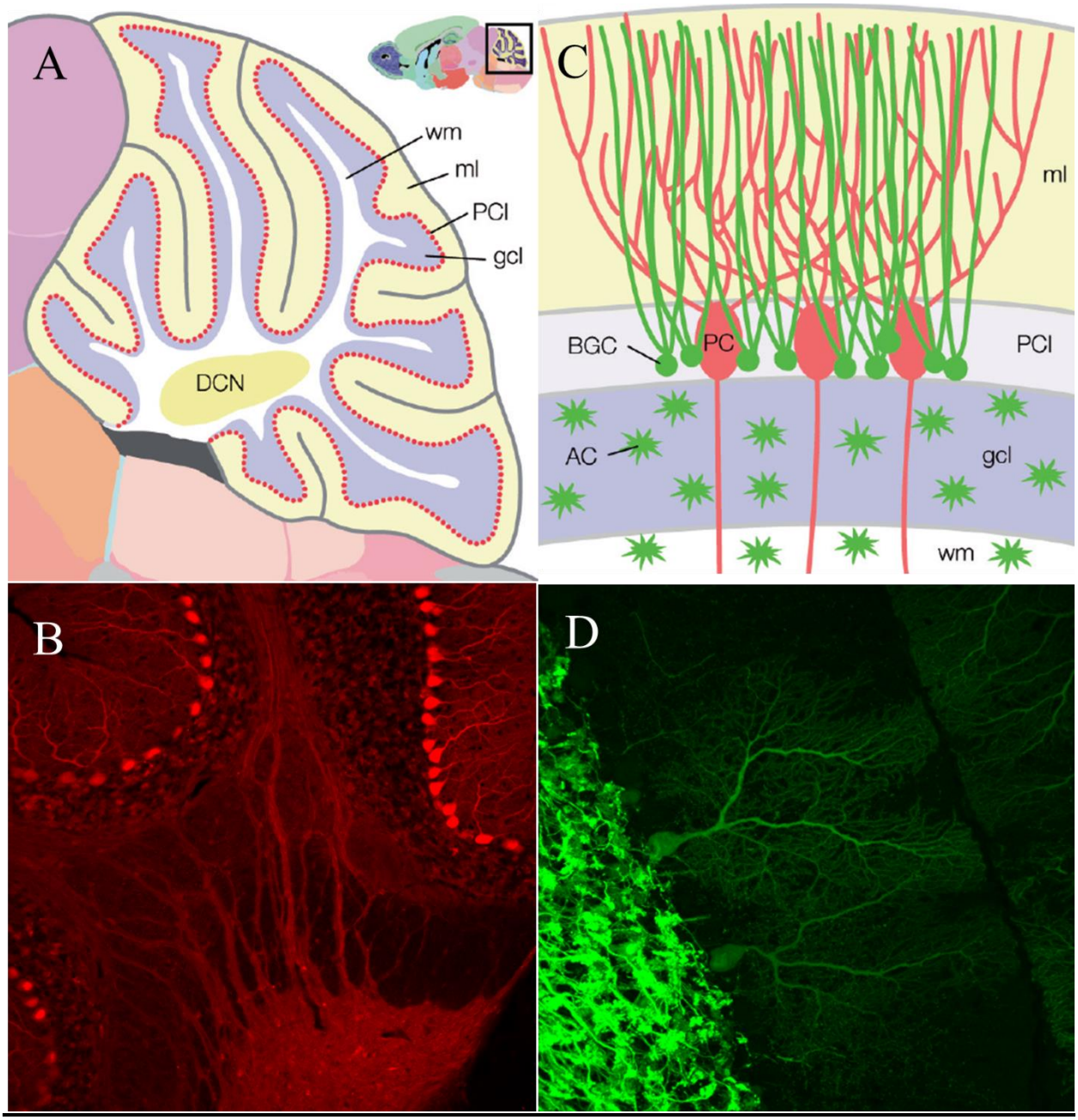

Figure 1.5 Organization of the cerebellum. (A) The cerebellum contains multiple folia (wrinkles) that contain 3 distinct functional layers: the outermost molecular layer (ml), the middle Purkinje cell layer (PCl), and the inner granular cell layer (gcl) where over 50% of the total neurons in the brain are located. The majority of communication to and from the cerebellum is mediated through the deep cerebellar nuclei (DCN). (B) Confocal microscopy of TdTomato

labeled neurons and their axons projecting to the DCN. (C) The Purkinje cell (PC) is the primary source of output from the cortex to the DCN in the cerebellum and is surrounded by supporting cells known as Bergmann glia (BGC). (D) Detailed confocal microscopy of YFP labeled Purkinje cells. Note the complex dendritic arborization. (A) and (C) were adapted from the publication "Connexin43 and Bergmann glial gap junctions in cerebellar function". http://dx.doi.org/10.3389/neuro.01.038.2008. Image in (B) and (D) were collected by Stroh MA during preliminary experiments using tamoxifen induced neuron-specific YFP and cre recombinase expression in mice possessing a floxed TdTomato allele.

CHAPTER 2

LOSS OF NCB5OR IN THE CEREBELLUM DISTURBS IRON PATHWAYS, POTENTIATES BEHAVIORAL ABNORMALITIES, AND EXACERBATES HARMALINE-INDUCED TREMOR IN MICE

2.1 ABSTRACT

Iron dyshomeostasis has been implicated in many diseases, including a number of neurological conditions. Cytosolic NADH cytochrome b5 oxidoreductase (NCB5OR) is ubiquitously expressed in animal tissues and is capable of reducing ferric iron in vitro. We previously reported that global gene ablation of NCB5OR resulted in early-onset diabetes and altered iron homeostasis in mice. To further investigate the specific effects of NCB5OR deficiency on neural tissue without contributions from known phenotypes, we generated a conditional knockout (CKO) mouse that lacks NCB5OR only in the cerebellum and midbrain. Assessment of molecular markers in the cerebellum of CKO mice revealed changes in pathways associated with cellular and mitochondrial iron homeostasis. ^{59}Fe pulse-feeding experiments revealed cerebellum-specific increased or decreased uptake of iron by 7 weeks and 16 weeks of age, respectively. Additionally, we characterized behavioral changes associated with loss of NCB5OR in the cerebellum and midbrain in the context of dietary iron deprivation-evoked generalized iron deficiency. Locomotor activity was reduced and complex motor task execution was altered in CKO mice treated with an iron deficient diet. A sucrose preference test revealed that the reward response was intact in CKO mice, but that iron deficient diet consumption altered sucrose preference in all mice. Detailed gait analysis revealed locomotor changes in CKO mice associated with dysfunctional proprioception and locomotor activation independent of dietary iron deficiency. Finally, we demonstrate that loss of NCB5OR in the cerebellum and midbrain exacerbated harmaline-induced tremor activity. Our findings suggest an essential role for NCB5OR in maintaining both iron homeostasis and the proper functioning of various locomotor pathways in the mouse cerebellum and midbrain.

2.2 INTRODUCTION

Iron deficiency is the most prevalent nutrient deficiency worldwide (WHO, 2001). Iron plays critical roles in a myriad of cellular pathways and processes, ranging from metabolism to gene transcription. The importance of iron to cellular and systemic processes is evident when considering the wide variety of diseases either directly caused by or associated with iron dyshomeostasis (Fernandez-Real, McClain, & Manco, 2015). Maintenance of brain iron homeostasis is relevant to several neurological diseases and the importance of iron in neurocognitive development has been established (D. G. Thomas, Grant, & Aubuchon-Endsley, 2009). Alterations in brain-specific or global iron homeostasis have been directly observed or associated with neuropathological diseases like Alzheimer's disease, Parkinson's disease, and neurodegeneration with brain iron accumulation, as well as cognitive disorders including autism spectrum disorders, attention deficit hyperactivity disorder, schizophrenia, and many more (Belaidi & Bush, 2015; Insel, Schaefer, McKeague, Susser, & Brown, 2008; Konofal et al., 2007; Zucca et al., 2015). A number of studies have evaluated the effects of maternal, neonatal, and adolescent iron deficiency. Whether changes in iron content or homeostasis are a means or an ends has yet to be determined, thus pathways and processes that alter or contribute to iron homeostasis are critical in understanding the underlying etiology and pathology of a number of diseases.

NCB5OR is a highly conserved, ubiquitously expressed oxidoreductase associated with the endoplasmic reticulum whose exact function remains unknown (H. Zhu et al., 2004b; H. Zhu et al., 1999). Naturally occurring polymorphism's in human NCB5OR have been shown result in increased proteasomal degradation (Kalman et al., 2013). Transgenic mice globally deficient in NCB5OR (GKO) have low birth weight (beginning at 2 weeks of age), petite skeletal

structure/build, impaired lipid storage and lipoatrophy, hypermetabolism, mitochondrial dysfunction, and early-onset diabetes from necrotic β-cell loss when compared to normal or wildtype (WT) control mice (Larade et al., 2008; W. F. Wang et al., 2011; Xie et al., 2004; Xu et al., 2011). We recently discovered that global loss of NCB5OR results in mild to moderate anemia, significant changes in iron related pathways, and iron deficiency in iron rich tissues such as the spleen and liver (H. Zhu et al., 2013). Further investigation using a radioactive pulse feeding assay combined with a non-heme iron assay revealed that the brains of GKO mice uptake significantly more circulating ^{59}Fe compared to WT controls, despite showing no apparent change in non-heme iron content (see footnote 1).

Changes in iron homeostasis, mitochondrial dysfunction, and diabetes and their correlation with neurodegenerative diseases (Stroh, Swerdlow, & Zhu, 2014) led us to ask what specific effects NCB5OR deficiency had on neural tissue. Ataxia with Oculomotor Apraxia (AOA2) and sideroblastic anemia with ataxia have been shown to be related to changes in iron homeostasis in the cerebellum. Additionally, Friedreich's ataxia results in mitochondrial iron dyshomeostasis, dorsal root ganglia degeneration, and atrophy of the dentate nuclei without changes in iron content (Solbach et al., 2014). Genes associated with these diseases are ubiquitously expressed; however alleles with mutations or expansions appear to have adverse effects on specific tissue types, namely neural tissue. A microarray study surveying changes in gene expression in Bergmann glia during the postnatal development of the mouse cerebellum revealed NCB5OR to be one of a few that were significantly up-regulated (~120 fold) beginning postnatal day 6 (Koirala & Corfas, 2010). This observation coincides with a sequential iron accumulation in chick Bergmann glia beginning postnatal day 2 as well as the localization of transferrin binding protein, ferritin, and iron in Bergmann glia (Cho, Shin, Lee, Hwang, &

Chang, 1998; J. Y. Kim et al., 2014). Loss of iron related genes in the cerebellum has been shown to alter locomotion and induce degeneration, ataxia, and developmental issues (Capoccia et al., 2015; LaVaute et al., 2001; Maccarinelli et al., 2015; Zhao, 2015). Additionally, cognate motor learning and execution of a complex motor task requires proper nigrostriatal function as well as efficient processing of proprioceptive input by the cerebellum (Salamone, 1992). Therefore, we investigated whether loss of NCB5OR in the cerebellum and midbrain would result in locomotor deficits and whether dietary iron deficiency would reveal or exacerbate any deficits.

2.3 RESULTS

2.3.1 Effective deletion of NCB5OR in the CKO cerebellum.

Mice expressing the En-1 driven cre recombinase showed effective recombination of a TdTomato reporter allele in the cerebellum and mid-brain (Figure 2.1). Quantitative PCR (qPCR) analysis of reverse transcribed mRNA with primers targeting exon 4, which is not deleted in CKO tissues, revealed a significantly reduced level of NCB5OR transcripts in the cerebellum of CKO mice relative to WT controls (CKO, 17.6±1.4; WT, 24.9±1.4; $p=0.003$, see table 1 for conditions). In addition, qPCR with primers targeting the floxed exon 3 revealed an absence of functional NCB5OR transcripts in CKO mice relative to WT controls (CKO, 0.33±0.64; WT, 8.33±0.64; $p<0.001$).

2.3.2 NCB5OR deficiency results in changes in iron related pathways and uptake of circulating ^{59}Fe.

To assess whether loss of NCB5OR in the cerebellum facilitated changes in iron related pathways we performed qRT-PCR analysis on mRNA isolated from the cerebellum of CKO mice and WT littermates (Table 2.1). At 7 weeks of age, CKO mice displayed significantly

elevated transcripts for many genes associated with or responsible for proper maintenance of cellular and mitochondrial iron homeostasis. Iron transport and import transcripts transferrin (Tf) and transferrin receptor (TfR1), respectively, were both significantly elevated. Interestingly, transcripts for the only known iron exporter ferroportin (Fpn1) were significantly increased. Transcripts of proteins responsible for iron storage (ferritin heavy chain, FtH, and ferritin light chain, FtL) were also found to be significantly elevated in CKO mice. Additionally, transcripts for amyloid precursor protein (APP) were elevated. APP has been shown to have ferroxidase activity and an iron-responsive element in the 5' untranslated region of the transcript (Duce et al., 2010; Rogers et al., 2002). Mitochondria-associated iron transcripts frataxin (Fxn) and mitoferrin 2 (MitoFn2) were elevated at 7 weeks as well. By 16 weeks of age, the majority of transcripts returned to levels comparable to WT control mice. However, transcripts for iron regulatory protein 2 (Irp2) and metallothionein 2 (Mt2) were found to be elevated at 16 weeks.

We also performed transcript analysis of cerebellar mRNA at 7 weeks of age after mice had been challenged for 4 weeks with an iron deficient diet for behavioral analysis (Table 2.2). Transcript levels from male CKO mice showed drastic increases for a number of genes compared to WT controls as well as chow fed controls. Conversely, female CKO mice showed significant decreases in transcripts compared to WT controls and their male counterparts.

Maintenance of iron homeostasis is heavily reliant on both transcriptional and translational regulatory mechanisms. To assess whether the transcript levels accurately reflected the status of TfR1, FtH, and APP protein levels we performed western blot analysis of total protein collected from the cerebellum of male CKO and WT mice at 7 weeks of age (Figure 2.2). Levels of TfR1 were significantly elevated (Figure 2.2A), while FtH levels were significantly

decreased (Figure 2.2B). Although CKO mice had elevated APP levels, they did not reach statistical significance when compared to WT (Figure 2.2A).

In order to evaluate whether the changes in iron-related pathways were indicative of actual changes in iron uptake we conducted an ^{59}Fe pulse feeding assay on CKO and WT mice at 7 and 16 weeks of age. At 7 weeks of age, CKO mice had significantly greater ^{59}Fe uptake in the cerebellum (Figure 2.3A - left), while uptake in control tissues remained unchanged (spleen - Figure 2.3B - left, and liver - data not shown). Surprisingly, by 16 weeks CKO mice had significantly lower ^{59}Fe uptake in the cerebellum (Figure 2.3A - right) and CKO males exhibited significantly less iron uptake in the spleen (Figure 2.3B - right). No recombination in the spleen was seen using PCR (data not shown). There were no changes in liver ^{59}Fe uptake at 16 weeks (data not shown). We tested whether the change in uptake was an indication of altered iron reserves in the form of non-heme iron content; however, measurement of non-heme iron content of the cerebellum and spleen of CKO mice revealed no changes in the cerebellum (Figure 2.3C) or spleen (Figure 2.3D) at 7 or 16 weeks of age.

2.3.3 NCB5OR deficiency results in less ferric iron staining in Purkinje cells.

The altered state of ^{59}Fe uptake combined with no observable difference in non-heme iron content at 16 weeks of age in CKO mice led us to question whether there was a shift in the ratio of free to stored iron content. A shift of this nature would result in different amounts of free iron in the ferrous state (Fe^{2+}) and stored iron in the ferric state (Fe^{3+}). In order to test this hypothesis we needed a test that would differentiate between the two oxidative states of iron. Therefore, we performed histological analysis of 16 week old male cerebellum sections combined with Perls' Prussian blue iron staining, which uses ferrocyanide to specifically stain for ferric iron. Perls iron staining in combination with DAB enhancer revealed distinct staining

in Purkinje cells of the cerebellum (Figure 2.4A). Iron positive and negative Purkinje cell counts revealed that CKO mice possessed a significantly reduced number of iron-positive Purkinje cells when compared to WT counterparts (Figure 2.4B). Control sections treated with only DAB (enhancer) and Nissl (counterstain) in the absence of Perls' iron stain revealed no positive staining, indicating iron-specific staining (data not shown).

2.3.4 Iron deficiency alters execution of complex motor tasks in CKO mice.

Based on the changes in iron uptake and related pathways, we hypothesized that loss of NCB5OR in the cerebellum and midbrain would result in locomotor defects. Additionally, we investigated whether generalized iron deficiency brought about by chronic dietary iron deprivation would exacerbate any underlying deficits. It is important to note that gross differences in body weight can contribute to significant changes in certain behavior measures. There were no body weight differences between CKO and WT mice in either the chow or low-iron diet fed groups, but we did note a significant difference in body weight of all mice between the chow and low-iron-diet treated groups during ages 4-7 weeks (Figure 2.5A).

While there were no apparent differences in performance of the beam walk task between chow-fed CKO and WT mice (Figures 2.6A and 2.6B), CKO mice on an iron-deficient diet took significantly longer to traverse an elevated beam at weeks 1,2, and 4 of low-iron-diet treatment. (Figure 2.5B) CKO mice also committed an increased number of paw slips (Figure 2.5C) compared to WT mice at weeks 2 and 3 of low-iron-diet treatment. Additionally, Rota-rod tests revealed that 7 week old CKO mice treated with an iron deficient diet for 4 weeks had a decreased latency to fall compared to WT mice (Figure 2.5D), indicating a deficit in coordination. When we compared the dietary effects within genotypes, we observed that the increased number of slips during the coordinated motor task was the result of the genotype

differences between CKO and WT mice (Figure 2.7A and 2.7B). However, the increased beam traversal time in the low-iron diet group was due to a hyperactive response in WT mice compared to no response in CKO mice (Figures 2.7C and 2.7D).

2.3.5 An iron-deficient diet decreases exploratory locomotor activity in CKO mice.

The resistance to a low-iron-diet-induced hyperactive response in CKO mice led us to investigate whether CKO mice had differences in locomotor activity when fed a low-iron diet. Force-plate actimeter data revealed no differences between CKO and WT mice on a chow diet (Figures 2.8A-D), with the exception of a difference in total distance traveled and spatial statistic during the initial 3 week age time point. However, treatment with a low-iron diet resulted in significantly reduced locomotor activity in CKO mice, yielding reduced total distance traveled (Figure 2.8E) and area measure (Figure 2.8F) compared to WT mice after 1-3 weeks of dietary iron deprivation. Spatial statistics also indicate that the reduced locomotor output correlated with lowered exploratory activity during weeks 1 and 2 of dietary iron deprivation, with CKO mice spending more time in one area, generating a higher spatial statistic (Figure 2.8G). It is possible that changes in total distance traveled and area measures are indicative of slower locomotion rather than reduced overall locomotor activity and exploratory behavior, however CKO mice displayed significantly more bouts of low mobility during weeks 1 and 2 of low-iron-diet treatment (Figure 2.8H), suggesting that they spent more time being immobile than their WT counterparts.

2.3.6 CKO mice display changes in locomotion independent of dietary treatment.

To our surprise, gait analyses revealed a number of significant changes in 7 week old CKO mouse locomotion that were present in both chow- and low-iron-fed mice that were ultimately unaffected by the dietary iron deficiency. Compared to WT mice, CKO mice had a

wider stance width (Figure 2.9B), decreased step angle (Figure 2.9C), and increased distance to fore limb-hind limb paw overlap (decreased occurrence of superimposed tracks; Figure 2.9D). Additionally, CKO mice displayed changes in the rate in which they reach full stance (increased max $\Delta A/\Delta T$, rate of change of paw area over time; Figure 2.9F) as well as an increase in the amount of paw drag (Figure 2.9G) from the time of full stance to liftoff.

In order to confirm locomotor changes independent of dietary treatment and assess whether age was in important factor we performed gait analysis on 16 week old CKO and WT mice fed a chow diet. Comparative gait analysis between 7 and 16 week old CKO mice revealed that CKO mice had significantly increased Max $\Delta A/\Delta T$ (Figure 2.10A), midline distance (Figure 2.10B), and distance to paw overlap (Figure 2.10C) regardless of age. In addition, CKO mice had decreased swing duration (Figure 2.10D), however this significance was not seen when comparing dietary influence at 7 weeks of age (data not shown).

2.3.7 Reward response remains intact in CKO mice.

Upon analysis of locomotor activity and Rota-rod performance, it became apparent that the effects of an iron-deficient diet not only had negative effects on CKO mice, but the effects appeared to be opposite that of WT mice exposed to a low-iron diet when compared to the chow diet. For example, CKO mice on a low-iron diet displayed decreased performance on the Rota-rod task compared to CKO mice on chow, while Rota-rod performance was greater in WT mice on a low-iron diet compared to WT mice on chow. The increased performance of the WT mice under iron-deficient conditions led us to question whether the ventral tegmental area (VTA) was affected in both WT and CKO mice on low-iron diets. Lesions in the tail of the VTA have been reported to result in increased Rota-rod performance in rats (Bourdy et al., 2014) and deletion of the dopamine D2 receptors in the VTA results in increased cocaine-induced locomotion.

Moreover, loss of dopamine D2 receptors in the VTA results in increased motivation for sucrose (de Jong et al., 2015).

Therefore, we used a sucrose preference test to determine whether the loss of NCB5OR and the low-iron diet altered behaviors associated with the VTA. In both chow-fed and low-iron-diet treated groups there were no significant differences between 6 week old CKO and WT mice for sucrose preference based on net consumption over a 24 hour period (Figures 2.11A and 2.11B). Interestingly, when comparing all mice treated with either a low-iron or chow diet, mice treated with a low-iron diet showed a significant shift away from sucrose preference compared to those on a chow diet (Figure 2.11C). This suggests that dietary iron deficiency alters the reward response such that there is less preference for sucrose without affecting total liquid consumption.

2.3.8 NCB5OR ablation in the cerebellum exacerbates peak harmaline-induced tremor.

Since CKO mice did not show signs of gait asymmetry or overt ataxia like those seen in mice with cerebellar or dorsal root ganglia lesion or degeneration, we hypothesized that pathways responsible for rhythmic, central pattern generation as well as gross limb movement were being affected by loss of NCB5OR in the cerebellum. These include the cerebelloreticular and cerebellorubral tracts (Figure 2.11D). In order to test these, we investigated subcutaneous harmaline tremor response, a commonly known pharmacological method of induced essential/cerebellar tremor that utilizes the suspect afferent and efferent pathways. Twenty-four (24) week old CKO and WT mice were placed in an actimeter that allowed for spectral analysis of power for vertical forces between 0-25 Hz (Figure 2.11E). Motion power percentages (MPP) for initial baseline session readings revealed no differences between CKO and WT mice. MPP's for the initial onset of tremor activity (10 minutes post injection) in the 10-17 Hz range did not differ between CKO and WT mice. By 20 minutes post injection, CKO mice exhibited

significantly greater MPP's than WT mice (Figure 2.11F). The significant difference continued through 30 minutes post injection.

2.4 DISCUSSION AND SUMMARY

Our study aimed to characterize iron-related and behavioral effects due to absence of a reductase, NCB5OR, in the mouse cerebellum and midbrain. To avoid complications of previously described phenotypes and changes associated with global loss of NCB5OR, we generated a cerebellum/midbrain specific conditional knockout (CKO) mouse. Strategic ablation of NCB5OR in the cerebellum and the midbrain allowed us to investigate the specific molecular effects of NCB5OR deficiency on neural tissue as well as evaluate changes in locomotive behavior due to loss of NCB5OR in areas known to affect locomotion. We demonstrated that ablation of NCB5OR in the cerebellum resulted in altered profiles of gene transcripts and proteins critical to iron metabolism and proper maintenance of cellular iron homeostasis. Normally, pathways responsible for iron uptake and export respond in accordance with cellular iron status. During times of iron sufficiency, import and export of iron are regulated such that there is not significant uptake or release of iron, since cytosolic iron stores should compensate for any immediate increase in demand. However, in times of iron deficiency, export is inhibited and uptake is increased, allowing for the accumulation of more iron without significant loss. In our model, loss of NCB5OR resulted in an abnormal response to normal iron bioavailability. At 7 weeks of age, neural tissue devoid of NCB5OR simultaneously acquired and exported available iron, consistent with observed changes in iron uptake (Tf and TfR) and export-related transcripts (Fpn1, APP, CP). Nutritional iron deficiency helped confirm our initial observations and led to interesting observations regarding sexual dimorphism in the iron-deprivation response. However, at 16 weeks no differences in levels of these transcripts were observed while less iron

was acquired by NCB5OR deficient tissue. It is important to note that we did observe elevated IRP2 and MT2 transcripts in 16 week old CKO mouse cerebellum. IRP2 is a regulator of iron-related transcript translation and therefore plays an important role in the abundance of proteins directly responsible for iron homeostatic maintenance (B. Guo, Yu, & Leibold, 1994; Samaniego, Chin, Iwai, Rouault, & Klausner, 1994). Levels of IRP2 protein are inversely correlated with iron content and are therefore increased in iron-depleted cells (Iwai, Klausner, & Rouault, 1995). Increased IRP2 transcript levels could indicate a shift from a transcriptional to a protein regulatory response to NCB5OR deficiency. MT2 also plays a role in metal homeostasis by regulating everything from heavy metal scavenging to zinc (Zn) acquisition and signaling. A role for Zn and metallothionein's in autism spectrum disorders has been of growing interest (Russo, 2009; Vela et al., 2015). Faber *et al* reported that the Zn/Cu ratio in children with autism spectrum disorder's was abnormally low, suggesting alterations in metallothionein related pathways (Faber, Zinn, Kern, & Kingston, 2009).

The stark contrast in transcript and iron uptake response to NCB5OR deficiency at 7 and 16 weeks of age may indicate a pattern of compensatory response and a subsequent compensated state, respectively. That is to say that by 16 weeks the loss of NCB5OR led to a shift in major iron homeostatic pathways as well as pathways dependent on iron. This resulted in the establishment of new homeostatic criteria, negating a need for a compensatory cellular response. This suggests not only an abnormal iron homeostatic response, but also abnormal iron flux, sensing, and pathway crosstalk. We used spleen and liver ^{59}Fe levels as positive and negative controls, respectively, during our uptake experiments due to previous findings showing significantly elevated ^{59}Fe uptake in the spleen and unchanged uptake in the liver of NCB5OR global knockout mice. As expected, at 7 weeks of age we observed no differences in ^{59}Fe uptake

in either the spleen or the liver. However, at 16 weeks we were surprised to find significantly decreased uptake in the spleens of male CKO mice. PCR confirmed no loss of NCB5OR in the spleen (data not shown). Direct communication and regulation from brain to the spleen moderated by cholinergic innervation has been identified and may contribute to this observation, and there is significant evidence demonstrating the existence of 'brain-spleen inflammatory coupling' (For review see (Rasouli, Lekhraj, Ozbalik, Lalezari, & Casper, 2011)). Histological analysis of iron staining in the cerebellum revealed further evidence of an altered homeostatic state in 16-week-old CKO mice. The results, along with the observation of no alteration in total non-heme iron content, suggest that CKO mice may possess altered homeostatic criteria that allow for more ferrous (labile) iron. The latter is known to potentiate oxidative stress *via* the classical Fenton reaction mechanism.

Brain iron homeostasis has been the focus of numerous studies, especially those focusing on the effects of neonatal/adolescent iron deficiency. In fact, iron deficiency, dietary or otherwise, has been linked to a number of neurological and psychiatric conditions including restless leg syndrome and attention deficit hyperactivity disorder (Capoccia et al., 2015; Connor et al., 2003; Earley, Connor, Beard, Clardy, & Allen, 2005; Konofal et al., 2007; Konofal, Lecendreux, Arnulf, & Mouren, 2004; Konofal et al., 2008; Maccarinelli et al., 2015; Percinel, Yazici, & Ustundag, 2015; Provini & Chiaro, 2015; Qu et al., 2007). An investigation into the effects of iron deficiency and iron deficiency anemia in young Zanzibari children demonstrated lower motor activity scores and less time in locomotion in affected children (Olney et al., 2007). However, there is evidence that early dietary iron deficiency can result in either reduced or increased locomotion (Bourque, Iqbal, Reynolds, Adams, & Nakatsu, 2008; Fiset, Rioux, Surette, & Fiset, 2015). Targeted deletion of NCB5OR in the cerebellum and midbrain in the

present study did not result in overt changes in locomotion or coordination when mice were fed a chow diet with sufficient iron content. However, NCB5OR deficiency combined with dietary iron deficiency significantly altered locomotion and coordination. Interestingly, when compared to chow fed controls, the effects of dietary iron deficiency appeared to be opposite for CKO and WT mice, with CKO mice becoming hypoactive (or unaffected, as seen in the beam walk time to traverse) and WT mice becoming hyperactive. Given that multiple studies have reported opposing effects of dietary iron deficiency on locomotion, it is interesting to note that ablation of NCB5OR in the cerebellum and midbrain resulted in a resistant or hypoactive response to iron deficiency while WT counterparts responded in a hyperactive manner. Additionally, CKO mice fed an iron-deficient diet displayed decreased coordination and movement execution during complex motor tasks. These changes indicate possible detrimental effects of NCB5OR deficiency on nigrostriatal pathways in the context of dietary iron deficiency. Genetic variations resulting in altered iron content in ventral midbrain nuclei have been linked to changes in locomotor activity (Unger, Sterling, Jones, & Beard, 2008). Also, interactions between iron, dopamine, and neuromelanin-related pathways have been indicated in Parkinson's disease (Zucca et al., 2015).

Changes in gait and ataxia are commonly associated with dysfunction in the cerebellum or proprioceptive pathways (Miyajima et al., 2001). However CKO mice did not display overt changes in gait symmetry or exhibit progressive ataxia (as is common with cerebellar lesion, degeneration, or altered proprioceptive input) compared to WT controls. Additionally, when compared to WT controls, CKO mice did not display changes in fore limb or whole body grip strength (data not shown), ruling out confounding factors of muscle weakness. It is important to

note that while there were no genotype differences in the chow and low-iron diet groups, the low-iron diet did induce a mildly ataxic phenotype in all mice.

The VTA contributes both to reward response and locomotor integration in reward-associated tasks. Since CKO mice exhibited locomotor effects opposite those of WT mice when treated with a low-iron diet, we evaluated whether CKO mice in the low-iron diet treated group harbored changes in reward response compared to WT mice. Results indicate that reward response was intact in CKO mice and was comparable to that of WT mice in both chow and low-iron diet groups. This suggests that the diet-dependent effects of NCB5OR deficiency are likely not originating from the VTA or VTA control over substantia nigral pathways. However, a low-iron diet significantly reduced sucrose preference in all mice, indicating that iron dyshomeostasis or deficiency does alter reward response in mice. Dopaminergic neurons in the VTA are thought to be the largest contributors to VTA mediated reward response. Since we suspect that dopaminergic pathways in the substantia nigra are at the root of the diet dependent effects of NCB5OR ablation, the lack of genotype-diet interaction in VTA-dopaminergic-neuron- mediated behavior might indicate genetic susceptibility of certain dopaminergic neuron populations over others.

We observed a number of changes in CKO mouse locomotion that were independent of and unaffected by dietary iron deficiency, suggesting that regions outside of the nigrostriatal and mesolimbic pathways may be affected. Gait analyses revealed that CKO mice had gait alterations indicating altered proprioception and central pattern-generated locomotion, resulting in hypometric hindlimb movements. In addition, these changes were found to occur in chow fed CKO mice regardless of age, confirming previous observations. However, the absence of ataxia and gait asymmetry in CKO mice suggests that changes may be due to physiological rather than

pathological mechanisms. We suspected the origins of diet-independent changes to be of lower, non-cognate motor task-associated pathways. We investigated whether pathways responsible for central pattern-generated locomotion (reticulospinal, rubrospinal, and associated tracts) were being affected by altered cerebellar input by using a harmaline-induced tremor assay. Harmaline treatment results in rhythmic burst firing in the medial accessory olive (MAO) and dorsal accessory olive (DAO) nuclei that excites vermis and paravermis Purkinje cells in the cerebellum. The Purkinje cells project to the deep cerebellar nuclei (fastigial and interposed nuclei). Climbing fibers from the MAO and DAO also directly project to deep cerebellar nuclei. The deep cerebellar nuclei stimulate reticulospinal and rubrospinal fibers which play a role in control of posture, locomotion, and central pattern generation of locomotion (F. C. Martin, Le, & Handforth, 2005; Mori et al., 1998). At the cellular level, harmaline administration results in increased intraneuronal Ca^{2+} spikes in oscillating olivary neurons, leading to greater excitability (F. C. Martin et al., 2005). The increased response to harmaline tremor in CKO mice could indicate changes in other metal ion (i.e. Ca^{2+}, Zn^{2+}, Na^{+}) homeostatic maintenance pathways in the absence of NCB5OR. Increased serotonin has also been shown to potentiate a greater response to harmaline-induced tremor. These are important considerations when exploring further explanation of the changes seen in CKO mice.

In summary, our study has shown that genetic alterations leading to iron dyshomeostasis can affect a range of movement-related neural pathways, especially when combined with environmental factors such as generalized iron deficiency. These data suggest that NCB5OR deficiency results in alterations in iron homeostasis, but do not prove that NCB5OR directly contributes to iron homeostasis. Although further experimentation is needed to address the latter, our current findings show that NCB5OR related iron dyshomeostasis, and pathways and

processes affected by iron, is of significance to the proper functioning of multiple neural pathways, specifically those contributing to quantitative and qualitative locomotor output.

CHAPTER 2 - TABLES AND FIGURES

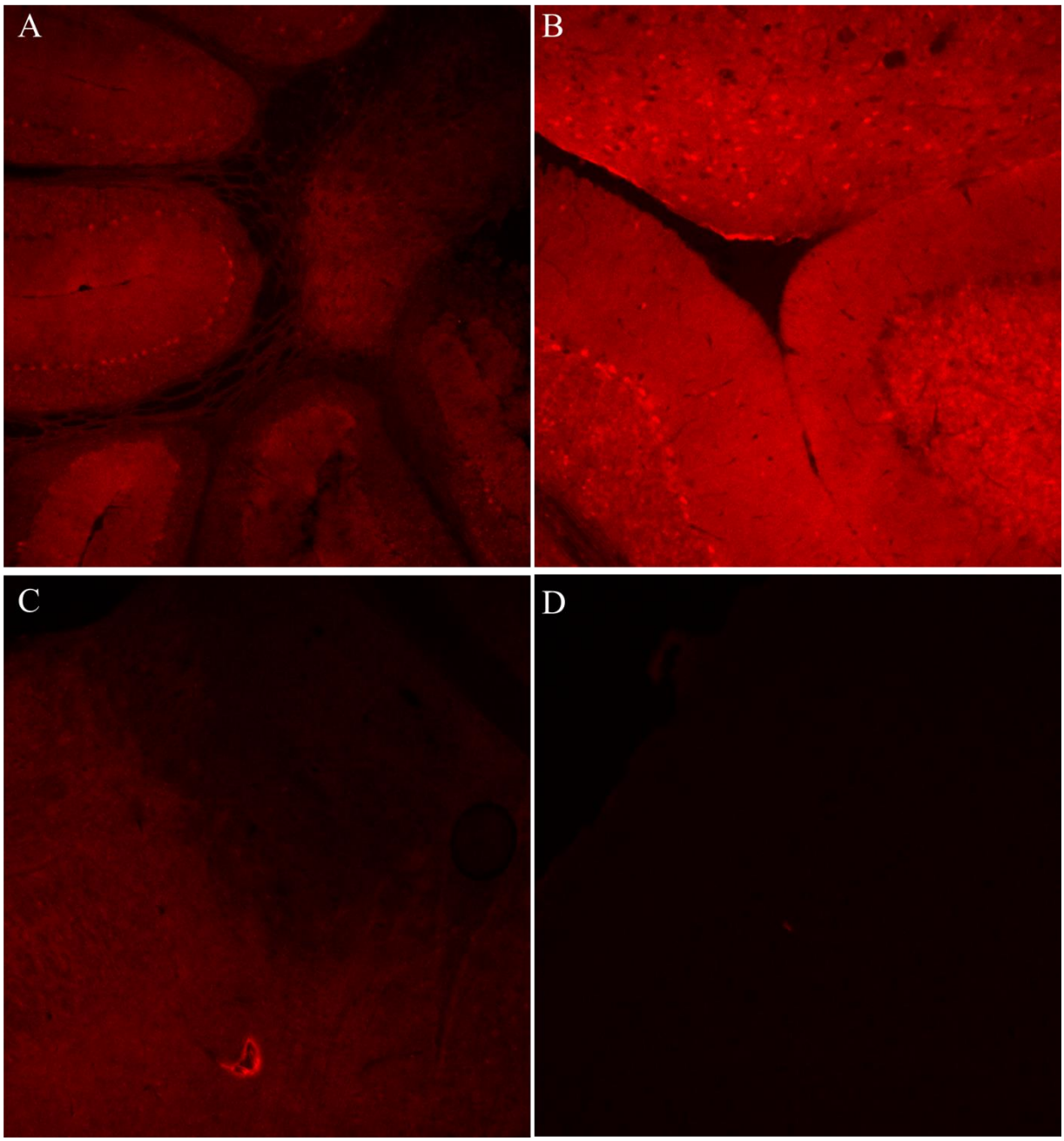

Figure 2.1 EN-1 Cre driven recombination in the mouse brain. TdTomato reporter shows recombination in CKO mice. (A) Cerebellum, (B) Cerebellum and midbrain at 4th ventricle, (C) Midbrain transition to thalamus, and (D) Cortex. Note the loss of recombination in (C) and (D).

Gene	Group	Chow – 7 weeks			Chow – 16 weeks		
		CKO	WT	CKO/WT	CKO	WT	CKO/WT
FtL	M	191.97±12	146.59±13	***1.31****	145.68±8.7	140.62±8.7	1.04
	F	166.98±15	145.17±13	1.15	126.19±8.7	107.19±8.7	1.18
	All	179.48±9.6	145.88±9.3	***1.23****	135.94±6.1	123.91±6.1	1.10
FtH	M	812.85±58	517.59±65	***1.57****	677.57±46	577.82±46	1.17
	F	668.55±75	457.95±65	1.46	559.83±46	522.71±46	1.07
	All	740.7±48	487.77±46	***1.52****	618.7±33	550.26±33	1.12
Dmt1	M	4.38±0.3	4.14±0.4	1.06	3.34±0.2	3.66±0.2	0.91
	F	3.97±0.4	3.98±0.4	1.00	2.57±0.2	2.75±0.2	0.93
	All	4.18±0.3	4.06±0.3	1.03	2.95±0.1	3.21±0.1	0.92
Tfr1	M	50.64±4.0	32.37±4.5	***1.56****	28.84±2.3	22.70±2.3	1.27
	F	35.50±5.2	29.26±4.5	1.21	22.70±2.3	13.80±2.3	0.91
	All	43.07±3.3	30.81±3.2	***1.40****	21.32±1.6	18.96±1.6	1.12
Irp2	M	57.40±4.2	40.79±4.7	***1.41****	44.21±2.5	36.09±2.5	***1.23****
	F	47.18±5.4	37.72±4.7	1.25	26.26±2.5	22.83±2.5	1.15
	All	52.29±3.4	39.26±3.3	***1.33****	35.24±1.7	29.46±1.7	***1.20****
TF	M	118.88±8.1	58.18±9.1	***2.04*****	107.7±6.5	92.50±6.5	1.16
	F	97.86±10.5	65.59±9.1	***1.49****	69.42±6.5	60.24±6.5	1.15
	All	108.37±6.6	61.83±6.4	***1.75*****	88.56±4.6	76.37±4.6	1.16
Fxn	M	4.67±0.3	3.44±0.3	***1.36****	2.29±0.3	2.21±0.3	1.04
	F	3.91±0.4	3.50±0.3	1.12	1.54±0.3	1.36±0.3	1.13
	All	4.29±0.3	3.47±0.2	***1.24****	1.92±0.2	1.78±0.2	1.08

Gene	Group	Chow – 7 weeks			Chow – 16 weeks		
		CKO	WT	CKO/WT	CKO	WT	CKO/WT
Hmox	M	1.98±0.1	1.34±0.1	***1.48*****	1.24±0.1	1.00±0.1	1.24
	F	1.60±0.1	1.20±0.1	***1.33****	0.86±0.1	0.74±0.1	1.16
	All	1.79±0.1	1.27±0.1	***1.41*****	1.05±0.1	0.87±0.1	1.20
APP	M	396.03±33	257.95±37	***1.54****	173.6±16	153.9±16	1.13
	F	283.46±42	244.36±37	1.16	91.6±16	74.9±16	1.22
	All	339.74±27	251.15±26	***1.35****	132.6±11	114.4±11	1.16
Fpn1	M	3.73±0.3	1.97±0.3	***1.89*****	1.29±0.2	1.35±0.2	0.96
	F	2.63±0.4	2.04±0.3	1.29	1.20±0.2	1.14±0.2	1.05
	All	3.18±0.2	2.01±0.2	***1.59*****	1.24±0.1	1.25±0.1	1.00
Mt2	M	201.14±66	272.01±74	***1.84****	333.1±43	187.6±43	***1.78****
	F	383.69±86	352.24±74	1.09	138.9±43	151.7±43	0.92
	All	442.42±54	312.12±52	1.42	236.0±30	169.7±30	1.39
Mt3	M	582.28±61	353.02±68	***1.65****	336.1±39	278.11±39	1.21
	F	487.36±79	272.64±68	1.79	188.43±39	159.23±39	1.18
	All	534.82±50	312.83±48	***1.71*****	262.67±27	218.67±27	1.20
MitoFn2	M	8.01±0.5	6.34±0.5	***1.26****	6.39±0.6	6.13±0.6	1.04
	F	7.31±0.6	6.50±0.5	1.12	4.58±0.6	4.33±0.6	1.06
	All	7.66±0.4	6.42±0.4	***1.19****	5.49±0.4	5.23±0.4	1.05
Cp-GPI	M	5.75±0.4	3.55±0.5	***1.62*****	3.33±0.4	2.46±0.4	1.35
	F	3.46±0.5	2.12±0.5	1.63	1.53±0.4	1.46±0.4	1.05
	All	4.61±0.3	2.84±0.3	***1.62*****	2.43±0.3	1.96±0.3	1.24

Table 2.1 Transcript levels of genes involved in iron metabolism and homeostatic maintenance in the cerebellum of CKO and WT mice. Transcript levels were determined by defining the internal reference, 18S rRNA, as 10^6. APP, amyloid precursor protein; Cp-GPI, GPI linked cerruloplasmin; Dmt1, divalent metal transporter 1; Fpn1, ferroportin; FtH, ferritin heavy chain; FtL, ferritin light chain; Fxn, frataxin; Hmox, heme oxygenase; Irp2, iron regulatory protein 2, MitoFn2, mitoferrin 2; MT2, metallothionein 2; MT3, metallothionein 3; TF, transferrin; TfR1, Transferrin receptor 1. Values are presented as mean +/- SEM (standard error of mean). n=8 WT (4 Male, 4 Female) and n=8 CKO (5 Male, 3 Female) at 7 weeks. n=8 WT (4 Male, 4 Female) and n=8 (4 Male, 4 Female) at 16 weeks. *, $p<0.05$; **, $p<0.01$; ***, $p<0.005$.

Gene	Group	Chow – 7 weeks			Low Fe – 7 weeks		
		CKO	WT	CKO/WT	CKO	WT	CKO/WT
FtL	M	192±12	147±13	***1.31****	89.9±10.7	50.9±11.9	***1.77****
	F	167±15	145±13	1.15	48.8±13.8	93.7±11.9	***0.52****
	All	180±10	146±9	***1.23****	69.4±8.7	72.3±8.4	0.95
FtH	M	813±58	518±65	***1.57****	439±54	282±60	1.55
	F	669±75	458±65	1.46	247±69	411±60	0.60
	All	741±48	488±46	***1.52****	343±43	347±42	0.99
Dmt1	M	4.38±0.30	4.14±0.40	1.06	3.12±0.40	2.27±0.40	1.37
	F	3.97±0.40	3.98±0.40	1.00	2.36±0.50	3.05±0.40	0.77
	All	4.18±0.30	4.06±0.30	1.03	2.74±0.30	2.66±0.30	1.03
Tfr1	M	50.6±4.0	32.4±4.5	***1.56****	24.2±2.8	11.8±3.2	***2.04****
	F	35.5±5.2	29.3±4.5	1.21	10.5±3.7	26.4±3.2	***0.39****
	All	43.1±3.3	30.8±3.2	***1.40****	17.3±2.3	19.1±2.3	0.91
TF	M	118.9±8.1	58.2±9.1	***2.04****	79.0±8.5	29.4±9.5	***2.68****
	F	97.9±10.5	65.6±9.1	***1.49****	30.0±11.0	53.9±9.5	0.72
	All	108.4±6.6	61.8±6.4	***1.75****	59.0±6.9	41.6±6.7	1.41
Fxn	M	4.67±0.30	3.44±0.30	***1.36****	2.61±0.40	1.21±0.40	***2.16****
	F	3.91±0.40	3.50±0.30	1.12	0.94±0.50	2.61±0.40	***0.36****
	All	4.29±0.30	3.47±0.20	***1.24****	1.77±0.30	1.91±0.30	0.92

Gene	Group	Chow – 7 weeks			Low Fe – 7 weeks		
		CKO	WT	CKO/WT	CKO	WT	CKO/WT
APP	M	396±33	258±37	***1.54****	152±20	68±22	***2.24****
	F	284±42	244±37	1.16	55±25	133±22	***0.41****
	All	340±27	251±26	***1.35****	103±16	100±15	1.03
Fpn1	M	3.73±0.30	1.97±0.30	***1.89*****	1.30±0.16	0.74±0.18	***1.74****
	F	2.63±0.40	2.04±0.30	1.29	0.52±0.21	1.13±0.18	***0.46****
	All	3.18±0.20	2.01±0.20	***1.59*****	0.91±0.13	0.94±0.13	0.96
Mt2	M	201±66	272±74	***1.84****	133±19	119±21	1.12
	F	384±86	352±74	1.09	89±24	157±21	0.57
	All	442±54	312±52	1.42	111±15	138±15	0.81
Mt3	M	582±61	353±68	***1.65****	224±30	125±34	***1.79****
	F	487±79	273±68	1.79	105±39	178±34	0.59
	All	535±50	313±48	***1.71*****	165±25	151±24	1.09
MitoFn2	M	8.01±0.50	6.34±0.50	***1.26****	4.78±0.51	2.90±0.57	***1.65****
	F	7.31±0.60	6.50±0.50	1.12	2.63±0.66	3.74±0.57	0.70
	All	7.66±0.40	6.42±0.40	***1.19****	3.71±0.42	3.32±0.41	1.12
Cp-GPI	M	5.75±0.40	3.55±0.50	***1.62*****	1.64±0.30	0.73±0.33	***2.26****
	F	3.46±0.50	2.12±0.50	1.63	0.68±0.38	1.53±0.33	0.44
	All	4.61±0.30	2.84±0.30	***1.62*****	1.16±0.24	1.13±0.23	1.03

Table 2.2 Transcript levels of genes involved in iron metabolism and homeostatic maintenance in the cerebellum of 7 week old CKO and WT mice fed either a chow or low-iron diet. Transcript levels were determined by defining the internal reference, 18S rRNA, as 10^6. APP, amyloid precursor protein; Cp-GPI, GPI linked cerruloplasmin; Dmt1, divalent metal transporter 1; Fpn1, ferroportin; FtH, ferritin heavy chain; FtL, ferritin light chain; Fxn, frataxin; MitoFn2, mitoferrin 2; MT2, metallothionein 2; MT3, metallothionein 3; TF, transferrin; Tfr1, Transferrin receptor 1. Values are presented as mean +/- SEM (standard error of mean). n=8 WT (4 Male, 4 Female) and n=8 CKO (5 Male, 3 Female) at 7 weeks for chow and low-iron diet treated. *, $p<0.05$; **, $p<0.01$; ***, $p<0.005$.

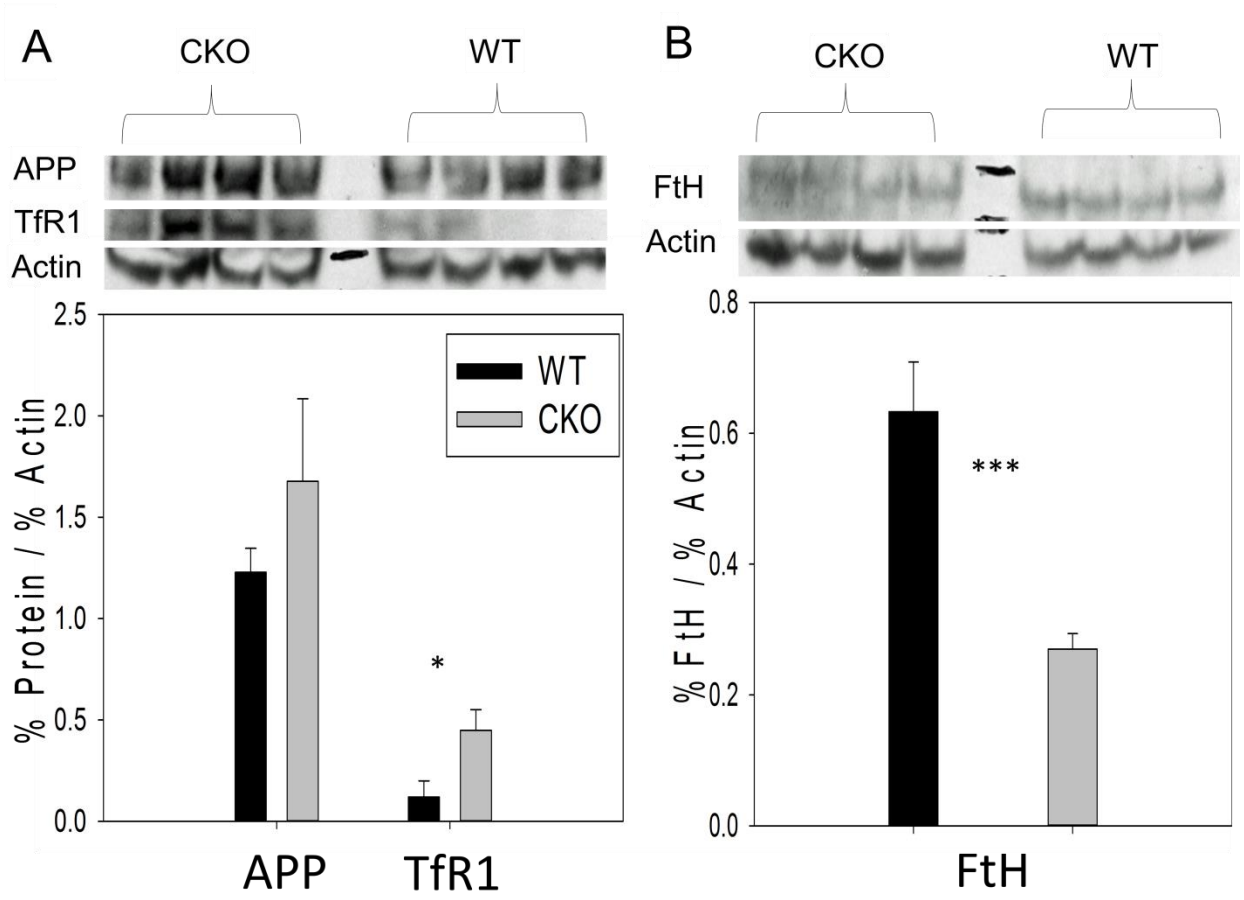

Figure 2.2 Iron-processing-relevant protein levels in the cerebellum of CKO and WT mice. Specific protein levels were measured using western blot analysis of whole protein extracted from mouse cerebellum at 7 weeks of age. (A) Amyloid precursor protein (APP) was unchanged in CKO mice, but levels of the iron import protein transferrin receptor (TfR1) were significantly elevated. (B) Iron storage protein ferritin heavy chain (FtH) was significantly reduced in CKO mice, suggesting an iron-deficient status. Values are presented as mean +/- SEM (standard error of mean). n=4:4 (CKO:WT). *, $p<0.05$; ***, $p<0.005$.

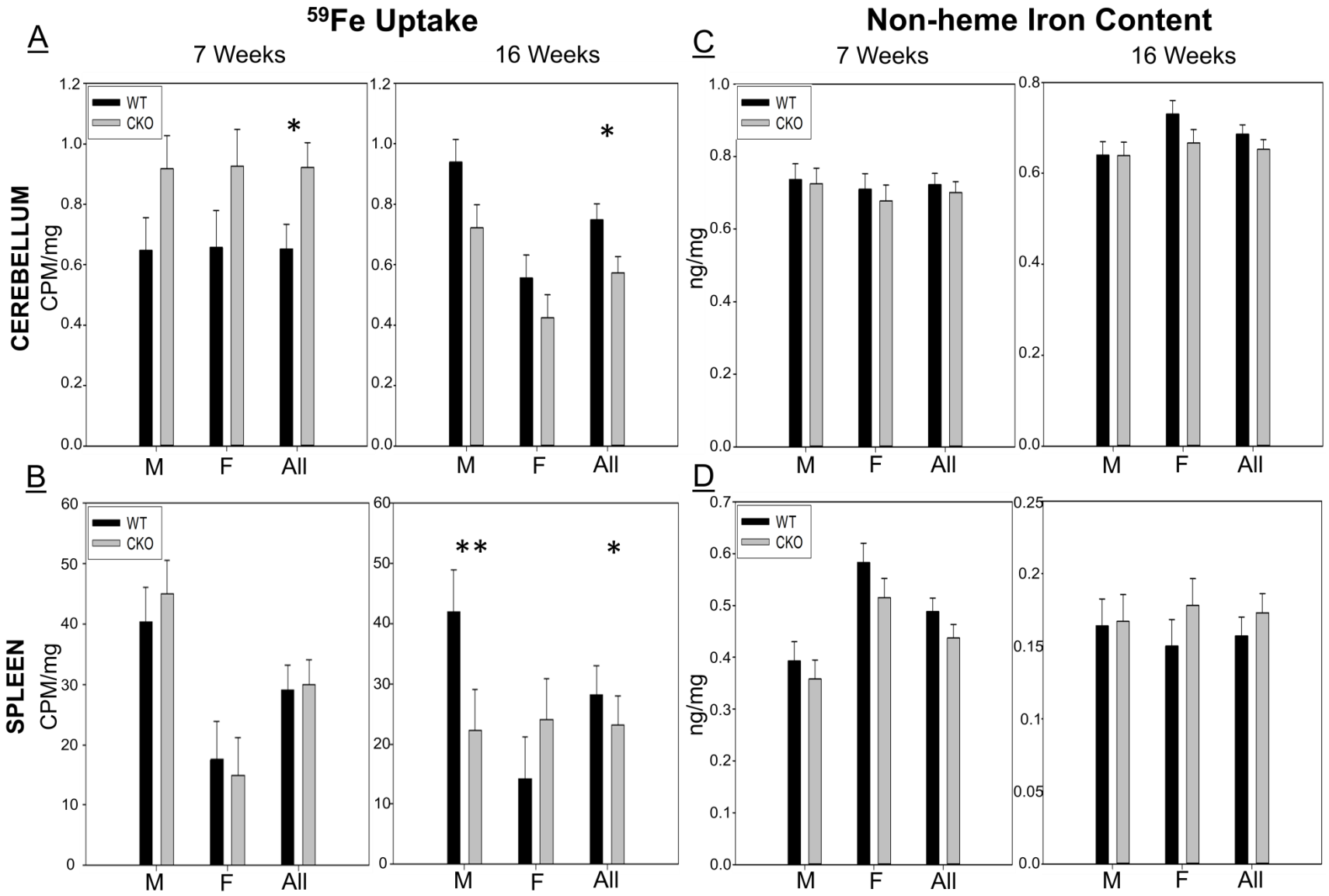
59Fe Uptake
Non-heme Iron Content
A
B
C
D
7 Weeks
16 Weeks
CEREBELLUM
SPLEEN
CPM/mg
ng/mg
WT
CKO
M
F
All
*
**

Figure 2.3 Altered iron uptake in CKO mice. ^{59}Fe pulse feeding assay revealed (A) significantly elevated ^{59}Fe uptake in the cerebellum of 7 week old CKO mice and significantly decreased uptake by 16 weeks of age. (B) Serving as a control, at 7 weeks the spleen showed no change in iron uptake. 16 week male CKO mice acquired significantly less ^{59}Fe. Non-heme iron content assays of the (C) cerebellum and (D) spleen from 7 and 16 week old CKO and WT mice showed no changes in non-heme iron content. Values are presented as mean +/- SEM (standard error of mean). 7 week; n=10 CKO (5 Male, 5 Female), n=10 WT (5 Male, 5 Female). 16 week; n=10 CKO (5 Male, 5 Female), n=10 WT (5 Male, 5 Female). *, $p<0.05$; **, $p<0.01$.

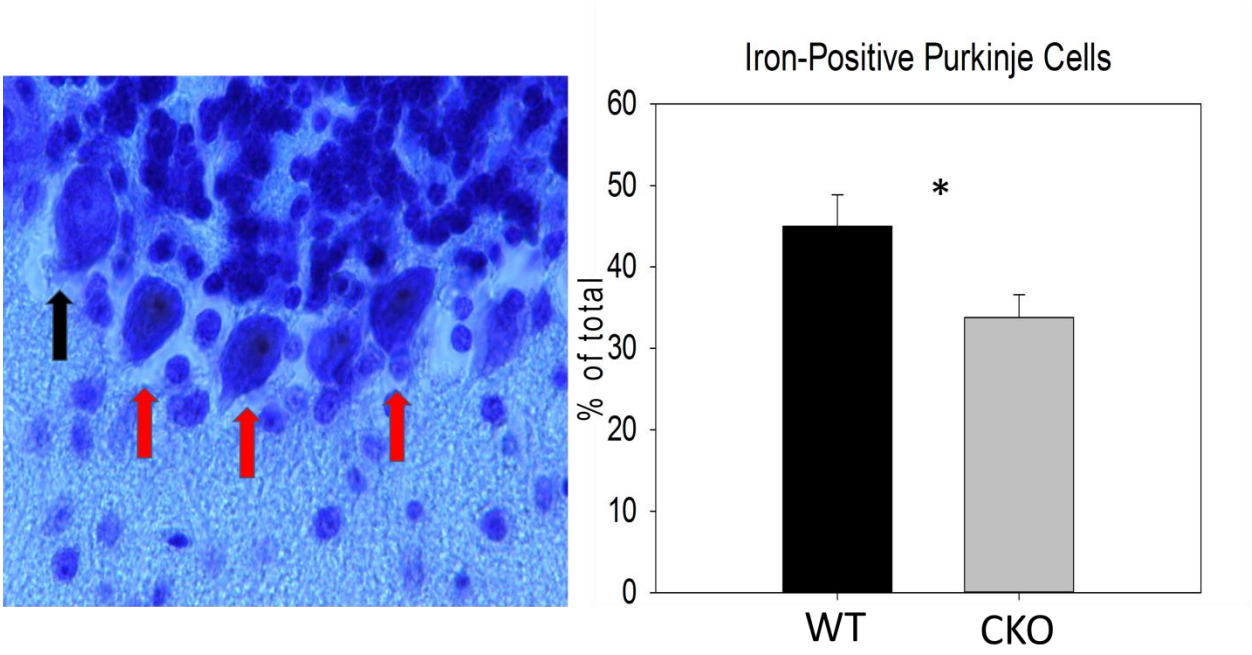

Figure 2.4 Reduced iron-positive Purkinje cells in male CKO mice. (Left) Perls iron staining in the CKO cerebellum with Nissl counterstaining. Note the positive staining (red arrows) and negative staining (black arrow) of purkinje cells. (Right) CKO mice have a reduced number of iron-positive Purkinje cells as a percentage of total Purkinje cells counted. Values are presented as mean +/- SEM (standard error of mean). Male mouse n=8 (4 CKO, 4 WT), sections used for quantification n=22 (10 CKO, 12 WT). *, $p<0.05$.

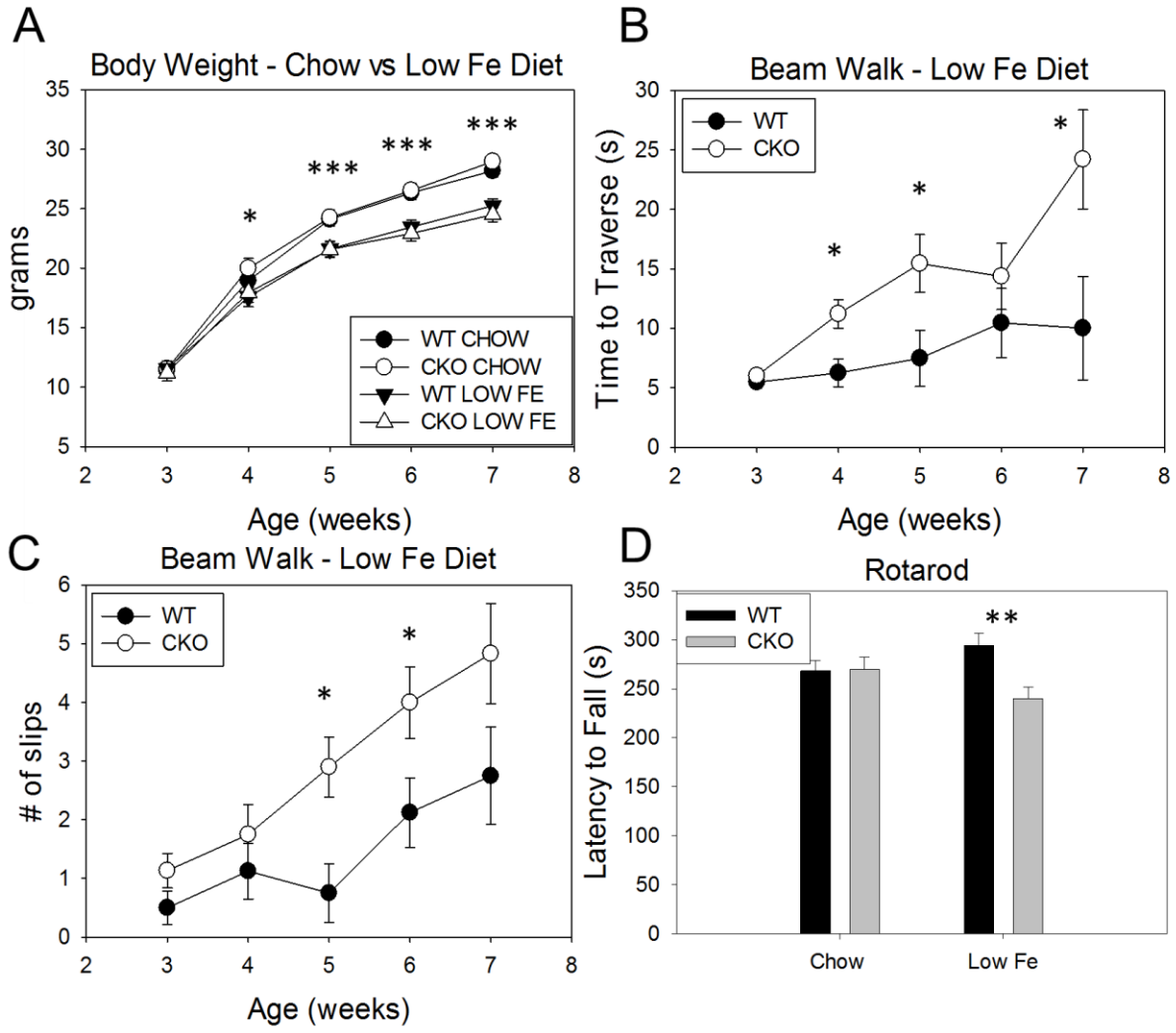

Figure 2.5 Diet-dependent effects of NCB5OR deficiency during a complex motor task. (A) There were no genotypic differences in weight within chow or low-iron-diet treated sets, however low-iron-diet treated animals weighed significantly less than the chow fed controls. CKO mice on a low iron diet challenged with a complex motor task (elevated beam walk) showed (B) increased beam traversal time accompanied by (C) increased slips/errors during traversal. Dietary iron deficiency also resulted in (D) a decreased latency to fall on an accelerating Rota-rod task. Values are presented as mean +/- SEM (standard error of mean). Chow; n=8:10 (CKO:WT). Low iron; n=8:8 (CKO:WT). *, $p<0.05$; **, $p<0.01$; ***, $p<0.005$.

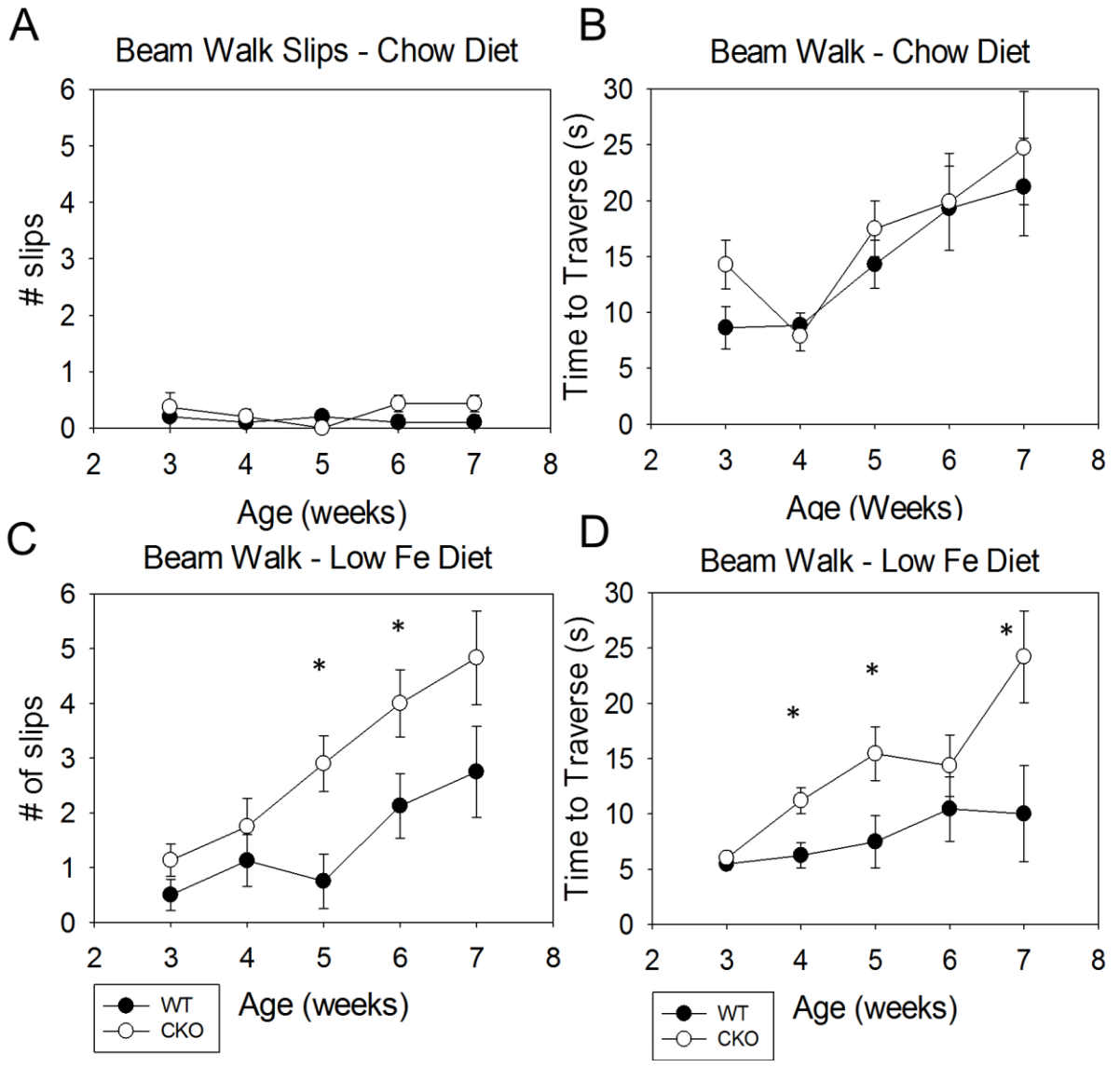

Figure 2.6 Chow and low-iron diet effects on beam walk task. On a chow diet, no difference between WT and CKO mice was seen in (A) the number of slips/errors or (B) time to traverse. However, CKO mice fed a low-iron diet showed (C) an increased number of slips/errors and (D) a significant difference in beam traversal time when compared to WT controls fed a low-iron diet. Values are presented as mean +/- SEM (standard error of mean). Chow; n=8:10 (CKO:WT). Low iron; n=8:8 (CKO:WT). *, $p<0.05$

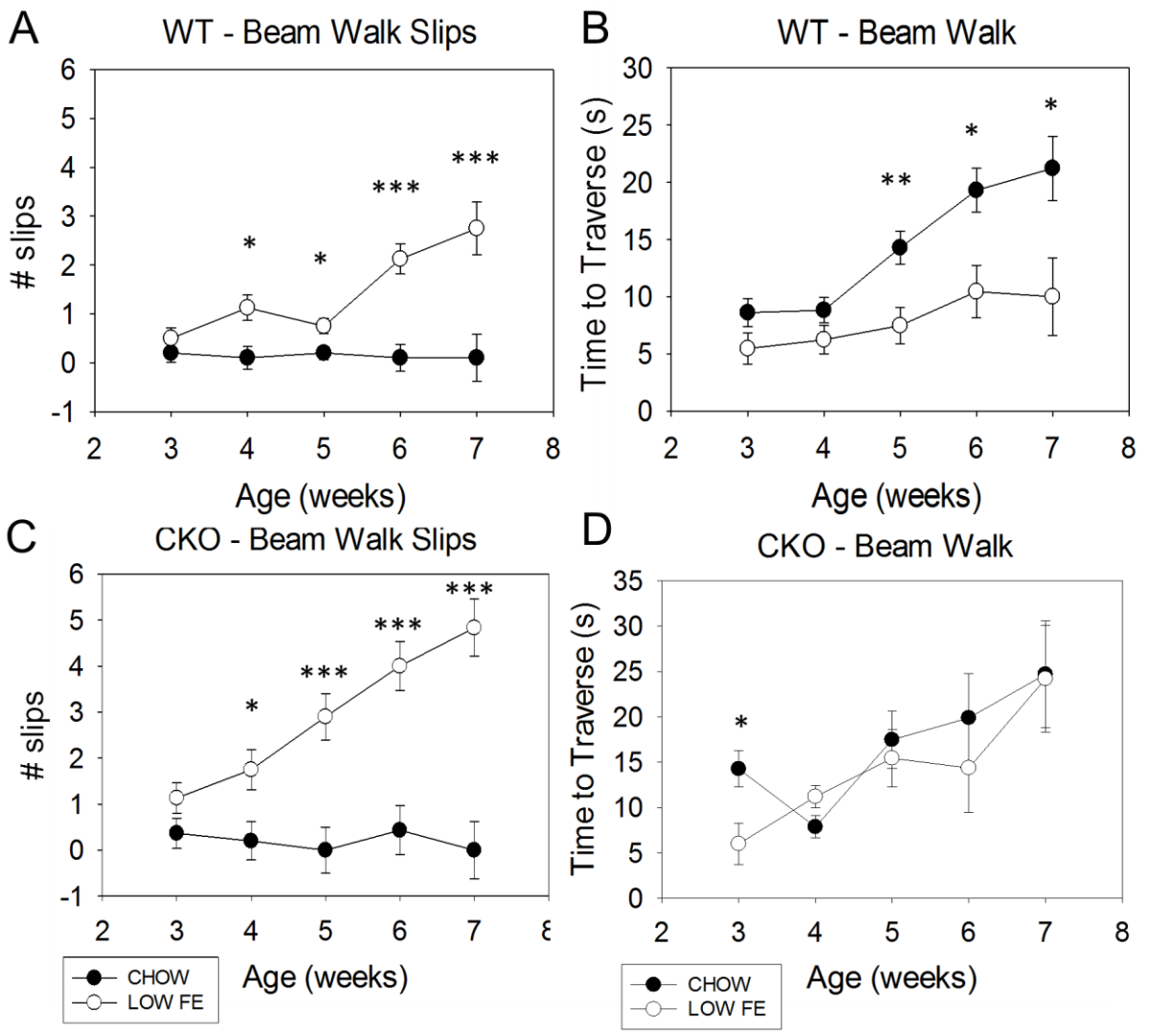

Figure 2.7 Comparison of dietary effects on genotype. (A) WT mice and (B) CKO mice made significantly more slips/errors on the beam walk as a result of dietary iron deficiency. However, dietary iron deficiency only affected the time to traverse in (C) WT mice, which showed a hyperactive response to the treatment. (D) CKO mice did not display the hyperactive response to the low-iron diet, suggesting resistance to the low iron diet impact. Values are presented as means +/- SEM (standard error of mean). Chow; n=8:10 (CKO:WT). Low iron; n=8:8 (CKO:WT). *, $p<0.05$; **, $p<0.01$; ***, $p<0.005$

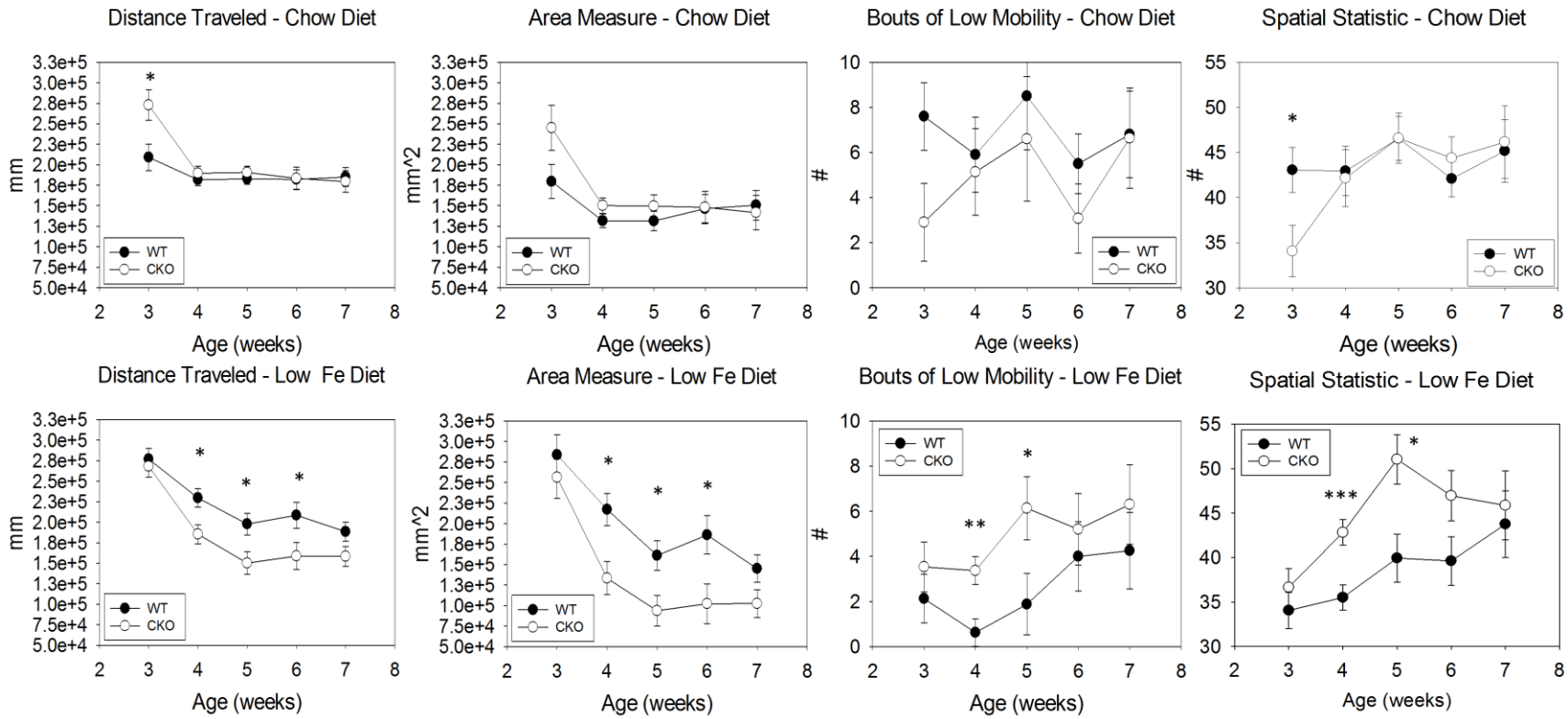
Distance Traveled - Chow Diet
Area Measure - Chow Diet
Bouts of Low Mobility - Chow Diet
Spatial Statistic - Chow Diet
Distance Traveled - Low Fe Diet
Area Measure - Low Fe Diet
Bouts of Low Mobility - Low Fe Diet
Spatial Statistic - Low Fe Diet
mm
mm^2
#
Age (weeks)
WT
CKO
*
**
***

Figure 2.8 Diet-dependent effects of NCB5OR deficiency on locomotion. Distance traveled, area measure, bouts of low mobility, and spatial statistic for mice fed a (A-D) chow diet or (E-H) low-iron diet. CKO mice on an iron-deficient diet had decreased total locomotor activity as indicated by (E) significant decreases in distance traveled and (F) area measure. CKO mice also exhibit reduced exploratory activity resulting in (G) high spatial statistics and (H) an increased number of low mobility bouts compared to WT. Spatial statistic scores: 100 = All time spent in one place, 1 = time spent evenly distributed across force plate. Bout of low mobility: 1 bout of low mobility = no change in distance or area (no movement) within a 10 second frame. Values are presented as means +/- SEM (standard error of mean). Chow; n=8:10 (CKO:WT). Low iron; n=8:8 (CKO:WT). *, $p<0.05$; **, $p<0.01$; ***, $p<0.005$.

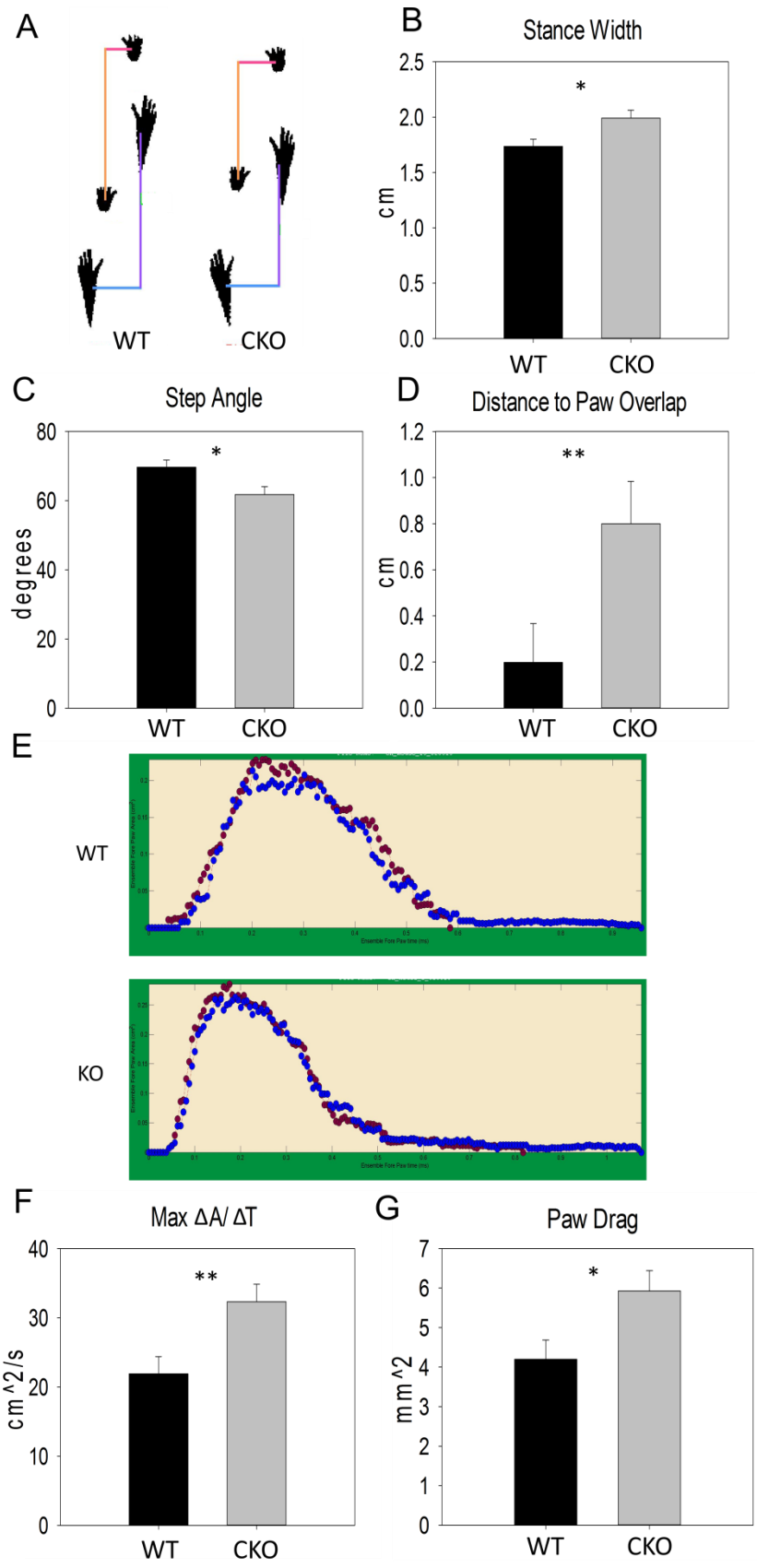
A
WT
CKO
B
Stance Width
2.5
2.0
1.5
1.0
0.5
0.0
cm
*
WT
CKO
C
Step Angle
80
60
40
20
0
degrees
*
WT
CKO
D
Distance to Paw Overlap
1.2
1.0
0.8
0.6
0.4
0.2
0.0
cm
**
WT
CKO
E
WT
KO
F
Max ΔA/ ΔT
40
30
20
10
0
cm^2/s
**
WT
CKO
G
Paw Drag
7
6
5
4
3
2
1
0
mm^2
*
WT
CKO

Figure 2.9 Diet-independent effects of NCB5OR deficiency on gait. (A) Posture plots of WT and CKO mice at 7 weeks. DigiGait analysis at 7 weeks revealed that CKO mice had (B) a wider stance width, (C) decreased step angle, and (D) a greater distance to paw overlap compared to WT mice. (E) A visual representation of change in paw area over time. CKO mice show significant changes indicative of hind limb paresis with increased (F) max $\Delta A/\Delta T$ and (G) paw drag. Max $\Delta A/\Delta T$ is the rate of change of paw area during paw placement and full stance. Paw drag is the paw area under the curve from full stance to liftoff. CKO mice were quick to load their paw and spent more time initiating the liftoff stage (flopping and dragging their paws). Values are presented as mean +/- SEM (standard error of mean). n=16:18 (CKO:WT) *, $p<0.05$; **, $p<0.01$

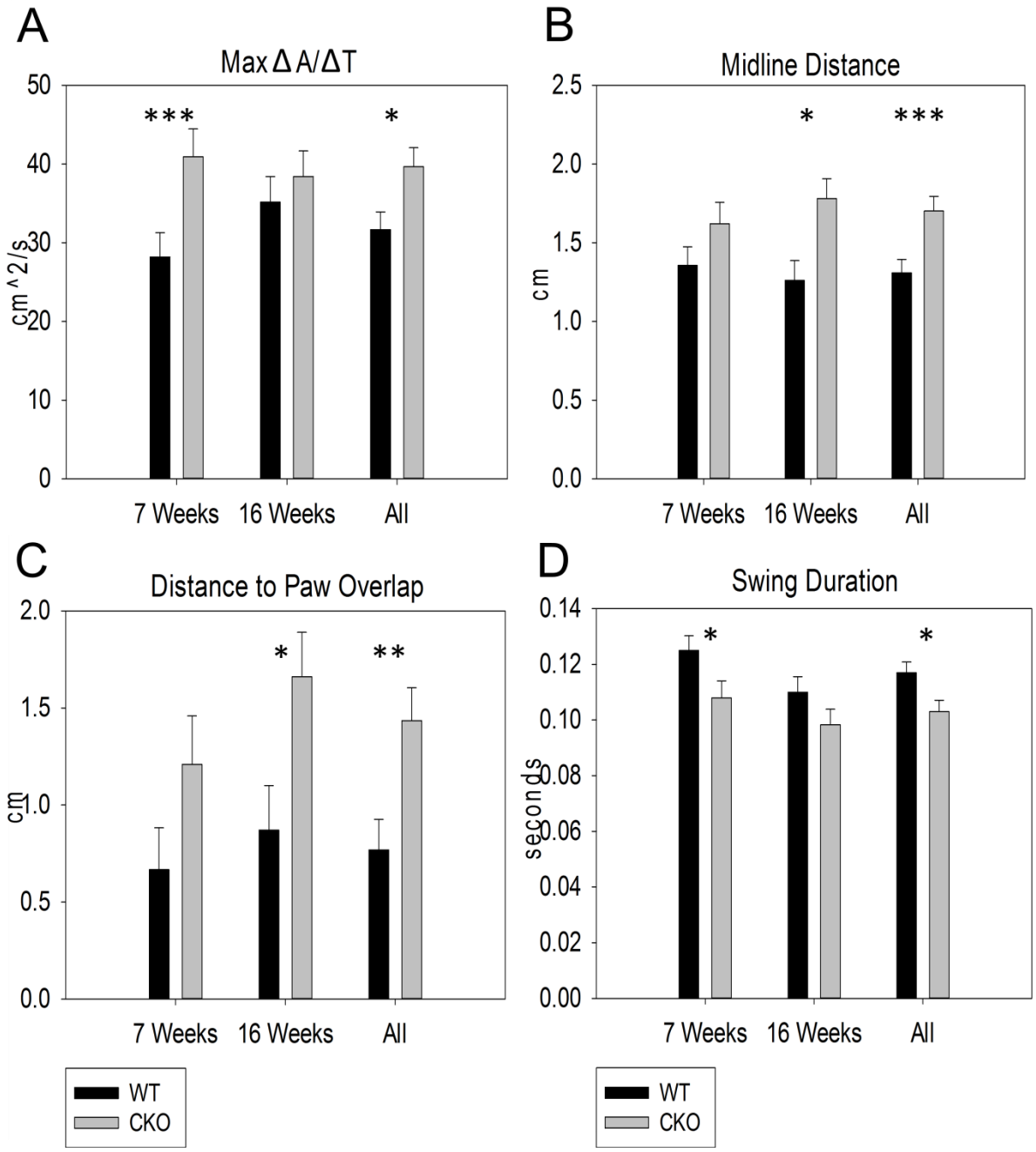

Figure 2.10 Age comparison of hind paw gait metrics in chow-fed CKO mice. (A) Similar trends in ΔA/ΔT were seen between 7 and 16 week old CKO mice. (B) Hind paws of CKO mice have an increased distance to the midline (transverse) regardless of age. (C) A greater distance to fore- paw-hind-paw overlap in 7 and 16 week old CKO mice. (D) CKO mice have a decreased swing duration at both 7 and 16 weeks of age. Values are presented as means +/- SEM (standard

error of mean). 7 week; n=8:10 (CKO:WT). 16 week; n=10:10 (CKO:WT). *, $p<0.05$; **, $p<0.01$; ***, $p<0.005$

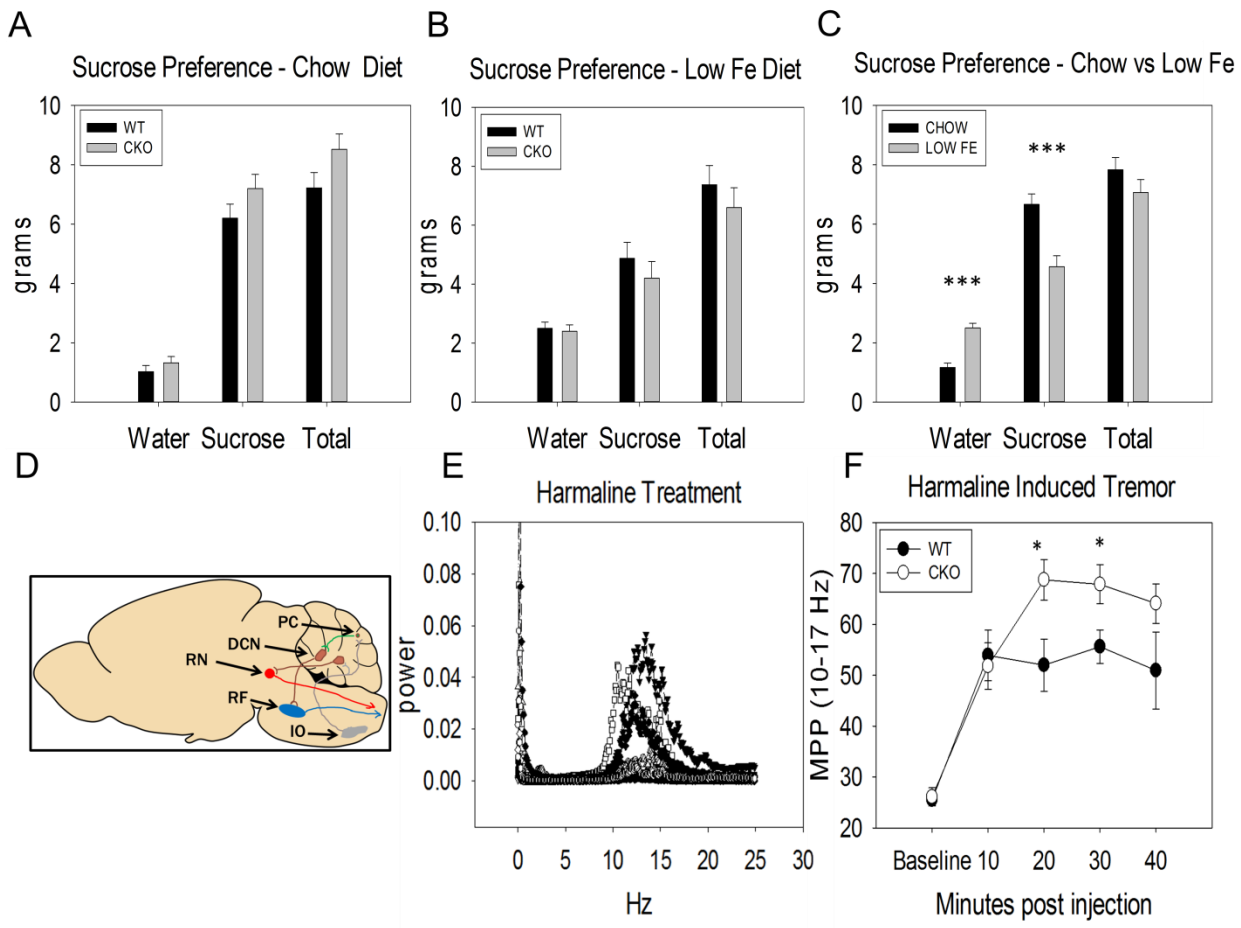

Figure 2.11 Intact reward response and increased peak harmaline tremor in CKO mice. Sucrose preference testing for CKO and WT mice fed a (A) chow diet and (B) low-iron diet. (C) A reduction in sucrose preference is seen when comparing the effects of a low-iron diet on all mice, suggesting that generalized iron deficiency significantly alters reward behavior in mice. (D) Treatment with subcutaneous harmaline results in rhythmic burst firing in the inferior olive and subsequent activation of rubrospinal and reticulospinal tracts via cerebellar efferents, generating a high frequency tremor. (E) Actimeter signals show a power spike in the 10-17 Hz range, indicative of a high frequency tremor. (F) CKO and WT mice had comparable motion power percentages (MPP) in the 10-17 Hz range during baseline and harmaline tremor onset (10 minutes post injection). However, by 20 and 30 minutes post injection CKO mice had

significantly elevated responses to harmaline-induced tremor over WT. Values are presented as mean +/- SEM (standard error of mean). DCN; deep cerebellar nuclei. IO; inferior olive. PC; Purkinje cell. RF; reticular formation. RN; red nucleus. For figures A-C: Chow; n=8:10 (CKO:WT). Low iron; n= 8:8 (CKO:WT). For figure F: n=10:10 (CKO:WT). *, $p<0.05$; ***, $p<0.005$. MPP = [(10 – 17 Hz) / (0 – 25 Hz)] x 100

CHAPTER 3

NCB5OR DEFICIENCY IN THE CEREBELLUM AND MIDBRAIN AFFECTS FASTED FEEDING BEHAVIOR, THIRST RESPONSE, AND VOLUNTARY EXERCISE IN MICE

3.1 ABSTRACT

Cytosolic NADH cytochrome b5 oxidoreductase (Ncb5or) is ubiquitously expressed in animal tissues. We have previously reported that global ablation of NCB5OR in mice results in early-onset lean diabetes with decreased serum leptin levels and increased metabolic and feeding activities. The conditional deletion of NCB5OR in the mouse cerebellum and midbrain (CKO mice) results in local iron dyshomeostasis and altered locomotor activity. It has been established that lesion to or removal of the cerebellum leads to changes in nutrient organization, visceral response, feeding behavior, and body weight, likely due to alterations in cerebellar-hypothalamic circuitry. This study assessed whether loss of NCB5OR in the cerebellum and midbrain altered feeding or metabolic activity and had an effect on serum T3, cortisol, prolactin, and leptin levels. Metabolic cage data revealed that 16-week-old male CKO mice had elevated respiratory quotients and decreased respiratory water expulsion, decreased voluntary exercise, and altered feeding and drinking behavior compared to wild-type littermate controls. Most notably, male and female CKO mice displayed over and under-consumption of food during refeeding after an overnight fast, respectively. Echo MRI revealed normal body composition but decreased total water content and hydration ratios in CKO mice. Serum leptin levels were significantly elevated in male CKO mice while prolactin, T3, and cortisol levels remain unchanged relative to WT controls. Taken together, these findings suggest potential alterations and dysfunction in cerebellar-hypothalamic circuitry as a result of NCB5OR deficiency. Further investigation is underway to elucidate the nature of changes resulting from NCB5OR deficiency in the cerebellum and midbrain.

3.2 INTRODUCTION

Metabolism arguably lies at the core of cellular function, with many pathways contributing to its regulation and virtually all pathways reliant upon sufficient energy production and availability. Thus changes in pathways influencing metabolism have the potential to severely impact a cell's vitality, function, and survival. Neurodegenerative diseases and diabetes mellitus are two clinically distinct disease classes that share common defects in metabolic influence (for review, see (Stroh et al., 2014)). Changes in bioenergetic homeostasis, influenced largely by mitochondrial and iron related pathways, lie at the nexus of these conditions.

NADH-Cytochrome-b5-oxidoreductase (NCB5OR) is a ubiquitously expressed, soluble, heme containing reductase associated with the endoplasmic reticulum (H. Zhu et al., 2004a; H. Zhu et al., 1999). Recently, naturally occurring non-synonymous mutations that lead to enhanced proteasomal degradation of NCB5OR have been identified in the human population (Kalman et al., 2013). To date, an exact function and pathway for NCB5OR has yet to be determined, however it is a potent reductase of iron and heme proteins (e.g. cytochrome c) *in vitro* and evidence suggests it plays a role in the maintenance of iron homeostasis and pathways critical to proper metabolic and mitochondrial function (H. Zhu et al., 2004a; H. Zhu, Wang, W.F., Wang H.P., Xu, M., E, L., and Swerdlow, R.H., 2013). Mice globally deficient for NCB5OR experience early-onset diabetes, growth retardation, decreased serum leptin levels, and increased food consumption despite maintaining a significantly reduced body weight relative to WT littermates (Y. Guo et al., 2012; Larade et al., 2008; Xie et al., 2004; Xu et al., 2011). We recently reported altered iron homeostasis, decreased iron-positive Purkinje cells, locomotor activity, and an increased response to harmaline-induced tremor in mice lacking NCB5OR in the cerebellum and the midbrain (CKO mice) (see footnote 1).

There exists a bidirectional network between the cerebellum and the hypothalamus (the cerebellar-hypothalamic circuit) that is known to play a role in circadian food anticipatory behavior, glucose sensing, satiety, metabolism, nutrient organization, thirst response, and body weight ((Mendoza, Pevet, Felder-Schmittbuhl, Bailly, & Challet, 2010), for review see (J. N. Zhu & Wang, 2008)). Therefore, we hypothesized that selective loss of NCB5OR in neural tissue would alter systemic metabolism, feeding/drinking behavior, and body weight. Through metabolic cage and biochemical analyses, we observed that CKO mice display significant changes in fasted feeding and *ad libitum* drinking behavior, fluctuation of body weight in response to overnight fasting, metabolic substrate utilization, and voluntary exercise with increases in serum leptin levels. These findings suggest potential alterations and dysfunction in cerebellar-hypothalamic circuitry as a result of NCB5OR deficiency in cerebellum and midbrain.

3.3 RESULTS

3.3.1 CKO mice had normal body weight and composition but less total and free water.

Body weights were collected and averaged for light and dark cycles during individual housing in the metabolic cage system. There were no discernable differences in body weight between CKO (light: 28.93±1.04 g, dark: 29.04±1.03 g) and WT mice (light: 31.62±1.04 g, dark: 31.27±1.03 g) in either the light or dark cycles. After metabolic cage experiments were concluded, body composition was assessed by measuring lean and fat mass via echo MRI. There were no differences in lean or fat mass between CKO (lean: 24.13±0.81 g, fat: 2.65±0.37 g) and WT mice (lean: 25.77±0.77 g, fat: 2.87±0.32 g), but CKO mice had significantly less total water (Figure 3.1A) and no changes in free water (Figure 3.1B) relative to WT controls. Hydration ratios calculated from Echo MRI data revealed that CKO mice had significantly reduced hydration ratios compared to WT controls (Figure 3.1C). However, these results were driven by

significantly reduced hydration ratios in male CKO mice while female CKO hydration ratios remained unchanged relative to WT controls.

3.3.2 Male CKO mice had decreased voluntary exercise and average energy expenditure.

Mice were allowed access to a running wheel for the entirety of their housing in the metabolic cage system. Both CKO and WT mice predictably traveled significantly greater distances on the running wheel during dark cycles compared to light cycles, indicating no strain differences in diurnal exercise trends (Figure 3.2A). However, this pattern was less clear when assessing strictly pedestrian locomotion (Figure 3.2B). While there were no apparent changes in diurnal trends, CKO mice exercised significantly less during the dark cycle compared to WT controls, with male CKO mice specifically showing a significant difference (Figure 3.2E). This change was not observed in pedestrian locomotion during the light or dark cycle or in exercise during the light cycle (Figures 3.2C, D, F). Note that the decreases in vO_2 and total energy expenditure in male CKO mice were observed only during the dark cycle when male CKO mice were also observed to have participated significantly less in voluntary exercise. In addition, CKO mice did not present with abnormalities in gait symmetry (Figure 3.3A) or Rota-rod performance (Figure 3.3B), indicating no overt ataxia.

The rate of oxygen consumption (vO_2) was used as an indicator to measure metabolic rate and total energy expenditure in CKO and WT mice (Figure 3.4). Although vO_2 were unchanged between CKO and WT mice during the light cycle (Figure 3.4A, C, E), a period when there is reduced activity and wheel running, we observed a marked decrease in vO_2 and energy expenditure in male CKO mice compared to WT controls during the dark cycle (Figure 3.4B, D), a period of time when mice are more active and perform more wheel running. However, resting energy expenditure was not different between male CKO and WT mice (Figure 3.4F), suggesting

that vO_2/energy expenditure differences were due to lower activity/wheel running in the CKO mice. Pearson correlation analysis revealed strong correlations between wheel activity and energy expenditure (0.77, p=0.006) and wheel activity and vO_2 (0.79, p=0.004).

3.3.3 Male CKO mice exhibited altered metabolic substrate preference, respiratory water expulsion, and water consumption behavior.

Using indirect calorimetry we explored a number of metrics that are indicative of the metabolic state of the mice being observed. Average respiratory quotients (RQ) (Figure 3.5A) of male CKO mice were significantly elevated during both the light (Figure 3.5B, top) and dark cycles (Figure 3.5C, top), indicating a greater reliance on carbohydrate utilization compared to WT controls. Elevated resting RQ values in male CKO mice during both the light (Figure 3.5B, bottom) and dark (Figure 3.5C, bottom) cycles confirmed the conditional independence of this observation.

An increased RQ is indicative of a metabolic preference for glucose utilization. Since the brain uses glucose as its primary metabolic substrate, we asked whether the cerebellum in CKO mice was hypermetabolic, resulting in an increase in uptake and utilization of glucose. In order to test this hypothesis in a simple manner we assessed whether there were changes in glucose uptake and key mRNA transcripts associated with brain glucose uptake and metabolism in the CKO cerebellum. We did not observe increased 2-deoxyglucose (2-DoG) uptake in CKO mice relative to WT controls (Figure 3.6A). In addition, qPCR analysis confirmed mRNA transcripts for glucose transporter's, lactate dehydrogenase, insulin, and insulin receptor were not increased in CKO mice compared to WT controls (Figure 3.6B). Notably, no functional NCB5OR transcripts were detected in the cerebellum of both male and female CKO mice (Figure 3.6B).

Interestingly, male CKO mice also exhibited a lowered rate of respiratory water expulsion (vH_2O) over WT controls during both the light (Figure 3.7A) and dark (Figure 3.7D) cycles. This corresponded with a significant decrease in total water consumption (Figure 3.7E) and number of drinking bouts (Figure 3.7F) in CKO male mice during the dark cycle. It is important to note that female CKO mice maintained a normal vH_2O (Figure 3.7D) when compared to controls but had an increased number of drinking bouts during the dark cycle (Figure 3.7F). These observations are consistent with a decreased hydration state in male, not female, CKO mice (Figure 3.1C).

3.3.4 Male CKO mice exhibited changes in fasted feeding behavior.

We observed no changes in normal feeding behavior between CKO and WT control mice (Figures 3.8A-D). While there were no overt changes in *ad libitum* feeding in CKO mice, we observed differences in feeding behavior under fasted and refeeding conditions (Figure 3.9A-C). Upon resumption of *ad libitum* feeding after an overnight fast, male CKO mice gained approximately 11.5% of their fasted body weight in the 24 hours after feeding had resumed compared to the 5% gained by male WT mice. Conversely, female CKO gained 2.5% of their fasted body weight compared to the 5% gained by female WT mice. All CKO and WT mice were allowed *ad libitum* access to water at all times.

3.3.5 Male CKO mice had normal serum T3, cortisol, and prolactin levels but elevated leptin levels.

Increased weight gain during refeeding after fasting, reduced voluntary exercise, and elevated RQ with no apparent explanation led us to investigate whether male CKO mice alterations in hypothalamic-pituitary-adrenal (HPA) axis function, hypothalamic-pituitary-thyroid (HPT) axis function, or hypothalamic response to satiety cues. . Therefore, we

evaluated serum T3, cortisol, prolactin, and leptin levels. When compared to WT controls, male CKO mice had normal serum T3 (Figure 3.10A), cortisol (Figure 3.10B), and prolactin levels (Figure 3.10C), but their leptin levels were significantly increased (Figure 3.10D).

3.4 DISCUSSION AND CONCLUSIONS

The cerebellum was once thought to influence only motor coordination, planning, and sensorimotor integration. This view has since changed with a growing body of evidence indicating an integral role for the cerebellum in non-somatic and visceral functions including feeding, micturition, immune function, and emotional and higher order cognate processes (for reviews see (Dietrichs, Haines, Roste, & Roste, 1994; Haines, Dietrichs, Mihailoff, & McDonald, 1997; Hoche et al., 2015; J. N. Zhu, Yung, Kwok-Chong Chow, Chan, & Wang, 2006)). This study provides evidence that absence of a reductase, NCB5OR, in the cerebellum and midbrain of mice results in changes consistent with altered cerebellar-hypothalamic pathway function.

Previous studies revealed an increased basal metabolic rate (vO_2) and lower body weight in mice globally deficient for NCB5OR (Xu et al., 2011). In the current study, initial observation indicated that deleting NCB5OR in the cerebellum and midbrain resulted in normal body weight accompanied by a lowered vO_2 and total energy expenditure in male CKO mice. Generally, such results would indicate a lower basal metabolic rate with decreased appetite and food intake. Theoretically, this combination would balance the lowered caloric energy expenditure with a lowered caloric intake, resulting in normal body weight. However we did not observe changes in *ad libitum* feeding behavior in CKO mice compared to WT. Further investigation revealed that male CKO mice had normal resting energy expenditure and participated significantly less in voluntary exercise during those times in which we observed lowered vO_2 and energy

expenditure. Therefore we concluded that CKO mice do not have changes in basal metabolic rate or resting energy expenditure. Rather, male CKO mice have decreased locomotor activity during times in which peak activity is expected (dark cycle). This observation is consistent with our previous study detailing altered locomotor behavior in CKO mice. However, the finding is novel in that these data indicate male CKO mice might have an aversion to voluntary wheel running in the absence of ataxia; an activity normally reveled by mice.

Respiratory quotients (RQ) provide information about the status of metabolic substrate utilization in an animal by dividing the amount of CO_2 eliminated by the amount of O_2 consumed during respiration. Normal RQ values generally range from 0.7, indicating pure fat oxidation, to 1.0, indicating pure carbohydrate oxidation. These values are helpful in assessing metabolic substrate preference and have been helpful in identifying metabolic deficiencies and trends in disease (Korenaga et al., 2013; Nakaya et al., 1998). During rest (e.g. sleep or prolonged periods of immobility) or in a fasted state, RQ values are expected to be close to 0.70 due to a reliance on fatty acid utilization. This preference is apparent in male WT mice during rest as indicated by resting RQ values of ~0.70. However, male mice lacking NCB5OR in the cerebellum and midbrain have elevated RQ values, even during rest, suggesting a state of mixed carbohydrate and fatty acid utilization. Since RQ values in male CKO mice indicated an increase in glucose utilization, it was within reason to consider the possibility that the neural tissue devoid of NCB5OR might have an increased basal metabolic rate comparative to the rest of the animal, causing increased glucose metabolism and the resulting elevated RQ values. However, transcript data for mRNA from CKO and WT mice failed to reveal increases in transcripts responsible for or attributed to changes in glucose uptake or demand in the brain. Transcript data would be unlikely to detect small changes in metabolic rate; however, considering the limited region in

which NCB5OR was deleted combined with the size of effect on RQ value, we posited that the change in metabolic activity would need to be sizeable, requiring significant changes in glucose uptake. In addition, a detectable increase in RQ value due to glucose preference derived from neural tissue would result in an increased basal metabolic rate (vO_2) since glucose is the primary source of energy for neural tissue. However, we did not observe any changes in resting vO_2 or energy expenditure in CKO mice. This data supports the observation that CKO mice do not have increased uptake of ^{14}C-labeled 2-deoxyglucose in the cerebellum.

Hydration and drinking behavior are controlled by extremely complex neuroendocrine mechanisms that have yet to be fully understood (for review see (Antunes-Rodrigues, de Castro, Elias, Valenca, & McCann, 2004)). Angiotensin II (AT_2) is a peptide hormone that plays a central role in the regulation of thirst and drinking behavior in the central nervous system ((Franci, Kozlowski, & McCann, 1989), for reviews see (Daniels, 2016; Thornton, 2011)). The expression of AT_2 receptors is generally restricted in the brain but has been confirmed in the cerebellum (Z. Huang et al., 2013; Lenkei, Palkovits, Corvol, & Llorens-Cortes, 1997). Direct projections from the deep cerebellar nuclei to osmoresponsive neurons in the paraventricular hypothalamus have been identified and neuroimaging evidence supports the theory that the cerebellum contributes to thirst (Parsons et al., 2000; Wen, Zhu, Zhang, & Wang, 2004). In our model, we observed significantly decreased levels of free and total water in CKO mice compared to WT controls. Changes indicative of altered thirst sensing were further observed in male CKO mice who had decreased water expulsion during exhalation (vH_2O) accompanied by decreased water intake. We did not see this trend in female CKO mice, which could be explained by the effects of estrogen on drinking behavior and fluid intake in females (Santollo & Daniels, 2015a, 2015b) as well as sexual dimorphism in AT_2 mediated processes (Xue, Johnson, & Hay, 2013).

Our data indicate that male CKO mice have an altered thirst response leading to a state of dehydration or hyperosmolality. Interestingly, hyperosmolality leads to a shift in metabolic substrate utilization similar to what is seen in male CKO mice: increased glucose utilization and decreased lipid oxidation leading to elevated RQ values (Keller, Szinnai, Bilz, & Berneis, 2003).

The hypothalamus controls whole body thermoregulation and energy expenditure; however the exact mechanism by which this occurs is not fully understood. In 2010 Lopez *et al* proposed and provided evidence for a mechanism by which T3 stimulates the ventromedial nucleus of the hypothalamus (VMH) which results in up regulated thermogenic markers in brown adipose tissue (Lopez et al., 2010). Investigators demonstrated phenotypes consistent with hyperthyroidism including weight loss due to increased energy expenditure and decreased fat mass after intracerebroventricular treatment with T3. While we observed no differences in body weight under *ad libitum* feeding conditions, we did observe a significant difference in male CKO body weight after an overnight fast. Since serum T3 levels were unchanged, it is possible that the VMH in male CKO mice has an altered response to T3 stimulation under conditions of caloric restriction, possibly mediated by reciprocal cerebellar-hypothalamic circuitry. However, further experimentation is needed to understand the nature of these changes.

A role for the cerebellum in the modulation of appetite and feeding behavior has been proposed based on mounting evidence that dysfunction or lesion in the cerebellum can result in changes in feeding behavior. Evidence for a circadian oscillator involved in food anticipatory behavior has been found in mice with the hotfoot mutation (*Grid2*$^{ho/ho}$), which results in altered cerebellar function and an ataxic phenotype (Mendoza et al., 2010). Interestingly, food-restricted hotfoot mutant mice lacked food anticipatory behavior in the presence of normal corticosterone levels. HPA-regulated corticosterone levels play an integral role in food anticipatory behavior

and change according to food anticipatory trends (Diaz-Munoz, Vazquez-Martinez, Aguilar-Roblero, & Escobar, 2000), suggesting that cerebellar modulation might involve the integration of peripherally expressed signals. However, we did not observe alterations in *ad libitum* feeding in the presence of normal corticosterone levels in CKO mice, indicating that corticosterone-mediated regulation of *ad libitum* food intake is intact in CKO mice.

Another peripherally expressed modulator of feeding behavior is leptin. Leptin is expressed by adipose tissue and plays a central role in mediating satiety during feeding (Friedman & Halaas, 1998). A vast majority of studies on leptin action in the brain have focused around the hypothalamus (van Swieten, Pandit, Adan, & van der Plasse, 2014), however leptin receptor expression in the brain appears to be widespread, suggesting that leptin may play more complex roles than previously thought (Bennett et al., 1998). Studies have confirmed the presence of leptin receptors in the cerebellum, with the active isoform found to be most densely expressed in the cerebellum (Burguera et al., 2000; Guan, Hess, Yu, Hey, & vanderPloeg, 1997). Leptin has also been shown to promote cell survival in cerebellar Purkinje neurons as well as modulate posterior cerebellar morphology in response to food cues in adults who are genetically-deficient for leptin (Berman et al., 2013; Oldreive, Harvey, & Doherty, 2008). In our study, male mice deficient for NCB5OR in the cerebellum and midbrain were found to gain significantly more weight as a result of *ad libitum* feeding after an overnight fast even in the presence of significantly elevated leptin levels. Interestingly, female CKO mice had an opposite response to the fasted and refeeding conditions compared to their male counterparts with results demonstrating significant reductions in weight gained after resumption of feeding compared to WT controls. The reason for the difference in this response is not immediately evident, although previous studies show sexually dimorphic responses to fasting as it pertains to corticosterone and

hypothalamic activation (Forbes, Herzog, & Cox, 2012; Fukushima et al., 2015). These changes are suggestive of an abnormal peripheral response to fasting conditions between the two genotypes and an abnormal response to satiety cues in the central nervous system (CNS).

The regulation of leptin secretion from adipocytes has been linked to a number of different factors, including prolactin mediated inhibition of leptin secretion (42). Previous studies demonstrating interaction and reciprocal regulation of prolactin and leptin lead us to hypothesize that lowered prolactin levels might explain increased leptin levels in male CKO mice. However, there were no significant differences in serum prolactin levels between CKO and WT mice. Prolactin release is negatively regulated by hypothalamic dopaminergic stimulation of pituitary dopamine D2 receptors (D2R) and has been shown to be stimulated by chronic elevation of leptin levels (43-45). Therefore, the lack of increased prolactin levels in the presence of increased basal leptin levels might indicate a decreased response to leptin. It is important to note that this response may not be an indication of changes in leptin sensitivity specifically, but rather increased hypothalamic dopaminergic tone leading to subsequent increased inhibition of prolactin release. We have previously observed changes in CKO mice indicative of altered dopaminergic function (see footnote 1) as well as significantly elevated dopamine levels in the brains of mice globally deficient for NCB5OR (unpublished data). Dopaminergic signaling in leptin-mediated processes has been explored and leptin modulation of dopaminergic tone in the ventral tegmental area (VTA) has been shown to reduce the reward response to running, leading to decreased voluntary exercise (46, 47). Direct dopaminergic projections from the VTA to the cerebellum have also been described (48). In addition, the actions of leptin-mediated satiety cues have been shown to be increased in the absence of hypothalamic D2R (49), and stimulation of adipocyte D2R has been shown to increase leptin secretion (50). While CKO mice display

characteristic changes of altered hypothalamic function, the effects of leptin, prolactin, and dopamine on food intake in the CNS are considerably complex processes involving many factors. Therefore, the effect of NCB5OR deficiency on hypothalamic function and leptin response in the CNS cannot be determined from the present findings and warrants future study.

In summary, this study provided evidence that loss of NCB5OR in the cerebellum and midbrain likely affects pathways and processes mediated by cerebellar-hypothalamic circuitry, specifically, by altering the integration of peripheral signals regulating feeding and drinking behavior. Lack of NCB5OR in the cerebellum and midbrain altered neuroendocrine thirst regulation in a manner that resulted in dehydration and subsequently elevated RQ values due to a shift to glucose utilization. In addition, NCB5OR deficiency in the cerebellum and midbrain reduced energy expenditure due to lowered voluntary wheel running, which may be an indication of altered leptin-mediated reward response to exercise. Although further experimentation is needed to investigate the mechanism, our current data demonstrate a role for NCB5OR in maintaining the integrity of cerebellar-hypothalamic circuitry and hypothalamic response to satiety cues.

CHAPTER 3 - TABLES AND FIGURES

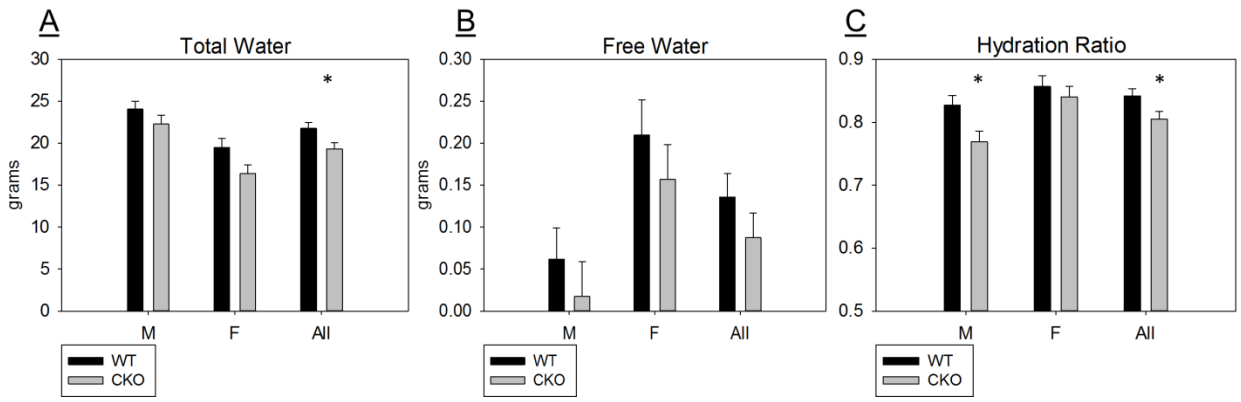

Figure 3.1 Hydration status of CKO and WT mice. (A) Total water was significantly reduced in CKO mice compared to WT mice. (B) CKO mice had comparable free water content relative to WT controls. (C) Hydration ratios in male CKO mice were significantly lower than those of WT controls, while female CKO hydration ratios remained unchanged. See materials and methods for definitions and calculations. Values are presented as means ± SEM (standard error of mean). *, $p < 0.05$. n=8 for CKO (4 Male, 4 Female) and n=9 for WT (5 Male, 4 Female).

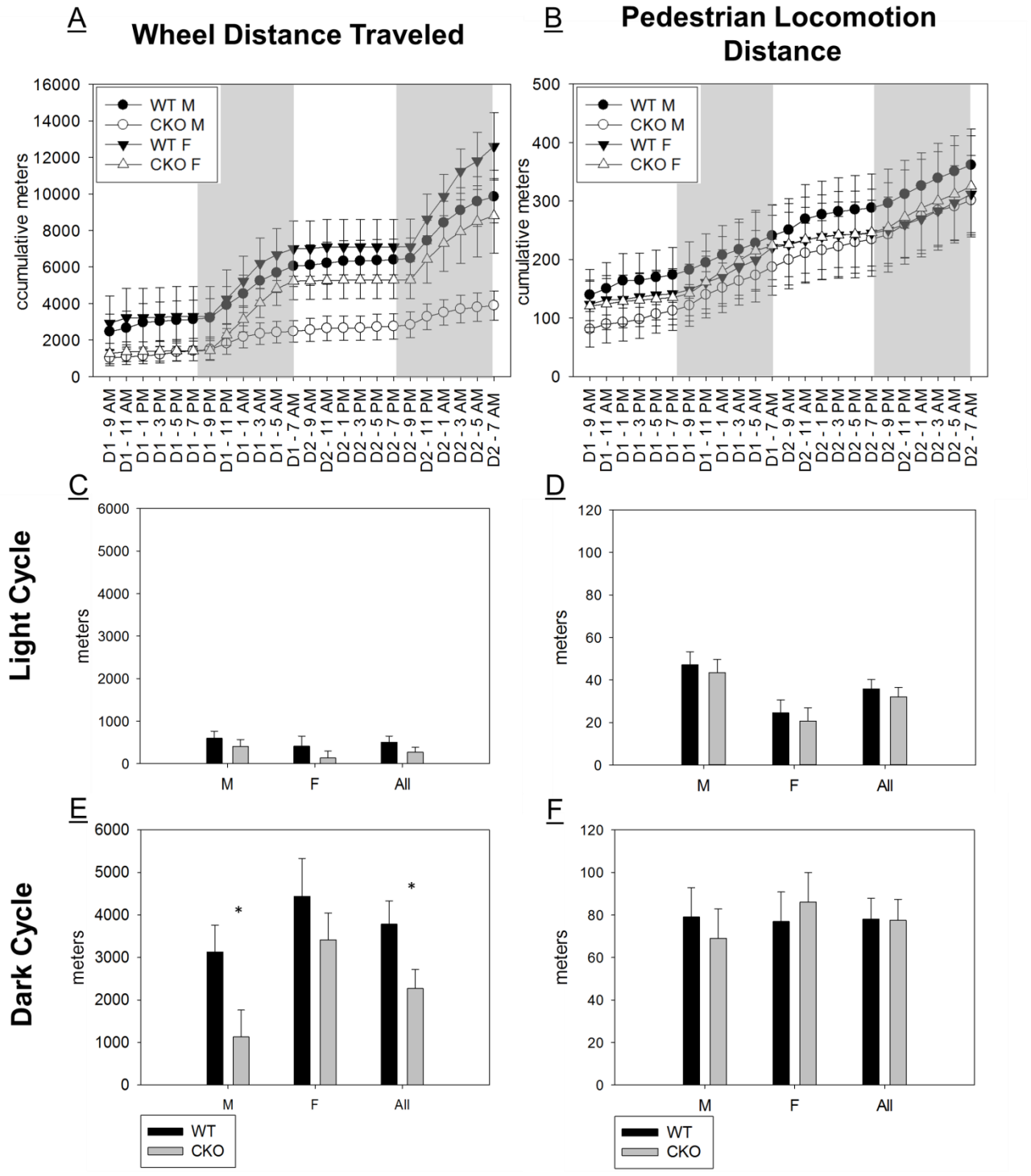

Figure 3.2 Exercise trends in CKO and WT mice. (A, B) Longitudinal representations of cumulative meters during two consecutive light and dark cycles. Note the lack of distance accumulation during the light cycle in (A). There were no differences between CKO and WT

mice during the light cycle for (C) average wheel distance traveled per cycle and (D) average pedestrian locomotion distance per cycle. Significantly lowered average wheel distance traveled in male CKO mice compared to WT during the dark cycle is shown in (E), while there were no differences in pedestrian locomotion (F). See materials and methods for definitions. Values are presented as means ± SEM (standard error of mean). Light and shaded areas in (A) and (D) represent light and dark cycles, respectively. *, $p<0.05$. n=12 for CKO (6 Male, 6 Female) and n=12 for WT (6 Male, 6 Female).

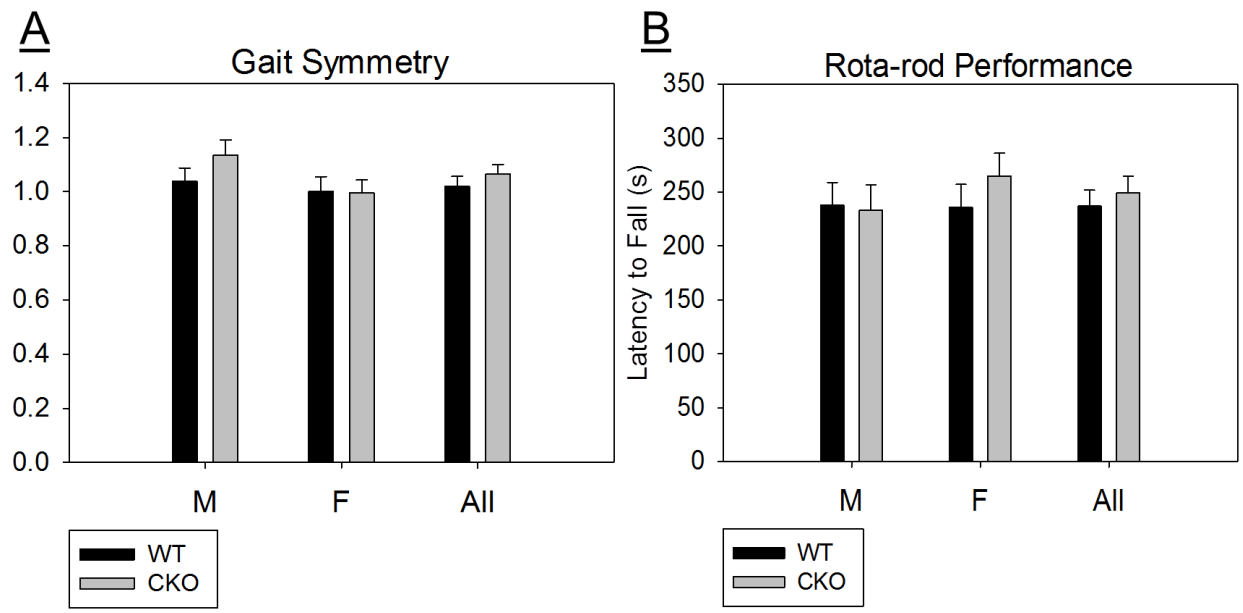

Figure 3.3 Gait analysis and Rota-rod performance in CKO mice. (A) CKO mice did not display changes in gait symmetry or (B) Rota-rod performance, indicating no overt signs of ataxia. Values are presented as means ± SEM (standard error of mean). n=9 for CKO (4 Male, 5 Female) and n=10 for WT (5 Male, 5 Female).

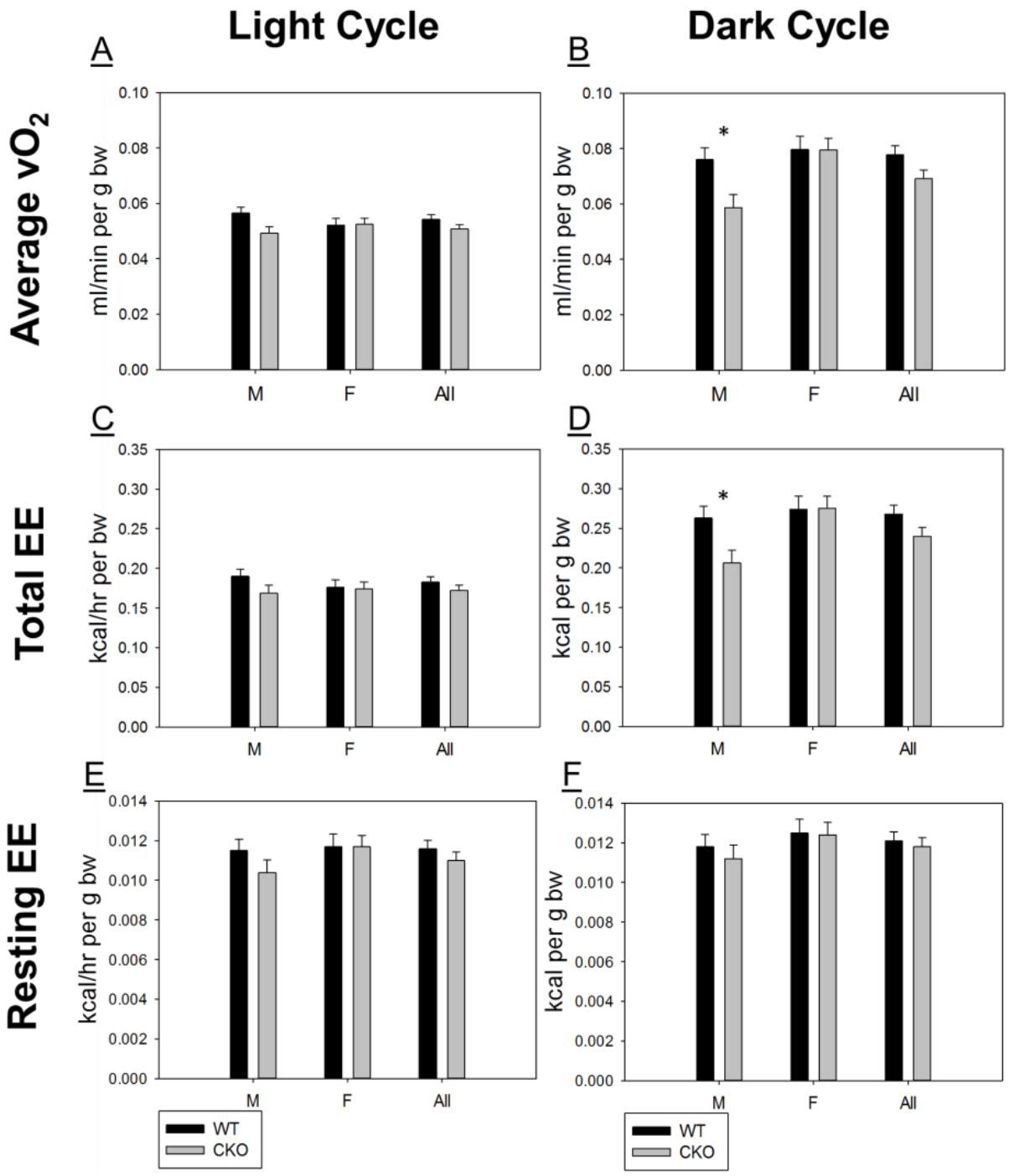

Figure 3.4 Energy expenditure and oxygen consumption in CKO and WT mice. Average rate of oxygen consumption (vO_2) was comparable between WT and CKO mice during the light cycle (A), but was lower in male CKO mice during the dark cycle (B). (C) Total energy expenditure (EE) was unchanged in CKO mice during the light cycle, but (D) was lower in male CKO mice

during the dark cycle. (E, F) Resting EE was unchanged between WT and CKO mice during both light and dark cycles. See materials and methods for definitions. Values are presented as means ± SEM (standard error of mean) and were normalized to body weight (per g bw). *, $p<0.05$. n=12 for CKO (6 Male, 6 Female) and n=12 for WT (6 Male, 6 Female).

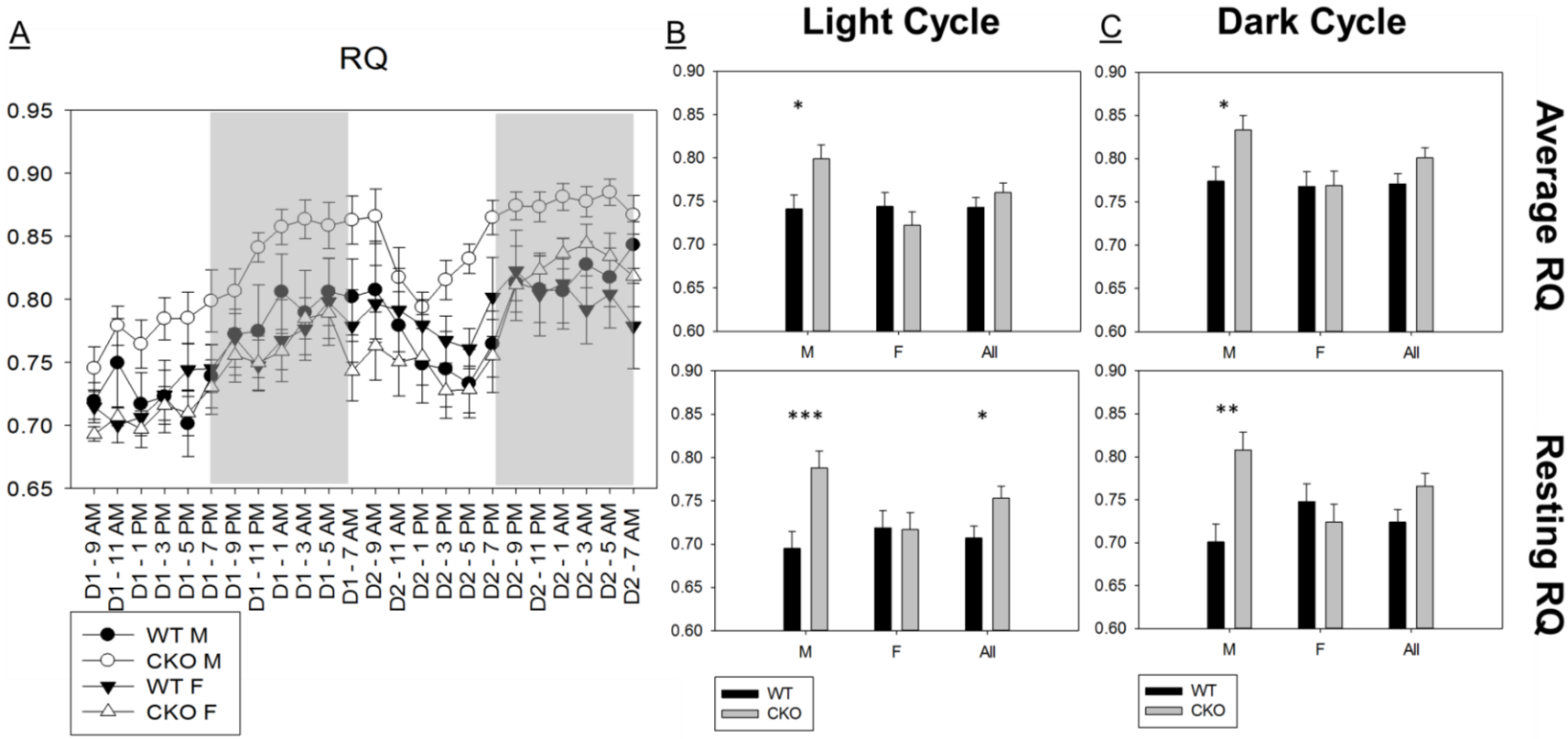

Figure 3.5 Metabolic substrate utilization in CKO and WT mice. (A) A longitudinal representation of average respiratory quotients during two consecutive light and dark cycles. Note that male CKO RQ values were consistently higher. (B) During the light cycle, male CKO mice had significantly elevated average RQ values (top) and resting RQ values (bottom). The same trend was seen in (C, top and bottom). See materials and methods for definitions and calculations. Values are presented as means ± SEM (standard error of mean). Light and shaded areas in (A) represent light and dark cycles, respectively. *, $p<0.05$; **, $p<0.01$; ***, $p<0.005$. n=12 for CKO (6 Male, 6 Female) and n=12 for WT (6 Male, 6 Female).

A

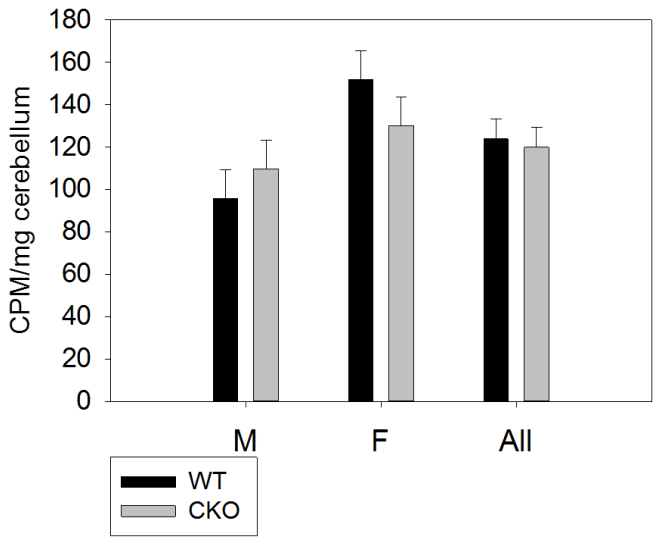

B

Gene	Group	16 weeks		
		CKO	WT	CKO/WT
Ncb5or	M	0.325±0.90	9.61±0.90	0.03
	F	0.336±0.90	7.05±0.90	0.05
	All	0.330±0.64	8.33±0.64	0.04
Ins2	M	0.061±0.02	0.078±0.02	1.07
	F	0.063±0.02	0.038±0.02	0.78
	All	0.062±0.02	0.058±0.02	1.07
InsR	M	9.55±1.51	8.65±1.51	1.10
	F	3.97±1.51	3.68±1.51	1.08
	All	6.76±1.06	6.16±1.06	1.10
LdhA	M	25.5±3.22	29.2±3.22	0.87
	F	10.5±3.22	12.7±3.22	0.82
	All	17.9±2.27	20.9±2.27	0.86
Glut1	M	21.8±3.18	16.8±3.18	1.30
	F	10.9±3.18	12.5±3.18	0.87
	All	16.3±2.25	14.6±2.25	1.11
Glut3	M	16.4±1.84	19.8±1.84	0.83
	F	10.5±1.84	12.8±1.84	0.82
	All	13.5±1.30	16.3±1.30	0.83

Figure 3.6 Status of glucose uptake in the CKO cerebellum. (A) CKO mice do not show altered uptake of ^{14}C labeled 2-DoG in the cerebellum relative to WT controls. (B) Transcript levels of genes involved in glucose transport and lactate metabolism in the cerebellum of 16 week old CKO and WT mice. Transcript levels were determined by defining the internal reference, 18S rRNA, as 10^6. Ins2, insulin; InsR, insulin receptor; LdhA, lactate dehydrogenase A; Glut1, glucose transporter 1, Glut3, glucose transporter 3. For 2-DoG uptake, n=10 WT (5 Male, 5 Female) and n=10 CKO (5 Male, 5 Female). For qPCR n=8 WT (4 Male, 4 Female) and n=8 KO (5 Male, 3 Female). Values are presented as means ± SEM (standard error of mean). CPM is counts per minute.

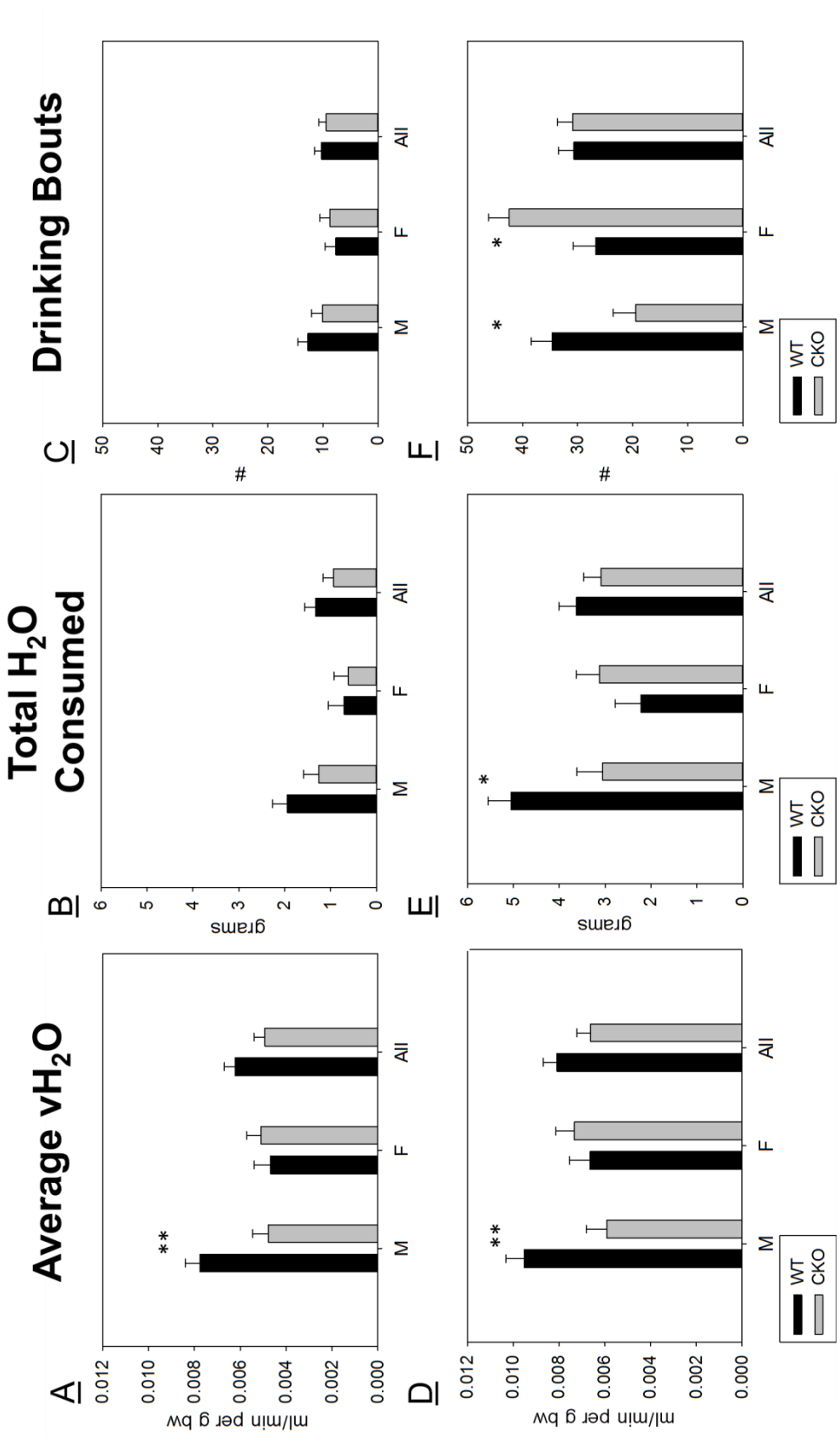
A
Average vH2O
Light Cycle
ml/min per g bw
0.012
0.010
0.008
0.006
0.004
0.002
0.000
**
M
F
All
B
Total H2O Consumed
grams
6
5
4
3
2
1
0
C
Drinking Bouts
#
50
40
30
20
10
0
D
Dark Cycle
E
F
WT
CKO
*

Figure 3.7 Respiratory water expulsion and water consumption behavior. During the light cycle, male CKO mice had (A) lowered average respiratory water consumption (vH_2O) but consumed comparable amounts of water (B) and had comparable average number of bouts (C) compared to WT mice. During the dark cycle, male CKO mice had (D) lowered average vH_2O along with decreased average water consumption (E) and average number of drinking bouts (F). Note that in (F), female CKO mice had an elevated number of drinking bouts converse that of their male counterparts. See materials and methods for definitions. Values are presented as means ± SEM (standard error of mean) and were normalized to body weight (per g bw) in (A, D). *, $p<0.05$; **, $p<0.01$. n=12 for CKO (6 Male, 6 Female) and n=12 for WT (6 Male, 6 Female).

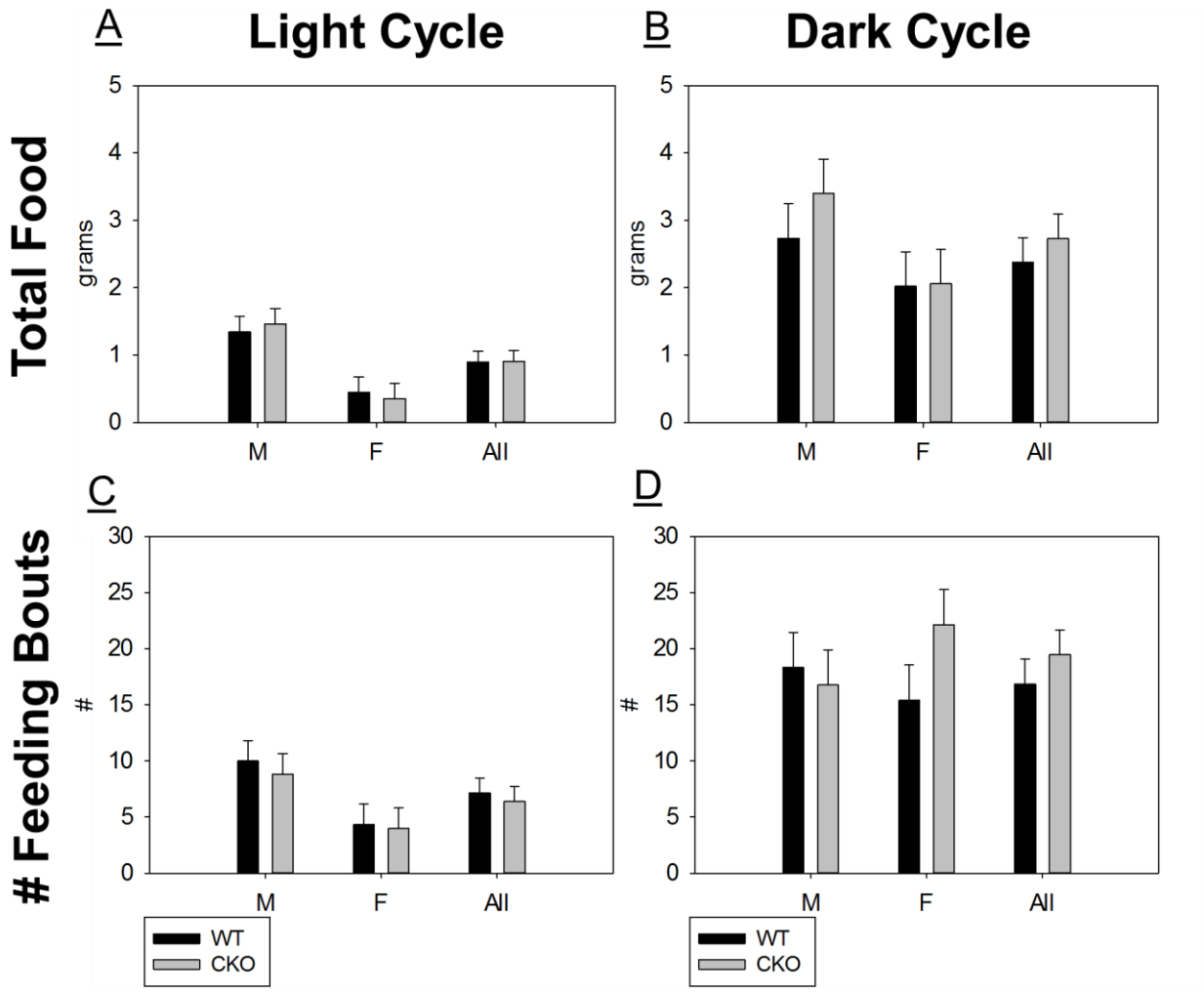

Figure 3.8 Feeding behavior of individually housed CKO and WT mice. CKO mice consumed the same amount of food compared to WT mice during both the light cycle (A) and dark cycle (B). There were no differences in the number of feeding bouts between WT and CKO mice during either the light cycle (C) or the dark cycle (D). Values are presented as means ± SEM (standard error of mean). n=12 for CKO (6 Male, 6 Female) and n=12 for WT (6 Male, 6 Female).

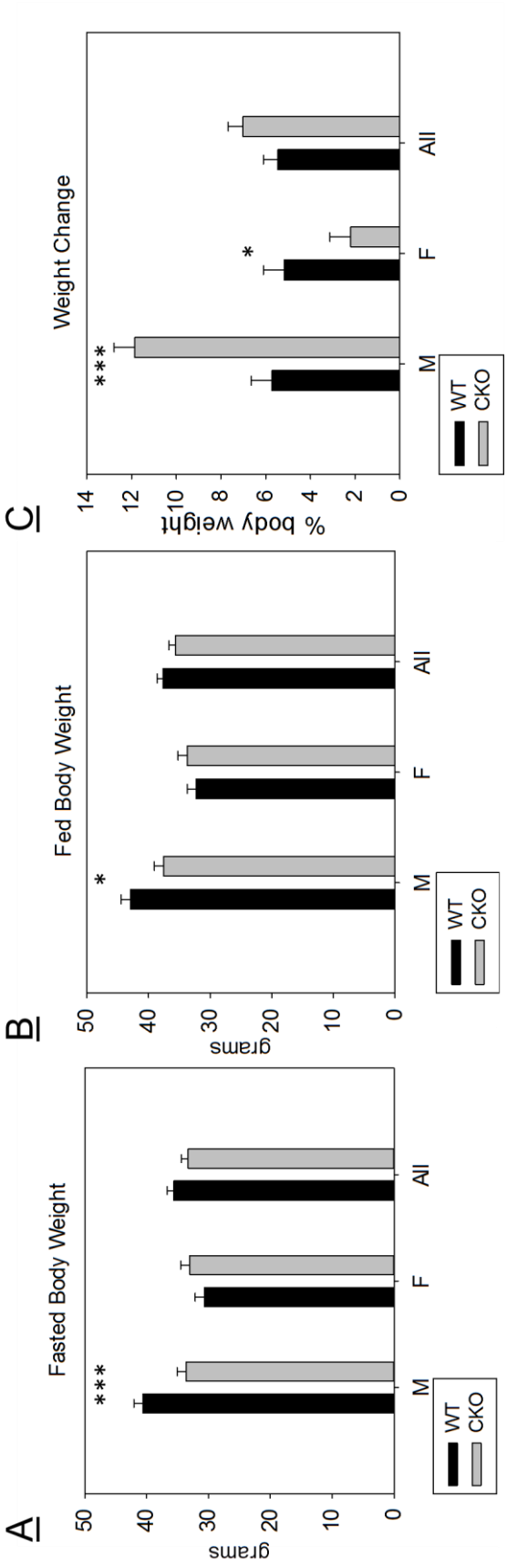
A
Fasted Body Weight
grams
50
40
30
20
10
0
***
M
F
All
WT
CKO
B
Fed Body Weight
grams
50
40
30
20
10
0
*
M
F
All
WT
CKO
C
Weight Change
% body weight
14
12
10
8
6
4
2
0
***
*
M
F
All
WT
CKO

Figure 3.9 Fasted feeding weight change in CKO mice. (A) Male CKO mice displayed decreased body weight after an overnight fast and (B) after resuming *ad libitum* feeding for 24 hours. (C) Male CKO mice gained significantly more body weight after refeeding while female CKO gained less compared to WT controls. All mice have access to water *ad libitum* at all times. Values are presented as means ± SEM. * $p<0.05$; ***, $p<0.005$. n=12 for CKO (6 Male, 6 female) and n=12 for WT (6 male, 6 female).

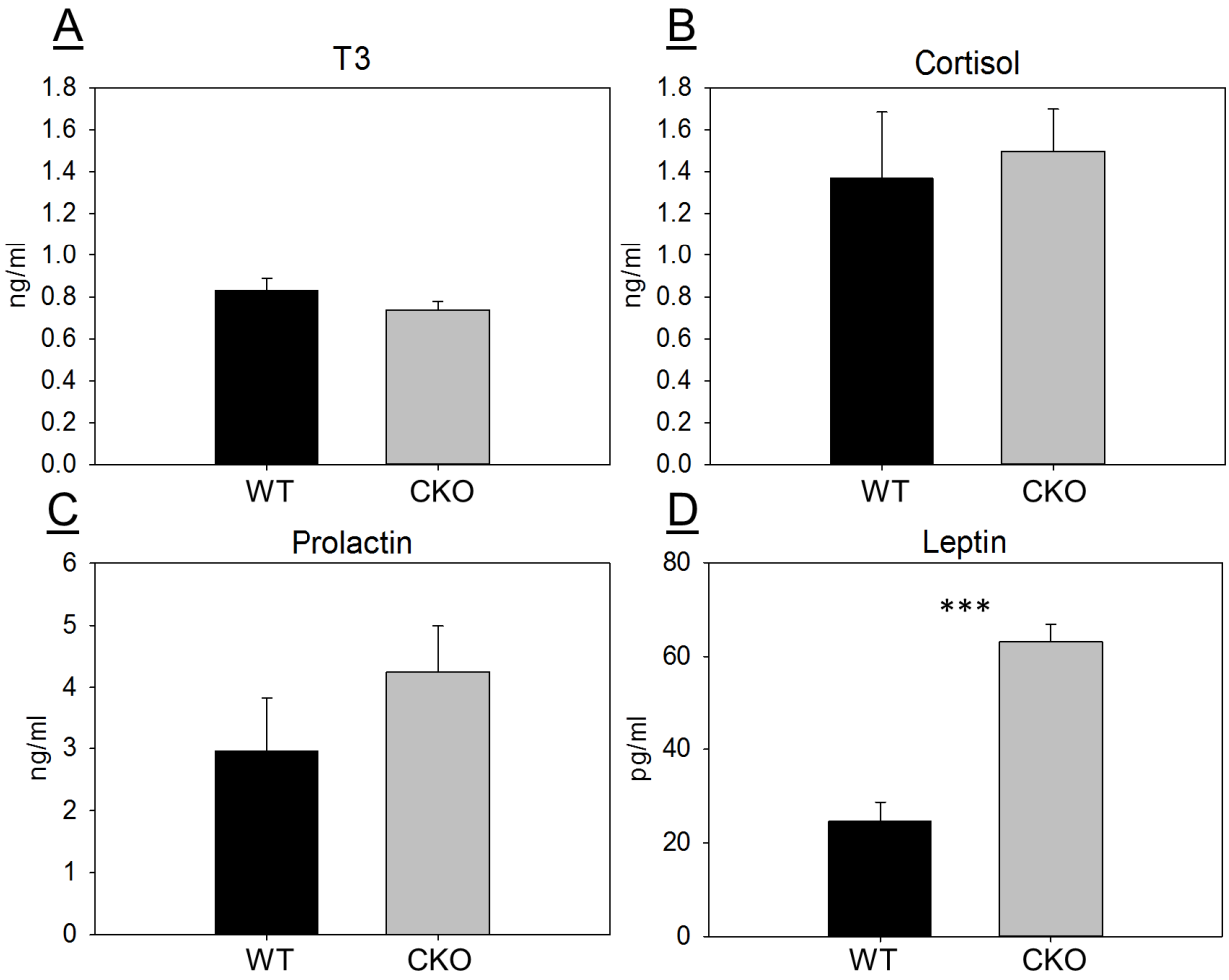

Figure 3.10 Serum T3, cortisol, prolactin, and leptin levels in male CKO mice. There were no differences in serum T3 (A), cortisol (B), or prolactin (C) levels between male CKO and WT mice. However, male CKO mice had significantly elevated serum levels of leptin (D) relative to WT controls. Values are presented as means ± SEM (standard error of mean). ***, $p<0.005$. n=13 (7 CKO, 6 WT), all male.

CHAPTER 4

EVALUATION OF NEUROTRANSMITTER LEVELS IN THE NCB5OR-DEFICIENT CEREBELLUM AND CORTEX USING HILIC UPLC-MS/MS

4.1 ABSTRACT

Iron is an essential nutrient required for proper brain development and function. Early studies established that early life brain iron deficiency, genetic or otherwise, affects neurotransmitter levels, ultimately altering proper development and functioning of neural pathways. Ablation of NCB5OR in the mouse cerebellum has been shown to affect iron homeostasis, feeding behavior, and locomotor activity. This study aimed to assess whether loss of NCB5OR in the mouse brain resulted in changes in four primary neurotransmitters in the cerebellum and frontal cortex: serotonin (5-HT), dopamine (DA), gamma aminobutyric acid (GABA), and L-glutamic acid (Glut). Using hydrophilic interaction liquid chromatography (HILIC) ultra-performance liquid chromatography coupled electrospray tandem mass spectrometry (UPLC-MS/MS) we determined that 10 week old, non-diabetic female mice globally deficient for NCB5OR (GKO mice) had normal levels of 5-HT, GABA, and Glut in the cerebellum and cortex compared to wildtype controls. However, cortex DA levels were found to be significantly elevated in GKO mice while cerebellar DA levels remained unchanged relative to wild type controls.

4.2 INTRODUCTION

Neurotransmitter levels are suspect in a number of neurological and psychological diseases. As such, metabolic pathways and receptors responsible for neurotransmitter synthesis, breakdown, and signal transduction are often key targets in etiological and pharmacological studies. There is a growing body of evidence that neurological diseases and disorders may be strongly influenced by a number of environmental factors, including nutrition. Iron deficiency has long been recognized as the number one nutritional deficiency in the world (WHO, 2001). Early studies investigated the impact of dietary iron deficiency on neurotransmitter levels and behavior as well as the functions of enzymes and pathways responsible for the synthesis, breakdown, and action of many neurotransmitters (J. L. Beard, Chen, Connor, & Jones, 1994; Oski, Honig, Helu, & Howanitz, 1983; Youdim & Green, 1978). The revelation that iron status alters neurotransmitter networks has since resulted studies investigating neurotransmitter composition and brain function in diseases, genetic models, and conditions in which iron homeostasis is known to be perturbed (Bakoyiannis et al., 2015; J. Beard, 2003; Johnstone & Milward, 2010; J. Kim & Wessling-Resnick, 2014).

We recently reported that global ablation of a reductase, NCB5OR, results in iron dyshomeostasis and hyperactivity in mice (see Chapter 1, footnotes 2 and 3). In addition, we observed alterations in iron pathways, iron uptake, and locomotor response to dietary iron deficiency in mice deficient for NCB5OR only in the cerebellum and midbrain (see Chapter 2). These changes led us to hypothesize that loss of NCB5OR would alter neurotransmitter levels in the brain. Therefore we investigated whether global loss of NCB5OR would lead to changes in serotonin (5-HT), dopamine (DA), γ-Aminobutyric acid (GABA), and L-glutamic acid (Glut)

levels in the mouse cerebellum and cortex using hydrophilic interaction ultra-performance liquid chromatography tandem mass spectrometry (HILIC UPLC-MS/MS).

The separation and quantification of pure monoamine neurotransmitters using HILIC UPLC-MS/MS has been previously described methodologically (Danaceua, 2012). However, the use of HILIC to assess neurotransmitter levels in biological samples, namely brain tissue, has yet to be described. In addition, non-monoamine neurotransmitters such as GABA and Glut were not included in the previous method description. Therefore we modified and optimized the previously described method for simultaneous separation of 5-HT, DA, GABA, Glut and 3,4-dihydroxybenzylamine (DHBA). DHBA is a dopamine analog and is used as an internal standard (IS) in our study. In addition, we developed a method to effectively extract quantifiable amounts of all 4 neurotransmitters from mouse brain tissue.

4.3 METHOD VALIDATION AND RESULTS

4.3.1 Assay Optimization.

Chromatographic conditions were adjusted such that 5-HT, DA, GABA, Glut, and DHBA were independently identifiable peaks at consistent retention times (Figure 4.1). All five compounds were best detected in positive ion detection mode. The conditions for detection of the most abundant protonated ion peak ($[M + H]^+$ for each compound are described in Table 4.1. Using these conditions we were able to establish ranges in which the peak response was linearly correlated with known amounts of compound (Table 4.2) and we were able to identify the lower limits of quantitation (LOQ) for each compound. We did not determine the lower limit of detection (LOD) as the LOQ for all compounds was established using the lowest standard concentration, which was considered to be significantly lower than expected physiological levels.

User and auto injector accuracy were tested in order to determine an expected error of measurement from the processes and to confirm that there were no systematic errors in the method (Table 4.1). User accuracy was determined by quantifying mass spectra of injections from five independently prepared vials of a standard of known concentration. Auto injection accuracy was determined by quantifying mass spectra of five successive injections from one vial of a standard of known concentration. Accuracy was calculated as percent error. User sample preparation accuracy and auto injection accuracy were comparable and were below 5%.

4.3.2 Sample peak identification and assessment of matrix effects.

A recurrent problem when assaying brain tissue for endogenous compounds using liquid chromatography is the lack of available analyte matrix, which is used to assess whether the presence of other compounds in the solution have an effect on the analyte of interest. Therefore, test samples of cerebellar extract were used to identify compound peaks in the presence of matrix and to assess if matrix effects were present by utilizing a method of standard addition. Chromatography and mass spectra were collected for neurotransmitters and the internal standard (IS) DHBA from 5 μL and 2.5 μL injections of extract and diluted extract, respectively. The same samples were then spiked to a 50 μM concentration (within the determined linear range for all compounds) with standard stock solutions of 5-HT, DA, GABA, DHBA, and Glut. Mass spectra were collected for neurotransmitters and the IS from 5 μL and 2.5 μL injections of spiked extract or spiked diluted extract, respectively. Mass spectra of normal and spike extract were compared and peaks were identified according to elevated peak responses at expected retention times for individual compounds. There were no significant shifts in retention times (< 0.10 min) or changes in predicted peak response areas, indicating no apparent matrix effects (Figure 4.2).

4.3.3 Analysis of neurotransmitters in the GKO mouse cerebellum and cortex

Using the validated assay conditions for all compounds we established the best conditions for evaluating 5-HT, DA, GABA, and Glut levels in mouse brain tissue extract. We determined that the extraction method was sufficient to yield quantifiable levels of all neurotransmitters as well as the added IS. Since the levels of GABA and Glut are three and four orders of magnitude more abundant in mouse brain tissue, respectively, than 5-HT and DA, we determined that a 100 fold dilution was sufficient to produce peak responses in the linear ranges for GABA and Glut.

We used the above assay conditions to quantify the levels of 5-HT, DA, Glut, and GABA in the cerebellum and frontal cortex of GKO and WT mice for comparison. Quantification of 5-HT, DA, GABA, and Glut in the cerebellum revealed no significant differences in GKO mice relative to WT controls (Figure 4.3). However, we observed significantly elevated levels of DA in frontal cortex extracts from GKO mice while 5-HT, GABA, and Glut remained unchanged relative to controls (Figure 4.3B).

4.4 DISCUSSION

Data presented here detail the analysis of four endogenous neurotransmitters in mouse brain tissue derived from mice globally deficient for NCB5OR. We presented data pertaining to assay development and validation as well as the application of the assay to biological samples. Our data indicate that DA levels are modulated by loss of NCB5OR in the mouse frontal cortex but not in the cerebellum.

Manipulating brain iron levels has been shown to alter development, behavior, and neurotransmitter levels, and has been shown to have specific effects on dopamine and behaviors associated with dopaminergic function (for review see, (Lozoff, 2011)). Pioneering work by Dr. John Beard demonstrated regional alterations in brain dopamine levels as well as changes in

dopamine receptor densities as a result of iron deficiency (for review see, (J. Beard, 2003)). Studies have repeatedly demonstrated the specific effects of iron deficiency on dopamine levels, with dopamine levels elevating in the context of iron deficiency while other neurotransmitters remain unchanged (J. L. Beard et al., 1994; Erikson, Jones, Hess, Zhang, & Beard, 2001; Nelson, Erikson, Pinero, & Beard, 1997). In addition, studies support findings that suggest early life iron deprivation leads to permanent alterations in behavioral profiles and dopaminergic networks (for review see (Georgieff, 2011)).

Loss of NCB5OR in the mouse cerebellum and midbrain has been shown to lead to alterations in brain iron homeostasis as well as locomotor changes indicative of altered dopaminergic function (see Chapter 2). Mice globally deficient for NCB5OR display hyperactive behavior (see preliminary data, Chapter 1), a phenotype known to result from changes in both iron homeostasis and dopaminergic function in the mesocorticolimbic system (Ohno, 2003; Viggiano & Sadile, 2000). Hyperactivity in GKO mice is consistent with our observations of increased dopamine levels in the cortex of GKO mice. Iron deficiency has been shown to alter the activities of dopamine hydroxylase, monoamine oxidase, dopamine transporters, and dopamine receptors. This data, combined with observations presented in Chapters 2 and 3, suggest a significant impact of NCB5OR deficiency on dopaminergic networks. Still, significantly more work is needed to identify the exact mechanism by which NCB5OR deficiency modulates dopaminergic tone.

CHAPTER 4 – TABLES AND FIGURES

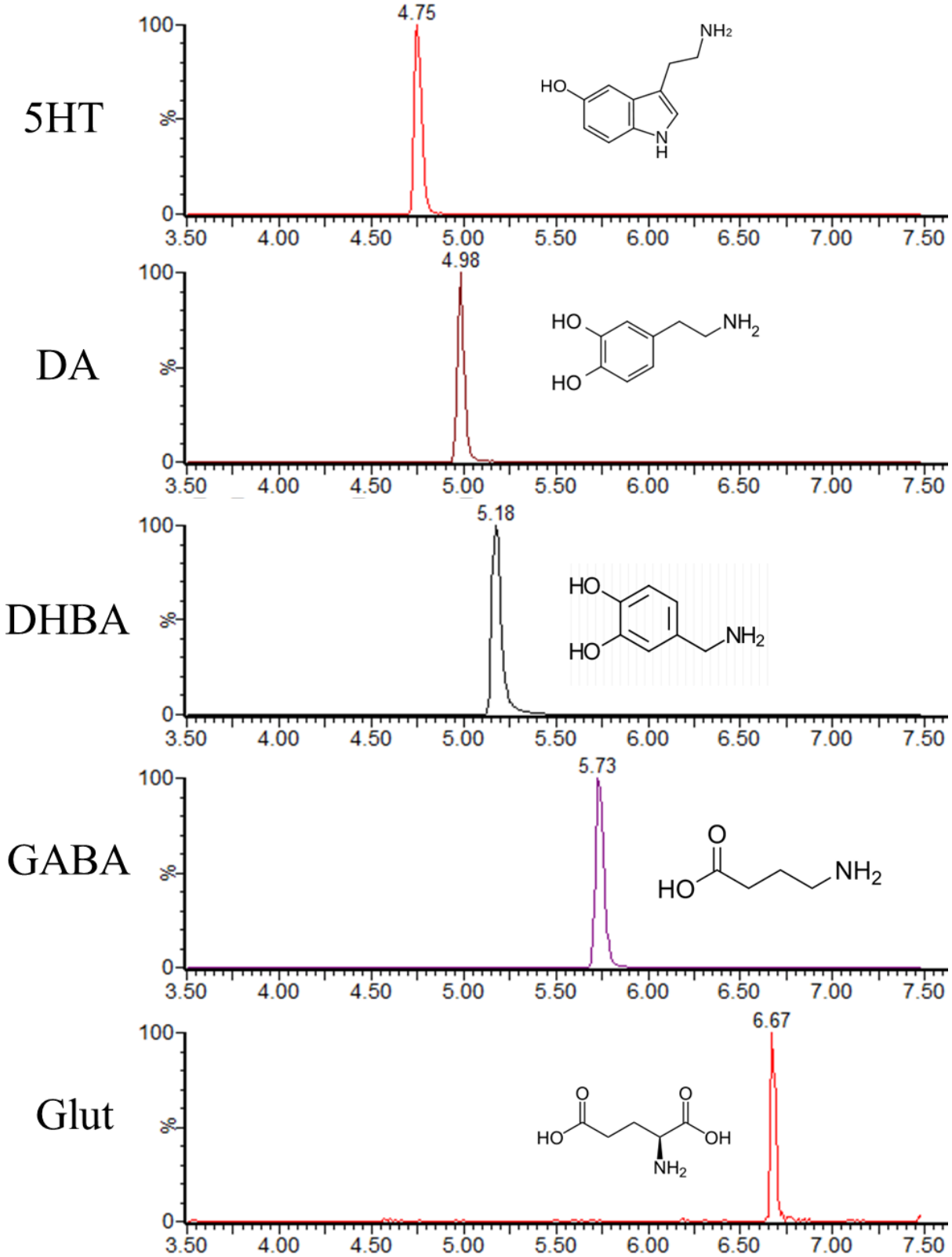
5HT
4.75
DA
4.98
DHBA
5.18
GABA
5.73
Glut
6.67
100
%
0
3.50
4.00
4.50
5.00
5.50
6.00
6.50
7.00
7.50
HO
NH2
N
H
O
OH

Figure 4.1 Chromatography of 5-HT, DA, DHBA, GABA, and Glut using HILIC UPLC MS/MS. Chromatographic conditions were optimized to allow for 7.5 minute run times and distinct and acceptable peak resolution and shape. Note that the most polar (hydrophilic) compounds had the shortest retention times. DHBA is an analog of DA that varies by only one methylene group, leading to their close, but distinct, retention times. All peak retention times were separated by more than 10 seconds.

Compound	Precursor Ion (*m/z*)[a]	Cone Voltage (V)	Collision energy (V)[b]	Product Ion[c]	Retention Time (min)	**Accuracy RE (%)**	
5-HT	177.5	20	11	160.8	4.75	User (sample prep)	Injection
DA	154.1	11	21	136.9	4.98		
GABA	103.9	16	15	86.6	5.74	3.2	4.8
Glut	148.1	22	9	83.8	6.67		
DHBA	140.2	20	11	77.4	5.18		

Table 4.1 LC-MS/MS analytical parameters. All compounds were best detected in positive ion mode. The most abundant $[M + H]^+$ peak was selected and used for quantification. 5-HT; serotonin. DA; dopamine. GABA; γ-aminobutyric acid. Glut; l-glutamic acid. DHBA; 3.4-dihydroxybenzylamine. RE; relative error. RE is an average of RE's obtained from 5 replicate measurements of a standard of known concentration and is expressed as a percentage.

Compound	Equations	Linear Range (ng)	Correlation Cooefficient (R^2)	LOD (ng)	LOQ (ng)
5-HT	y=0.0006x-0.4066	0.03-133	0.9950	< 0.02	0.02
DA (cer.)	y=0.0001x-0.0151	0.02-0.74	0.9966	< 0.02	0.02
DA (cort.)	y=0.00009x-0.0046	0.02-23.7	0.9973	< 0.02	-
GABA	y=0.0002x-0.1477	0.01-64.5	0.9997	< 0.02	0.03
Glut	y=0.0708x-1.1379	2.64-106	0.9999	< 0.02	0.02
DHBA (5-HT, DA)	y=0.0012x-0.0206	0.03-27.5	0.9997	< 0.02	0.02
DHBA (GABA, Glut)	y=0.0011x+0.0013	0.03-1.72	0.9990	< 0.02	-

Table 4.2 Compound calibration parameters for quantification using HILIC UPLC-MS/MS. Due to the wide detection range for each compound as well as relative abundance in normal and diluted biological samples, separate calibration curves were established for DA and DHBA. All calibration curves were established from the same standard curve run, but were adjusted based on detected range so as to provide more accurate quantitation. LOD; limit of detection. LOQ; limit of quantitation.

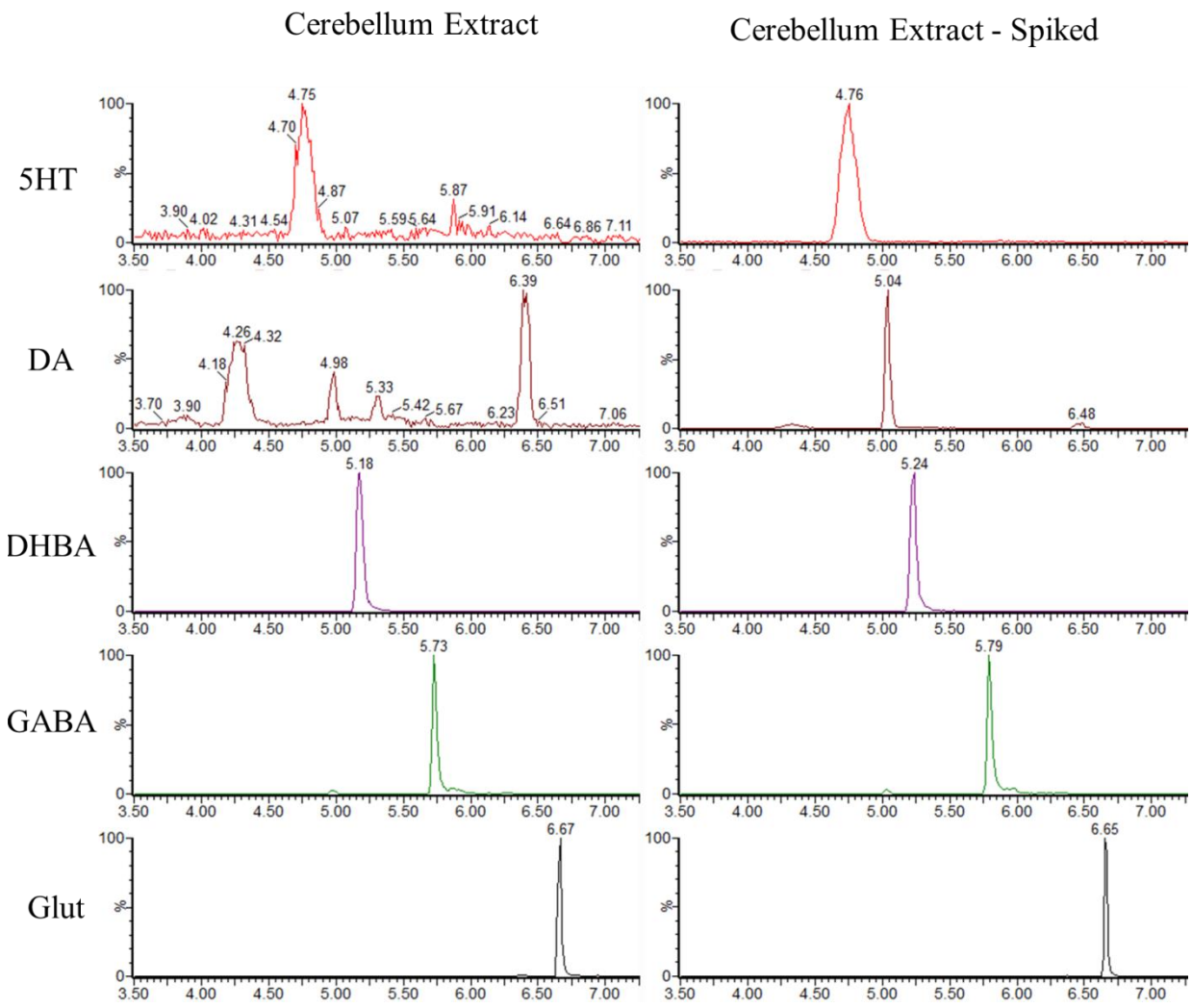

Figure 4.2 Identification of compound peaks and matrix effects in cerebellar extract. Pure cerebellar extract spiked with DHBA as an internal standard (IS) was evaluated for peak identification (LEFT). 5-HT and DA display multiple auxiliary peaks from unidentified endogenous compounds. Without a matrix blank to assess matrix effects, it is not possible to conclude that the peaks observed at the expected retention times are actually 5-HT and DA. (RIGHT) Addition of a pure compound standard to the cerebellum extract leads to enhanced peak response near the expected retention times of each compound, confirming the presence and placement of detectable endogenous 5-HT and DA. No significant shift in retention time or change in expected spike recovery values were observed, indicating no apparent matrix effects.

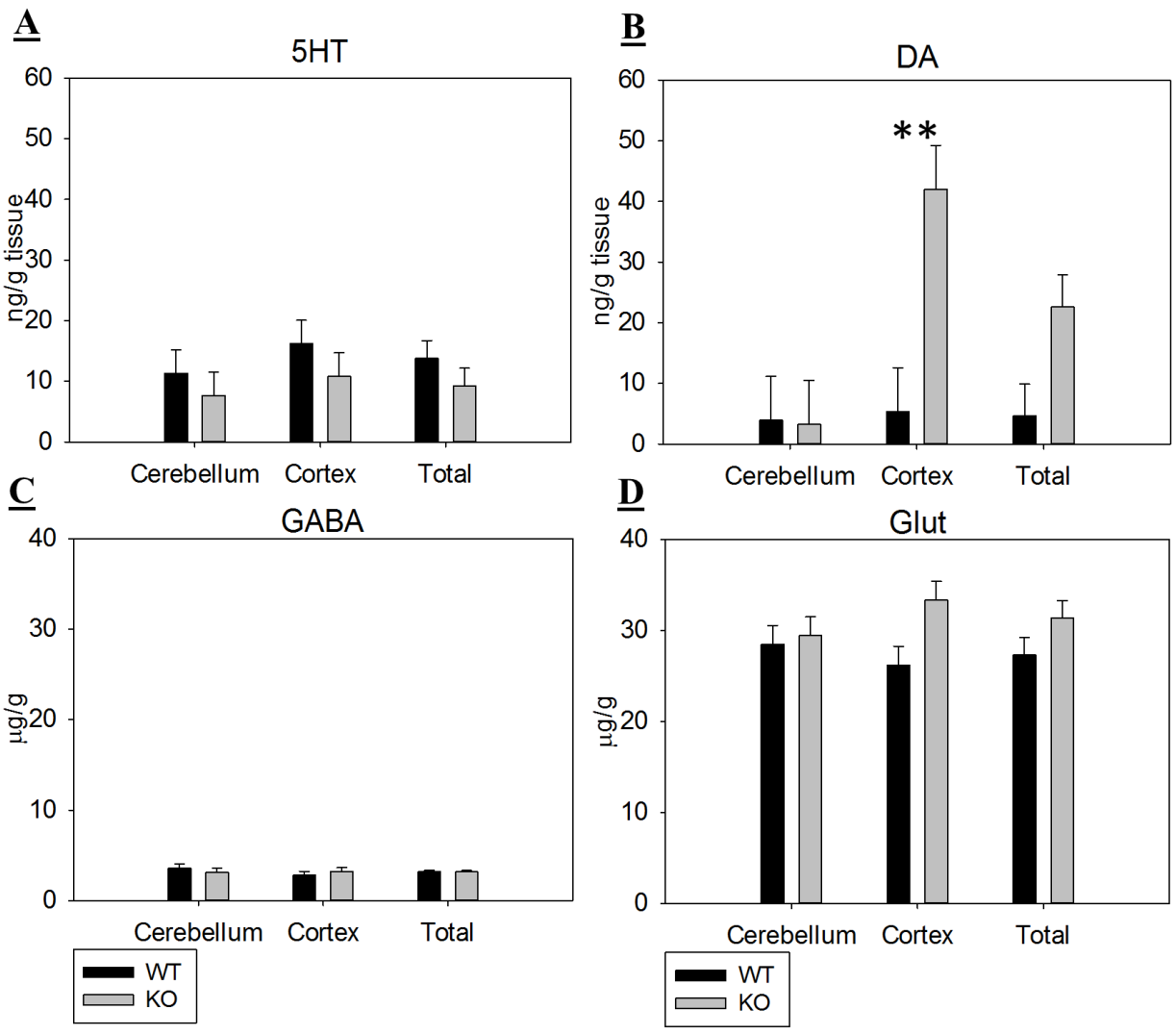

Figure 4.3 5-HT, DA, GABA, and Glut levels in the cerebellum and cortex of GKO and WT mice. (A) Levels of 5-HT were did not differ in the cerebellum or cortex of GKO mice relative to controls. (B) Cortex DA levels are significantly increased in GKO mice relative to controls while no change was observed in the cerebellum. (C&D) GABA and Glut levels were comparable between GKO and WT mice in the cerebellum and cortex. n= 3:3 (KO:WT). Values are presented as means ± SEM. **, $p<0.01$.

CHAPTER 5

MATERIALS AND METHODS

5.1 CHAPTER 2 MATERIALS AND METHODS

5.1.1 Conditional knock out and reporter mice.

All mice were of C57BL/6J background and treated according to the University of Kansas Medical Center's Institutional Animal Care and Use Committee approval protocol. The generation of mice with selective deletion of NCB5OR in the mouse cerebellum and midbrain (conditional knockout (CKO) mice) was achieved by crossing C57BL/6J mice homozygous for a floxed version of NCB5OR's exon 3 (detailed in Wang *et al,* see footnote 2) with *En1*$^{tm2(cre)Wrst}$ (The Jackson Laboratory stock no. 007916) mice that are known to excise floxed DNA regions in only the cerebellum and midbrain (Kimmel et al., 2000). To evaluate recombination activity, En1 Cre positive mice were crossed with *B6.Cg-Gt(ROSA)26Sor*$^{tm14(CAG-tdTomato)Hze/J}$ (stock no. 007914, Jackson Laboratory) which harbor a TdTomato locus with a *loxP*-flanked STOP cassette that was removed after Cre-mediated recombination, resulting in TdTomato expression. Mice carrying no copies of the Cre gene were considered as normal or wild-type (WT) and all mice used (CKO and WT) were littermates. Evaluation of recombination of NCB5OR was also conducted using qPCR and primer sets targeted to exon 3 and exon 4 of NCB5OR transcripts.

5.1.2 TdTomato reporter and confocal microscopy.

Tandem dimer Tomato (TdTomato) reporter mice underwent transcardial perfusion with 10 mL of PBS solution immediately followed by 10 mL of 4% paraformaldehyde. The cerebellum was collected and immediately post-fixed with 4% paraformaldehyde at room temperature for 1 hour. Tissue was then transferred to 20% sucrose solution and allowed to sit overnight at 4°C for cryoprotection. Tissues were then embedded in OCT and 12 µm sections were cut, placed on Superfrost Plus slide (Fisher, #12-550-15), and cover slipped. Confocal images of TdTomato were taken using a Nikon Eclipse 90i microscope.

5.1.3 Molecular analysis.

Quantitative Reverse Transcription PCR (qRT-PCR) was performed on RNA extracted from WT and CKO whole mouse cerebellum after the mice had been fasted for 4 hours. Purity of isolated RNA was assessed by A_{260}/A_{280} ratio. Reverse transcription of 1ug total RNA was performed using M-MLV Reverse transcriptase and standard protocol from Life Technologies (Cat # 28025-013). The qPCR reaction was performed on an Applied Biosystems 7900 Fast Real-Time PCR System using SYBR Green master mix from ThermoFisher (Cat. No. 4367659) and all results were normalized to 18S rRNA with the ΔΔCt method. Primer sequences are available upon request. Total protein was isolated from whole mouse cerebellum using a lysis buffer as previously described (Lemaire-Vieille et al., 2013), with the addition of the SigmaFAST protease inhibitor cocktail (s8830). Protein content was determined using a DC assay from Bio-Rad, and total protein was diluted with SDS loading buffer containing β-mercaptoethanol and boiled briefly at ~95°C for 5 minutes. Ninety (90) µg of total protein per sample underwent gel electrophoresis on a mini protean TGX gel 4-15% from BioRad (Cat. No. 456-1084). Protein was transferred to a nitrocellulose membrane via cold transfer at 200 mA for 2 hours while at 4°C. Transfer buffer was composed of 25 mM Tris-base (pH 8.8), 192 mM glycine, and 20% methanol. All antibodies are against mouse antigen: Actin (Sigma, # A1978), APP (Cell Signaling, 2452), ferritin heavy chain/FtH (Santa Cruz Biotechnology, sc-14416), and transferrin receptor 1/TfR1 (Invitrogen, 13-6800). Densitometry was performed using ImageJ software. Percentages represent percentage of signal that is attributed to protein band over the background noise (% Protein or % FtH). Densitometry signal of each protein is normalized against actin (% Actin).

5.1.4 ^{59}Fe uptake.

Iron uptake in the cerebellum, spleen, and liver was determined by oral ^{59}Fe ingestion. Mice were fasted overnight (14-16 hours) but allowed water *ad libitum*. Each mouse underwent intragastric feeding with a solution containing 10 µCi/mL of ^{59}Fe, 30 µg/mL carrier iron, and 1 M ascorbic acid in phosphate-buffered saline as previously described (Du et al., 2008). Each mouse received 2 µCi ^{59}Fe per 10 grams of body weight. One (1) hour post oral gavage, feeding of chow was resumed *ad libitum*. Approximately 24 hours post-gavage the brain, cerebellum, spleen, and liver were collected. Radioactivity was measured (each in a total volume < 1 mL) using a Perkin Elmer 1470 Wizard gamma counter.

5.1.5 Non-heme iron content.

Tissue non-heme iron content was measured as previously described (Torrance & Bothwell, 1968). Whole cerebellum and spleen from mice were dried at 55°C for > 48 hours, ground into powder, weighed, and then digested in 200 µL or 1 mL of 10% trichloroacetic acid/10% HCl at 55°C for > 48 hours, respectively. Samples were then centrifuged at 16,000 rcf for 10 minutes and 100 µL of the supernatant collected. Ten (10) µL of supernatant was then mixed well in a clear-bottom 96-well plate with 190 µL of chromogen solution, allowed to incubate for 10 minutes at room temperature, and the absorbance at 535nm was determined using a Tecan Plate Reader. Chromogen solution consisted of 0.01% bathophenanthroline-disulfonic acid, 0.1% thioglycolic acid, and 7 M sodium acetate. Iron concentration was determined by a standard curve dilution from an iron standard (Sigma, St. Louis, MO). All measurements were performed in duplicates.

5.1.6 Histology and iron staining.

Sixteen (16) week old male CKO and WT mice were fasted for 4 hours and then sacrificed. Whole blood and cerebellum were collected. The cerebellum was immediately placed in 4% paraformaldehyde and allowed to sit at room temperature for 1-2 hours and then placed at 4°C overnight. The paraformaldehyde was then replaced with 70% ethanol and the cerebellum was stored at 4°C until processing. The cerebellum underwent dehydration processing and was embedded in paraffin wax for sectioning. Ten (10) µM sections were taken and placed on Superfrost Plus slide (Fisher, #12-550-15).

Perls' Prussian blue iron staining with DAB enhancement was performed on sections, as previously described (Moos & Mollgard, 1993; Nguyenlegros, Bizot, Bolesse, & Pulicani, 1980; Roschzttardtz, Conejero, Curie, & Mari, 2010; M. A. Smith, P. L. R. Harris, L. M. Sayre, & G. Perry, 1997). Prior to staining, sections were rehydrated and during the rehydration sequence a 3% H_2O_2 step was added before the final rehydration step for quenching of endogenous peroxidases. Sections were then stained with 3% HCl / 3% potassium ferrocyanide / 2% Triton 100X solution for 30 minutes and subsequently washed with distilled H_2O for 10 minutes. DAB enhancement was performed for 15 minutes according to the manufacturer's protocol (Thermo Fisher cat. No. 34065B). Sections were counterstained with Nissl (cresyl violet). Iron positive and total Purkinje cell counting was performed with a manual counter in real time on a total of 22 sections (10 CKO, 12 WT; 8047 total cells counted). Observer was blinded to genotype during counting.

5.1.7 Dietary treatment.

Mice were switched to a low-iron diet (TD10210, Teklad Harlan) and allowed to feed *ad libitum* beginning at weaning (3 weeks of age) and continued for 4 weeks until 7 weeks of age.

5.1.8 Longitudinal behavior assays and gait analysis.

Beginning at 3 weeks of age mice fed either a chow or low-iron diet were screened using a battery of behavioral tests on a weekly basis until 7 weeks of age. The battery of behavioral tests included stationary elevated beam walk, Force-plate Actimetry (BASi), and fore/whole body grip strength. Mice were tested beginning early in the morning (around the beginning of the programmed light cycle of 7 a.m.) and testing was finished prior to noon (12 p.m.) so as to avoid cortisol-associated effects on outcomes. At 7 weeks of age, mice were tested on the Rota-rod and underwent gait analysis using a DigiGait apparatus (Mouse Specifics) prior to euthanasia. Force-plate Actimeter measurements were obtained during 10 minute recording sessions and DigiGait analysis was conducted at a walking speed of 10 cm/s. Rota-rod data were collected at an accelerating speed of 4 to 40 rpm for a maximum of 5 minutes.

5.1.9 Sucrose preference test.

At 6 weeks of age, mice fed a low-iron or chow diet were individually housed in a two bottle system cage with both bottles containing water. After 1 day of acclimation, one bottle was replaced with a pre-weighed bottle of 4% sucrose solution and the amount of water in the non-sucrose bottle was measured. The positions of water and sucrose solutions were randomized between cages. After 24 hours both the water and sucrose solution weights were recorded and the net consumptions for water, sucrose, and total liquid were determined.

5.1.10 Harmaline-induced tremor.

At 24 weeks of age, mice were subject to a harmaline-induced tremor assay using subcutaneous injection of harmaline saline solution and assessment of tremor activity on a Force-plate actimeter as previously described (F. C. Martin et al., 2005). An initial baseline reading of activity for frequencies from 0-25 Hz was obtained by allowing mice to explore the Actimeter

for 10 minutes pre-injection. The mice were removed and 4 mL/kg of harmaline stock solution (5 mg/mL harmaline in saline) was injected and the mice were immediately returned to the Actimeter for a 40 minute recording session. During this time recordings for signals from 0-25 Hz were collected. Subsequently, Fourier transformation of the force-time data facilitated power analysis across frequency and the data was binned into 4 different epochs of 10 minutes per epoch. The MPP normalizes the data to give the specific contribution of tremor activity (activity in the 10-17 Hz range) to total motion activity over the 0-25 Hz range, allowing for corrections for intra-animal total movement variation.

5.1.11 Statistical analyses.

One (1) way ANOVA was performed for genotype comparison of Western blot quantification and for iron staining quantification of Purkinje cells. Two (2) way ANOVA (sex and genotype) analysis was performed for qPCR, ^{59}Fe uptake, non-heme iron content, and all behavior tests. Three (3) way ANOVA (genotype, sex, and diet) was used to evaluate changes in body weight during the longitudinal studies, sucrose preference test data, and on all metrics from gait analyses. Three (3) way ANOVA (genotype, sex, and age) was used for gait analyses between 7 and 16 week old mice. Student-Newman-Keuls post hoc tests were performed for all ANOVA's. P-values of <0.05 were considered statistically significant. Values are presented as mean +/- SEM (standard error of mean).

5.2 CHAPTER 3 MATERIALS AND METHODS

5.2.1 Generation of conditional knockout mice (CKO) and animal husbandry.

All mice were treated according to the University of Kansas Medical Center's Institutional Animal Care and Use Committee approval protocol. All mice were of C57BL/6J background. The generation of CKO mice mice) was achieved as previously described (see

section 5.1.1). Deletion of NCB5OR in the cerebellum was confirmed through qPCR analysis of functional NCB5OR transcripts, of which the loss of sequences corresponding to exon 3 results in a premature "stop" codon and a highly truncated protein product of 89 residues. All measurements were performed on mice at 16 weeks of age. Mice were fed a standard chow diet from PicoLab (5053). Chow diet total calorie composition: 62.4% carbohydrates, 24.5% proteins, and 13.1% fat.

5.2.2 Transcript Analysis.

Quantitative Reverse Transcription PCR (qRT-PCR) was performed on RNA extracted from WT and CKO whole mouse cerebellum after mice had been fasted for 4 hours. Total RNA purity was assessed by A_{260}/A_{280} ratio. One (1) μg of total RNA underwent reverse transcription using the M-MLV Reverse transcriptase and random primers from Life Technologies (Cat # 28025-013 and 48190-011, respectively). The qPCR reaction was performed on an ABI 7900 HT thermo system using SYBR Green master mix from ThermoFisher (Cat # 4367659) and all results were normalized to 18S rRNA with the ΔΔCt method. Primer sequences are available upon request.

5.2.3 Serum T3, Cortisol, Prolactin, and Leptin levels.

Blood serum levels of T3, cortisol, prolactin, and leptin were evaluated using enzyme linked immunosorbent assay (ELISA) kits (T3, Sigma–SE120091; Cortisol, Sigma-SE120082; Prolactin, Sigma-RAB0408; Leptin, Abcam-ab100718). Sixteen (16) week old male CKO mice and WT littermate controls were fasted for 4-6 hours and whole blood was collected in BD Serum Separator Tube (Fisher Cat # 02-675-188) and centrifuged at 9,000 rcf for 10 minutes at 4°C. Blood serum was then collected and immediately frozen using liquid N_2 and stored at -80°C for use at a later date. ELISA's were performed according to manufacturer's protocol.

5.2.4 Metabolic, feeding, drinking, and locomotion detection.

Sixteen (16) week old CKO mice (n=12; 6 male, 6 female) and WT littermates (n=12; 6 male, 6 female) were individually housed and analyzed using the Promethion Indirect Calorimetry System (Sable Systems, Inc., North Las Vegas, NV). All mice were provided access to running wheels. Measurements of feeding, drinking, metabolism, sleeping, and locomotor activity were recorded for 3 days (3 light-dark cycles). Data collected from the first day (1st light-dark cycle) were discarded to avoid unintended effects and noise during acclimation. Light-dark cycles were in 12 hour intervals with the light cycle commencing from 0700 to 1900 and the dark cycle commencing from 1900 to 0700.

5.2.5 Gait analysis and Rota-rod performance.

Conditional knockout and WT mice underwent gait analysis using a DigiGait apparatus (Mouse Specifics) and were tested on the Rota-rod as described in more detail elsewhere (see section 5.1.8). Briefly, DigiGait analysis was conducted under walking conditions at a speed of 10 cm/s, and Rota-rod measurements were collected at an accelerating speed of 4 to 40 rpm for no longer than 5 minutes.

5.2.6 Fasted-feeding assay.

Mice were deprived of food overnight (~ 14 hours) before being allowed ad libitum access to food for 24 hours. Mice were allowed ad libitum access to water at all times.

5.2.7 Echo MRI.

Animal body composition was assessed using the EchoMRI-1100 system (EchoMRI LCC, Houston TX).

5.2.8 2-deoxyglucose (2-DoG) uptake.

Mice were fasted for 4-6 hours prior to intraperitoneal injection of 0.15 uCi per gram body weight of 14C 2-deoxyglucose (Perkin Elmer, Cat # NEC-945A). Whole cerebellum was collected 2 hours later and was placed in 1 mL of lysis buffer containing proteinase K, homogenized, and rotated at 55°C overnight. Whole homogenate was then mixed with a scintillation fluid (ScintiVerse BD cocktail, Fisher Cat # SX18-4) and 5 minute β-scintillation counts were obtained on a Beckman Coulter LS6500 Multi-purpose scintillation counter. The composition of the lysis buffer was as follows (final concentration): 100 mM Tris-HCl pH 8.8, 5 mM EDTA, 0.2% SDS, 200 mM NaCl, 10 μg/mL proteinase K.

5.2.9 Statistical analyses.

Two (2)-way ANOVA (sex and genotype) with Student-Newman-Keuls post hoc test analysis was performed for qPCR and ECHO MRI. Two (2)-way ANOVA (sex and genotype) analysis with Student-Newman-Keuls post hoc test analysis was performed for all metabolic, locomotor, and feeding metrics after values had been split into light and dark cycles and averaged for two consecutive light and dark cycles. One (1)-way ANOVA (genotype) analysis was performed for all ELISA results. Simple linear regression analysis was performed in R for correlation between wheel activity and total energy expenditure and correlation between wheel activity and vO_2. Pearson correlation analysis was performed in R for correlations between wheel activity and total energy expenditure and correlations between wheel activity and vO_2 and a t-test was applied to individual correlations. Pearson correlation values are presented as Pearson correlation coefficients. All other values are presented as means ± SEM (standard error of mean). P-values of <0.05 were considered statistically significant. *Alternative statistical analysis*: In order to confirm observations made using the above statistical analysis, metabolic cage data were

analyzed using a three part analysis in R. First, interactions between all three independent variables (genotype, sex, and cycle) were analyzed using a linear mixed effects (LME) model. This allowed for interactions between all three independent variables to be analyzed while avoiding an artificially inflated 'n' due to measures of light and dark cycles being from the same mice (e.g. 22 measurements for mice during the light cycle and 22 measurements for the mice during the dark cycle should be analyzed using an 'n' of 22 instead of 'n' of 44). Next, ANOVA analysis was performed using results from the LME analysis. Finally, those interactions that yielded significant p-values ($p<0.05$) were further analyzed using a correlation matrix approach to delineate which interactions within the groups were significant. For example, if a significant interaction was found between genotype and sex, further analysis was used to determine if the significant difference between genotypes was found in the male or female populations. This analysis confirmed results and conclusions drawn from the original statistical analysis of metabolic cage data.

5.3 CHAPTER 4 MATERIALS AND METHODS

5.3.1 Chemicals and reagents.

Pure analyte, internal standard, and antioxidant were purchased from Sigma: Serotonin (5-HT, 14927), Dopamine hydrochloride (DA, PHR1090), L-glutamic acid monosodium salt hydrate (Glut, 01495), γ-Aminobutyric acid (GABA, A2129) 3,4-Dihydroxybenzylamine hydrobromide (DHBA, 858781), L-Ascorbic acid (AA, A92902). Reagents and HPLC grade liquids used for mobile phase preparation were purchased from Fisher: Ammonium Formate (A666), formic acid (A119P), Acetonitrile (A998), Water (W5).

5.3.2 Preparation of Reagents and Standard Solutions.

Mobile phase A (MPA) consisted of 95% ammonium formate (100 mM) set at pH 3.0 with formic acid and 5% acetonitrile. Mobile phase B (MPB) consisted of 85% acetonitrile and 15% ammonium formate (30 mM) set at pH 3.0 using formic acid. A 10 mM standard stock solution mix of DA, 5HT, GABA, and DHBA was made in HPLC grade methanol solution containing 1N HCl (2.5%) and ascorbic acid (1 mg/mL) to prevent oxidation. A 10 mM standard stock solution of Glut was made in a solution of HPLC grade H_2O with 0.1% formic acid. It is important to note that in the presence of methanol and acidic conditions, L-glutamic acid will form a methyl ester adduct (L-glutamic acid methyl ester). The stock solution and standard dilutions were made on the same day that standard curve and sample measurements were obtained. The standard stock solution mix underwent serial dilution to the desired concentrations with MPB diluent. The stock solutions ranged from 10 picomolar to 500 micromolar. Standard curves were collected by injecting 1.25 microliters of standard onto the column, resulting in picomoles-on-column values ranging from 0.12 to 625 picomoles. A separate internal standard stock solution of 10 mM DHBA was made HPLC grade methanol solution containing 1N HCl (2.5%) and ascorbic acid (1 mg/mL) to serve as the internal standard during extraction. DHBA internal standard stock solution was stored at -80˚C between extractions.

5.3.3 Chromatographic Instrumentation and Software.[4]

LC-MS/MS experiments were conducted on a Waters Acquity (Waters Co., Milford, MA, USA) UPLC whose effluent was directed into the electrospray source of a Waters Quattro Premier XE tandem quadrupole mass spectrometer. Both instruments were controlled and data acquired using Waters MassLynx 4.1 SCN 805 software. Peak integration and analyte quantitation was accomplished using Waters Quanlynx 4.1 software.

[4] Sections 5.3.3-5.3.6: Details provided in part by Dr. Robert Winefield, Director of Analytical Core, KUMC

5.3.4 Chromatography conditions.

Brain extract samples and mixtures of purified neurochemicals used for external calibration (1.25 µL) were applied to a Waters BEH-Amide HILIC column (1.7 µm particle size, 2.1 x 150 mm) protected by a Waters BEH-Amide Vanguard pre-column. DA and 5-HT levels were assessed with 5 µL injections of undiluted extract and GABA and Glut levels were assessed with 2.5 µL injections of diluted extract. Subsequent to loading the initial injection conditions (300 µL/min, 100% MPB, 30 ºC) were maintained for 1 minute (and the effluent directed to waste) to desalt the sample, then the compounds were resolved with a convex gradient (MPB decreasing to 70% over 5 min at 300 µL/min). The column was washed at 70% MPB at 1 mL/min for 30 seconds before being ramped to 100% MPB (1 mL/min) in 11 sec and re-equilibrated at 100% MPB (1 mL/min) for 38 seconds. Finally, the flow rate was decreased to 300 µL/min (100% MPB) over 51 seconds. The total chromatographic run-time was 7.5 minutes. Quality control runs of standard solutions and blank solutions were run after every 12^{th} sample in order to confirm proper chromatographic performance and assess whether residual compound was present.

5.3.5 Mass Spectra Acquisition.

The column eluent was directed (via a divert valve) into the electrospray source of a Waters Quattro Premier XE tandem quadrupole mass spectrometer that was operated in positive ion mode. The following electrospray and collision-induced ionization parameters were maintained throughout the experiment: Source block and desolvation gas temperatures were set to 100°C and 350°C. The N_2 (g) flow through the source block and ESI probe's desolvation assembly were 50 L/h and 350 L/h respectively. The 1st and 3rd quadrupoles were tuned to an average resolution of 0.93 amu at full width, half-height. Argon gas pressure in the collision cell

was maintained at approximately $6x10^{-3}$ mbar such that the ion beam was consistently attenuated by 30%. Pre-programmed multiple ion monitoring was used to quantify the analytes and the parameters of this program (parent ion, product ion, optimized cone voltage, and collision energy) for each compound are reported in Table 4.1.

5.3.6 Biological sample preparation and extraction.

Whole mouse cerebellum and frontal cortex tissue was isolated from GKO and WT mice and immediately placed in liquid N_2 and stored at -80˚C for future use. Individual tissue was allowed to thaw while being weighed and was subsequently placed in 160 μL of MPB containing DHBA internal standard (50 μM final concentration). Approximately whole cerebellum and approximately 50 mg of cortex tissue was used for extraction. The tissue was then homogenized well and underwent sonication for 30 seconds (12-13 pulses). Finally, 60 μL of MPB was used to wash the sides of the tube and the sample was spun at 16,100 rcf for 10 minutes at 4˚C. The supernatant was collected and used for analysis. Each extraction was handled individually and the resulting extract was immediately analyzed for neurotransmitter levels. All samples were run at room temperature. Due to the abundance of GABA and Glut in the tissue analyzed, primary extract was diluted 1:100 in MPB and mixed well prior to chromatographic separation and mass spectral analysis.

5.3.7 Animals and Diet.

GKO mice were generated as previously described and backcrossed into C57BL/6J for >12 generations (Xu, et al, JBC 2011; Wang, et al, BBA, 2011). Experiments were performed in non-diabetic females as specified in a protocol approved by the Institutional Animal Care and Use Committee at the University of Kansas Medical Center. GKO and WT mice were generated from heterozygous crosses and maintained in a pathogen-free facility at 24°C under a standard

12-hour light/12-hour dark cycle with free access to standard rodent chow (PicoLab 5053) and water.

5.3.8 Statistical analyses.

Linear regression analysis was used to determine linear response ranges for all analytes. Two (2)-way repeated-measures ANOVA analysis (genotype and tissue type) was performed for quantification of 5-HT, DA, GABA, and Glut levels in biological tissue extract. Duplicates were acquired for all samples.

CHAPTER 6

DISCUSSION AND CONCLUSIONS

6.1 PURPOSE AND SUMMARY OF FINDINGS

The work presented in this dissertation was conducted in order to characterize effects of genetic deficiency of NCB5OR in the mouse brain. Specifically, the studies aimed to characterize alterations in iron-related pathways, locomotor activity, and behavioral and molecular changes as they pertain to global regulation of metabolism and feeding and drinking behavior as a result of NCB5OR deficiency. Moreover, preliminary work was conducted to detect changes in neurotransmitters in the affected tissue as a means to elucidate mechanisms that could potentially be responsible for the observed phenotypes. The results presented demonstrate alterations in iron-related pathways, neurotransmitter levels, locomotion, locomotor response to dietary iron deficiency, and altered behavior associated with those regions in which NCB5OR was absent, suggesting that NCB5OR plays an indirect role in maintaining the integrity of neurological function.

6.1.1. NCB5OR contributes to pathways responsible for proper maintenance of iron homeostasis in neurological tissue.

The primary aims for studies in Chapter 2 were: 1.) To investigate the effects of NCB5OR deficiency on iron pathways in neural tissue. 2.) To investigate the interaction of dietary iron deficiency and genetic disruption of iron pathways in the cerebellum and midbrain on locomotion. We employed a number of molecular techniques as well as locomotor measurements to characterize dietary iron deficiency in mice lacking NCB5OR in the cerebellum and midbrain. Data presented in this chapter detailed changes in mRNA transcript and protein levels for elements critical to maintenance of iron homeostasis as a result of NCB5OR deficiency. In addition, mice lacking NCB5OR in the cerebellum and midbrain displayed altered

locomotion under normal conditions as well as deficits in locomotion as a result of dietary iron deficiency.

The response of CKO mice to dietary iron deficiency provides valuable insight into genetic and environmental interaction. Specifically, loss of NCB5OR in the cerebellum and midbrain produced an opposite reaction to dietary iron deficiency than that of their WT counterparts. Compared to chow fed controls, dietary iron deficiency elicited a hyperactive response in WT mice while CKO mice became hypoactive. Neurological conditions such as attention deficit/hyperactivity disorder (ADHD) and restless leg syndrome (RLS) are thought to be complex in that there are genetic and environmental influences that appear to contribute to the conditions. The NCB5OR model demonstrates this interaction between genetic background and environmental influence in a manner that could help better understand the complex nature of such diseases.

6.1.2. NCB5OR maintains the integrity of neurological systems responsible for eating and drinking behavior.

The work presented in Chapter 3 aimed to investigate the underpinnings of metabolic and feeding phenotypes observed in mice globally deficient for NCB5OR. The contribution of the cerebellum and midbrain to feeding and metabolic regulation has been well established. Therefore, we investigated whether loss of NCB5OR in the cerebellum and midbrain could contribute to previously described phenotypes of global knockout mice. Measurements from an indirect-calorimetry-based metabolic cage system revealed an increase in whole body glucose utilization, decreased voluntary exercise, and decreased thirst response in male CKO mice. In addition, male CKO mice had lowered hydration ratios, increased fasted feeding weight gain, and increased serum leptin levels.

The presence of sexual dimorphism in the NCB5OR model has been observed in a number of different phenotypes, with males dominating the phenotypic presentation in both severity and onset. We hypothesize that the sexual dimorphism in the CKO mouse model results from estrogen modulation of brain bioenergetics. However, significantly more work is needed to better understand the specific contribution of sex to NCB5OR-related phenotypes.

6.1.3 NCB5OR influences pathways responsible for balance of neurotransmitters.

Chapter 4 delivered data surrounding preliminary investigation of neurotransmitter changes as a result of NCB5OR deficiency. The use of HILIC UPLC-MS/MS to analyze extract from the cortex and cerebellum of NCB5OR global knockout mice revealed significantly elevated levels of dopamine in the cortex. This observation helps support preliminary data discussed in Chapter 1 that outlines hyperactivity in GKO mice. Changes in dopaminergic function are thought to lie at the heart of hyperactive phenotypes and have also been linked to iron deficiency.

It is important to note that GKO mice, which present with mild to moderate anemia and generalized iron deficiency, present with a hyper active phenotype that corresponds with elevated dopamine levels in the cortex. In contrast, the CKO mouse response to generalized iron deficiency is hypoactive. The reversal in response due to regional restriction of NCB5OR deficiency helps support previous studies indicating mesocorticolimbic function and associated dopaminergic tracts in hyperactive phenotypes.

6.2 LIMITATIONS

Regionally restricted disruption of NCB5OR provides a powerful tool for focused assessment of phenotypes; however behavioral phenotyping provides simplified views of effects on a number of complex neural pathways. The methods presented in this dissertation can

provide insight into, but not directly pinpoint, the exact pathways and modalities being affected by NCB5OR deficiency. For example, the widened stance width and changes in gait may not reflect purely proprioceptive changes, but could be complicated by or a reflections of vestibular dysfunction. Therefore these data stand only as initial insights into possible pathways and processes being affected by deletion of NCB5OR in the cerebellum and midbrain.

We observed no histological abnormalities in CKO mice as old as 16 weeks of age, indicating that the defects we observed were either of pathway dysfunction or progressive, but subtle, neurodegeneration. Our current histological approach focused on observing gross histological changes in the CKO cerebellum, namely overt signs of Purkinje cell number loss and atrophy of the molecular or granular layers. While we did not observe these changes initially, it is still possible that a careful stereotactic study of the CKO cerebellum would reveal regional and layer-specific signs of neurodegeneration.

These studies focused on CKO mice from 3 to 16 weeks of age, making the findings limited to that of early life. Neurodegenerative processes are generally progressive and usually do not present until the mid or later years of life. This should serve as a caution to the reader when assessing the impact of NCB5OR deficiency, as there may phenotypes, ranging in severity, that arise as a function of age.

6.3 FUTURE DIRECTIONS

Our current data clearly demonstrates dysfunctional neuronal pathways as a result of NCB5OR deficiency. The means by which these deficits occur have yet to be explored, leaving a number of questions unanswered. There are three important questions that are directing plans for future studies into the effects of NB5OR deficiency on neural tissue.

1.) What are the physiological effects of NCB5OR deficiency on action potential and signal transduction in neurons?

Current data suggests that NCB5OR maintains pathways critical to iron homeostasis, however microarray data suggests that NCB5OR deficiency results in changes in a myriad of pathways. Notably, there are significant changes in pathways responsible for maintenance of calcium homeostasis. Calcium is a cornerstone in the neuronal membrane potential, action potential, and signal transduction. Using single neuron recording, we aim to explore the effects of NCB5OR deficiency on neuron physiology and response to external cues.

2.) What are the bioenergetic ramifications of NCB5OR deficiency in neurons and glial cells?

Previous studies of NCB5OR deficiency have detailed abnormal fatty acid metabolism, altered mitochondrial ETC complex function, and changes in mitochondrial morphology and number. While the brain does not oxidize fatty acids energy, these observations point to altered bioenergetic pathways in NCB5OR deficient tissue. We did not observe increased 2-DoG uptake in the cerebellum of 16 week old CKO mice, however, this may reflect a compensating bioenergetic profile rather than a 'normal' bioenergetic state. We aim to explore mitochondrial function, morphology, and number in order to better understand the effects of NCB5OR deficiency on bioenergetics in neural tissue.

3.) Can NCB5OR deficiency protect against or postpone frataxin-deficiency related iron deposition and cell death?

Friedreich's ataxia arises through dorsal root ganglia degeneration and subsequent loss of proprioception as a result of the mitochondrial protein frataxin. The disease is generally accepted as arising through toxic iron dyshomeostasis and histological analysis of dorsal root

ganglia from patients shows iron deposition in mitochondria. A number of mouse models have arisen and model the disease fairly well. Our data indicate that NCB5OR deficiency results in iron dyshomeostasis, most likely in the form of altered iron storage and labile iron pool maintenance. In addition, loss of NCB5OR in the cerebellum results in elevated frataxin transcripts. We aim to investigate whether NCB5OR deficiency might prove beneficial in delaying the onset of phenotypes in mouse models of Friedreich's Ataxia and help to provide more insight into the role of cytosolic iron homeostasis and mitochondrial interaction in the pathology of the disease.

6.4 SIGNIFICANCE OF WORK

Findings presented in this dissertation are important when exploring two main concepts: 1) the specific contribution of NCB5OR to the integrity of neurological function and 2) the importance of genes whose function either directly or indirectly maintains bioenergetic homeostasis in the contribution to neurological disease. It is hoped that this work will aid in the search for unique mechanisms and approaches in exploring complex disease etiology.

REFERENCES

Adinolfi, S., Iannuzzi, C., Prischi, F., Pastore, C., Iametti, S., Martin, S. R., . . . Pastore, A. (2009). Bacterial frataxin CyaY is the gatekeeper of iron-sulfur cluster formation catalyzed by IscS. *Nature Structural & Molecular Biology, 16*(4), 390-396. doi: Doi 10.1038/Nsmb.1579

Aisen, P. S., & Vellas, B. (2013). Passive immunotherapy for Alzheimer's disease: what have we learned, and where are we headed? *J Nutr Health Aging, 17*(1), 49-50. doi: 10.1007/s12603-013-0001-3

Aiyar, L., Shuman, C., Hayeems, R., Dupuis, A., Pu, S., Wodak, S., . . . Davies, J. (2013). Risk estimates for complex disorders: comparing personal genome testing and family history. *Genet Med*. doi: 10.1038/gim.2013.115

Alexander, G. E., Chen, K., Pietrini, P., Rapoport, S. I., & Reiman, E. M. (2002). Longitudinal PET Evaluation of Cerebral Metabolic Decline in Dementia: A Potential Outcome Measure in Alzheimer's Disease Treatment Studies. *Am J Psychiatry, 159*(5), 738-745.

Andersen, G., Wegner, L., Rose, C. S., Xie, J., Zhu, H., Larade, K., . . . Pedersen, O. (2004). Variation in NCB5OR: studies of relationships to type 2 diabetes, maturity-onset diabetes of the young, and gestational diabetes mellitus. *Diabetes, 53*(11), 2992-2997.

Ansari, M. A., & Scheff, S. W. (2010). Oxidative Stress in the Progression of Alzheimer Disease in the Frontal Cortex. *Journal of Neuropathology and Experimental Neurology, 69*(2), 155-167.

Antunes-Rodrigues, J., de Castro, M., Elias, L. L., Valenca, M. M., & McCann, S. M. (2004). Neuroendocrine control of body fluid metabolism. *Physiol Rev, 84*(1), 169-208. doi: 10.1152/physrev.00017.2003

Arai, Y., Suzuki, A., Mizuguchi, M., & Takashima, S. (1997). Developmental and aging changes in the expression of amyloid precursor protein in Down syndrome brains. *Brain Dev, 19*(4), 290-294.

Aregbesola, A., Voutilainen, S., Virtanen, J. K., Mursu, J., & Tuomainen, T. P. (2013). Body iron stores and the risk of type 2 diabetes in middle-aged men. *Eur J Endocrinol, 169*(2), 247-253. doi: 10.1530/EJE-13-0145

Arntfield, M. E., & van der Kooy, D. (2011). beta-Cell evolution: How the pancreas borrowed from the brain. *Bioessays, 33*(8), 582-587. doi: DOI 10.1002/bies.201100015

Arvanitakis, Z., Wilson, R. S., Bienias, J. L., Evans, D. A., & Bennett, D. A. (2004). Diabetes mellitus and risk of Alzheimer disease and decline in cognitive function. *Arch Neurol, 61*(5), 661-666. doi: 10.1001/archneur.61.5.661

Atouf, F., Czernichow, P., & Scharfmann, R. (1997). Expression of neuronal traits in pancreatic beta cells. Implication of neuron-restrictive silencing factor/repressor element silencing transcription factor, a neuron-restrictive silencer. *J Biol Chem, 272*(3), 1929-1934.

Atwood, C. S., Huang, X. D., Moir, R. D., Tanzi, R. E., & Bush, A. I. (1999). Role of free radicals and metal ions in the pathogenesis of Alzheimer's disease. *Metal Ions in Biological Systems, Vol 36, 36*, 309-364.

Bakoyiannis, I., Gkioka, E., Daskalopoulou, A., Korou, L. M., Perrea, D., & Pergialiotis, V. (2015). An explanation of the pathophysiology of adverse neurodevelopmental outcomes in iron deficiency. *Rev Neurosci, 26*(4), 479-488. doi: 10.1515/revneuro-2015-0012

Barrientos, A., Casademont, J., Cardellach, F., Estivill, X., Urbano-Marquez, A., & Nunes, V. (1997). Reduced steady-state levels of mitochondrial RNA and increased mitochondrial DNA amount in human brain with aging. *Brain Res Mol Brain Res, 52*(2), 284-289.

Bauer, P. O., & Nukina, N. (2009). The pathogenic mechanisms of polyglutamine diseases and current therapeutic strategies. *J Neurochem, 110*(6), 1737-1765. doi: 10.1111/j.1471-4159.2009.06302.x

Beard, J. (2003). Iron deficiency alters brain development and functioning. *J Nutr, 133*(5 Suppl 1), 1468S-1472S.

Beard, J. L., Chen, Q., Connor, J., & Jones, B. C. (1994). Altered monamine metabolism in caudate-putamen of iron-deficient rats. *Pharmacol Biochem Behav, 48*(3), 621-624.

Beck-Nielsen, H., & Groop, L. C. (1994). Metabolic and genetic characterization of prediabetic states. Sequence of events leading to non-insulin-dependent diabetes mellitus. *J Clin Invest, 94*(5), 1714-1721. doi: 10.1172/JCI117518

Behl, C., Davis, J. B., Lesley, R., & Schubert, D. (1994). Hydrogen-Peroxide Mediates Amyloid-Beta Protein Toxicity. *Cell, 77*(6), 817-827. doi: Doi 10.1016/0092-8674(94)90131-7

Beisswenger, P. J., Howell, S. K., Russell, G. B., Miller, M. E., Rich, S. S., & Mauer, M. (2013). Early progression of diabetic nephropathy correlates with methylglyoxal-derived advanced glycation end products. *Diabetes Care, 36*(10), 3234-3239. doi: 10.2337/dc12-2689

Belaidi, A. A., & Bush, A. I. (2015). Iron neurochemistry in Alzheimer's disease and Parkinson's disease: targets for therapeutics. *J Neurochem*. doi: 10.1111/jnc.13425

Belin, A. C., Bjork, B. F., Westerlund, M., Galter, D., Sydow, O., Lind, C., . . . Olson, L. (2007). Association study of two genetic variants in mitochondrial transcription factor A (TFAM) in Alzheimer's and Parkinson's disease. *Neurosci Lett, 420*(3), 257-262. doi: 10.1016/j.neulet.2007.05.010

Belin, C., & Gatt, M. T. (2006). [Pain and dementia]. *Psychol Neuropsychiatr Vieil, 4*(4), 247-254.

Bennett, P. A., Lindell, K., Karlsson, C., Robinson, I. C., Carlsson, L. M., & Carlsson, B. (1998). Differential expression and regulation of leptin receptor isoforms in the rat brain: effects of fasting and oestrogen. *Neuroendocrinology, 67*(1), 29-36.

Berman, S. M., Paz-Filho, G., Wong, M. L., Kohno, M., Licinio, J., & London, E. D. (2013). Effects of leptin deficiency and replacement on cerebellar response to food-related cues. *Cerebellum, 12*(1), 59-67. doi: 10.1007/s12311-012-0360-z

Bierhaus, A., Fleming, T., Stoyanov, S., Leffler, A., Babes, A., Neacsu, C., . . . Nawroth, P. P. (2012). Methylglyoxal modification of Nav1.8 facilitates nociceptive neuron firing and causes hyperalgesia in diabetic neuropathy. *Nat Med, 18*(6), 926-933. doi: 10.1038/nm.2750

Bloss, C. S., Delis, D. C., Salmon, D. P., & Bondi, M. W. (2008). Decreased Cognition in Children with Risk Factors for Alzheimer's Disease. *Biological Psychiatry, 64*(10), 904-906. doi: DOI 10.1016/j.biopsych.2008.07.004

Boulton, A. J., Vinik, A. I., Arezzo, J. C., Bril, V., Feldman, E. L., Freeman, R., . . . American Diabetes, A. (2005). Diabetic neuropathies: a statement by the American Diabetes Association. *Diabetes Care, 28*(4), 956-962.

Bourdy, R., Sanchez-Catalan, M. J., Kaufling, J., Balcita-Pedicino, J. J., Freund-Mercier, M. J., Veinante, P., . . . Barrot, M. (2014). Control of the nigrostriatal dopamine neuron activity and motor function by the tail of the ventral tegmental area. *Neuropsychopharmacology, 39*(12), 2788-2798. doi: 10.1038/npp.2014.129

Bourque, S. L., Iqbal, U., Reynolds, J. N., Adams, M. A., & Nakatsu, K. (2008). Perinatal iron deficiency affects locomotor behavior and water maze performance in adult male and female rats. *J Nutr, 138*(5), 931-937.

Brehm, M. A., Powers, A. C., Shultz, L. D., & Greiner, D. L. (2012). Advancing Animal Models of Human Type 1 Diabetes by Engraftment of Functional Human Tissues in Immunodeficient Mice. *Cold Spring Harbor Perspectives in Medicine, 2*(5). doi: ARTN a007757 DOI 10.1101/cshperspect.a007757

Briggs, C. A., Schneider, C., Richardson, J. C., & Stutzmann, G. E. (2013). Beta amyloid peptide plaques fail to alter evoked neuronal calcium signals in APP/PS1 Alzheimer's disease mice. *Neurobiol Aging, 34*(6), 1632-1643. doi: 10.1016/j.neurobiolaging.2012.12.013

Brucher, J. M., Gillain, C., & Baron, H. (1989). [Cerebellar amyloid plaques in Alzheimer's disease]. *Acta Neurol Belg, 89*(3-4), 286-293.

Burguera, B., Couce, M. E., Long, J., Lamsam, J., Laakso, K., Jensen, M. D., . . . Lloyd, R. V. (2000). The long form of the leptin receptor (OB-Rb) is widely expressed in the human brain. *Neuroendocrinology, 71*(3), 187-195. doi: Doi 10.1159/000054536

Campuzano, V., Montermini, L., Molto, M. D., Pianese, L., Cossee, M., Cavalcanti, F., . . . Pandolfo, M. (1996). Friedreich's ataxia: Autosomal recessive disease caused by an intronic GAA triplet repeat expansion. *Science, 271*(5254), 1423-1427. doi: DOI 10.1126/science.271.5254.1423

Capoccia, S., Maccarinelli, F., Buffoli, B., Rodella, L. F., Cremona, O., Arosio, P., & Cirulli, F. (2015). Behavioral Characterization of Mouse Models of Neuroferritinopathy. *PLoS One, 10*(2). doi: ARTN e0118990 10.1371/journal.pone.0118990

Castellano, J. M., Kim, J., Stewart, F. R., Jiang, H., DeMattos, R. B., Patterson, B. W., . . . Holtzman, D. M. (2011). Human apoE isoforms differentially regulate brain amyloid-beta peptide clearance. *Sci Transl Med, 3*(89), 89ra57. doi: 10.1126/scitranslmed.3002156

Cheung, C. L., Cheung, T. T., Lam, K. S., & Cheung, B. M. (2012). High ferritin and low transferrin saturation are associated with pre-diabetes among a national representative sample of U.S. adults. *Clin Nutr*. doi: 10.1016/j.clnu.2012.11.024

Cho, S. S., Shin, D. H., Lee, K. H., Hwang, D. H., & Chang, K. Y. (1998). Localization of transferrin binding protein in relation to iron, ferritin, and transferrin receptors in the chicken cerebellum. *Brain Research, 794*(1), 174-178. doi: Doi 10.1016/S0006-8993(98)00303-5

Chowdhury, S. K., Dobrowsky, R. T., & Fernyhough, P. (2011). Nutrient excess and altered mitochondrial proteome and function contribute to neurodegeneration in diabetes. *Mitochondrion, 11*(6), 845-854. doi: 10.1016/j.mito.2011.06.007

Chowdhury, S. K., Smith, D. R., & Fernyhough, P. (2013). The role of aberrant mitochondrial bioenergetics in diabetic neuropathy. *Neurobiol Dis, 51*, 56-65. doi: 10.1016/j.nbd.2012.03.016

Cole, G., Williams, P., Alldryck, D., & Singharo, S. (1989). Amyloid plaques in the cerebellum in Alzheimer's disease. *Clin Neuropathol, 8*(4), 188-191.

Connor, J. R., Boyer, P. J., Menzies, S. L., Dellinger, B., Allen, R. P., Ondo, W. G., & Earley, C. J. (2003). Neuropathological examination suggests impaired brain iron acquisition in restless legs syndrome. *Neurology, 61*(3), 304-309.

Corral-Debrinski, M., Horton, T., Lott, M. T., Shoffner, J. M., Beal, M. F., & Wallace, D. C. (1992). Mitochondrial DNA deletions in human brain: regional variability and increase with advanced age. *Nat Genet, 2*(4), 324-329. doi: 10.1038/ng1292-324

Currais, A., Prior, M., Lo, D., Jolivalt, C., Schubert, D., & Maher, P. (2012). Diabetes exacerbates amyloid and neurovascular pathology in aging-accelerated mice. *Aging Cell, 11*(6), 1017-1026. doi: 10.1111/acel.12002

D'Angelo, E., Mazzarello, P., Prestori, F., Mapelli, J., Solinas, S., Lombardo, P., . . . Congi, L. (2011). The cerebellar network: from structure to function and dynamics. *Brain Res Rev, 66*(1-2), 5-15. doi: 10.1016/j.brainresrev.2010.10.002

Danaceua, J. P., Fountain, K.J., Chambers, E.E. (2012). Hydrophilic-Interaction Chromatography (HILIC) for LC-MS/MS Analysis of Monoamine Neurotransmitters using XBridge BEH Amide XP Columns. www.waters.com.

Daniels, D. (2016). Angiotensin II (de)sensitization: Fluid intake studies with implications for cardiovascular control. *Physiol Behav*. doi: 10.1016/j.physbeh.2016.01.020

de Jong, J. W., Roelofs, T. J., Mol, F. M., Hillen, A. E., Meijboom, K. E., Luijendijk, M. C., . . . Adan, R. A. (2015). Reducing Ventral Tegmental Dopamine D2 Receptor Expression Selectively Boosts Incentive Motivation. *Neuropsychopharmacology, 40*(9), 2085-2095. doi: 10.1038/npp.2015.60

De La Monte, S., Wands JR. . (2008). Alzheimer's Disease Is Type 3 Diabetes - Evidence Reviewed. . *Journal of diabetes science and technology (Online), 2*(6), 1101-1112.

de la Monte, S. M. (2014). Type 3 diabetes is sporadic Alzheimer's disease: Mini-review. *European Neuropsychopharmacology, 24*(12), 1954-1960. doi: 10.1016/j.euroneuro.2014.06.008

De Smet, H. J., Paquier, P., Verhoeven, J., & Marien, P. (2013). The cerebellum: Its role in language and related cognitive and affective functions. *Brain and Language, 127*(3), 334-342. doi: 10.1016/j.bandl.2012.11.001

Deng, Y., Zhang, Y., Li, Y., Xiao, S., Song, D., Qing, H., . . . Rajput, A. H. (2012). Occurrence and distribution of salsolinol-like compound, 1-acetyl-6,7-dihydroxy-1,2,3,4-tetrahydroisoquinoline (ADTIQ) in parkinsonian brains. *J Neural Transm, 119*(4), 435-441. doi: 10.1007/s00702-011-0724-4

Diaz-Munoz, M., Vazquez-Martinez, O., Aguilar-Roblero, R., & Escobar, C. (2000). Anticipatory changes in liver metabolism and entrainment of insulin, glucagon, and corticosterone in food-restricted rats. *Am J Physiol Regul Integr Comp Physiol, 279*(6), R2048-2056.

Dietrichs, E., Haines, D. E., Roste, G. K., & Roste, L. S. (1994). Hypothalamocerebellar and cerebellohypothalamic projections--circuits for regulating nonsomatic cerebellar activity? *Histol Histopathol, 9*(3), 603-614.

Du, X., She, E., Gelbart, T., Truksa, J., Lee, P., Xia, Y., . . . Beutler, B. (2008). The serine protease TMPRSS6 is required to sense iron deficiency. *Science, 320*(5879), 1088-1092. doi: 10.1126/science.1157121

Duara, R., Lopez-Alberola, R. F., Barker, W. W., Loewenstein, D. A., Zatinsky, M., Eisdorfer, C. E., & Weinberg, G. B. (1993). A comparison of familial and sporadic Alzheimer's disease. *Neurology, 43*(7), 1377-1384.

Duce, J. A., Tsatsanis, A., Cater, M. A., James, S. A., Robb, E., Wikhe, K., . . . Bush, A. I. (2010). Iron-export ferroxidase activity of beta-amyloid precursor protein is inhibited by zinc in Alzheimer's disease. *Cell, 142*(6), 857-867. doi: 10.1016/j.cell.2010.08.014

Durr, A., Cossee, M., Agid, Y., Campuzano, V., Mignard, C., Penet, C., . . . Koenig, M. (1996). Clinical and genetic abnormalities in patients with Friedreich's ataxia. *N Engl J Med, 335*(16), 1169-1175. doi: 10.1056/NEJM199610173351601

Earley, C. J., Connor, J. R., Beard, J. L., Clardy, S. L., & Allen, R. P. (2005). Ferritin levels in the cerebrospinal fluid and restless legs syndrome: effects of different clinical phenotypes. *Sleep, 28*(9), 1069-1075.

Edland, S. D., Silverman, J. M., Peskind, E. R., Tsuang, D., Wijsman, E., & Morris, J. C. (1996). Increased risk of dementia in mothers of Alzheimer's disease cases: evidence for maternal inheritance. *Neurology, 47*(1), 254-256.

Erikson, K. M., Jones, B. C., Hess, E. J., Zhang, Q., & Beard, J. L. (2001). Iron deficiency decreases dopamine D1 and D2 receptors in rat brain. *Pharmacol Biochem Behav, 69*(3-4), 409-418.

Faber, S., Zinn, G. M., Kern, J. C., & Kingston, H. M. S. (2009). The plasma zinc/serum copper ratio as a biomarker in children with autism spectrum disorders. *Biomarkers, 14*(3), 171-180. doi: Pii 909433093 10.1080/13547500902783747

Fan, R., Li, X., Gu, X., Chan, J. C., & Xu, G. (2010). Exendin-4 protects pancreatic beta cells from human islet amyloid polypeptide-induced cell damage: potential involvement of AKT and mitochondria biogenesis. *Diabetes Obes Metab, 12*(9), 815-824. doi: 10.1111/j.1463-1326.2010.01238.x

Fernandez-Real, J. M., Lopez-Bermejo, A., & Ricart, W. (2005). Iron stores, blood donation, and insulin sensitivity and secretion. *Clinical Chemistry, 51*(7), 1201-1205. doi: DOI 10.1373/clinchem.2004.046847

Fernandez-Real, J. M., McClain, D., & Manco, M. (2015). Mechanisms Linking Glucose Homeostasis and Iron Metabolism Toward the Onset and Progression of Type 2 Diabetes. *Diabetes Care, 38*(11), 2169-2176. doi: 10.2337/dc14-3082

Fischer, A., Fisher, E., Mohlig, M., Schulze, M., Hoffmann, K., Weickert, M. O., . . . Spranger, J. (2008). KCNJ11 E23K affects diabetes risk and is associated with the disposition index: results of two independent German cohorts. *Diabetes Care, 31*(1), 87-89. doi: 10.2337/dc07-1157

Fiset, C., Rioux, F. M., Surette, M. E., & Fiset, S. (2015). Prenatal Iron Deficiency in Guinea Pigs Increases Locomotor Activity but Does Not Influence Learning and Memory. *PLoS One, 10*(7). doi: ARTN e0133168 10.1371/journal.pone.0133168

Florez, J. C., Hirschhorn, J., & Altshuler, D. (2003). The inherited basis of diabetes mellitus: implications for the genetic analysis of complex traits. *Annu Rev Genomics Hum Genet, 4*, 257-291. doi: 10.1146/annurev.genom.4.070802.110436

Forbes, S., Herzog, H., & Cox, H. M. (2012). A role for neuropeptide Y in the gender-specific gastrointestinal, corticosterone and feeding responses to stress. *Br J Pharmacol, 166*(8), 2307-2316. doi: 10.1111/j.1476-5381.2012.01939.x

Ford, E. S., & Cogswell, M. E. (1999). Diabetes and serum ferritin concentration among US adults. *Diabetes Care, 22*(12), 1978-1983. doi: DOI 10.2337/diacare.22.12.1978

Franci, C. R., Kozlowski, G. P., & McCann, S. M. (1989). Water intake in rats subjected to hypothalamic immunoneutralization of angiotensin II, atrial natriuretic peptide, vasopressin, or oxytocin. *Proc Natl Acad Sci U S A, 86*(8), 2952-2956.

Friedman, J. M., & Halaas, J. L. (1998). Leptin and the regulation of body weight in mammals. *Nature, 395*(6704), 763-770. doi: 10.1038/27376

Fujita, T., Kobayashi, S., & Yui, R. (1980). Paraneuron concept and its current implications. *Adv Biochem Psychopharmacol, 25*, 321-325.

Fukushima, A., Hagiwara, H., Fujioka, H., Kimura, F., Akema, T., & Funabashi, T. (2015). Sex differences in feeding behavior in rats: the relationship with neuronal activation in the hypothalamus. *Front Neurosci, 9*, 88. doi: 10.3389/fnins.2015.00088

Furuyama, K., Kaneko, K., & Vargas, P. D. (2007). Heme as a magnificent molecule with multiple missions: Heme determines its own fate and governs cellular homeostasis. *Tohoku Journal of Experimental Medicine, 213*(1), 1-16. doi: Doi 10.1620/Tjem.213.1

Gabuzda, D., Busciglio, J., Chen, L. B., Matsudaira, P., & Yankner, B. A. (1994). Inhibition of energy metabolism alters the processing of amyloid precursor protein and induces a potentially amyloidogenic derivative. *J Biol Chem, 269*(18), 13623-13628.

Gasparini, L., Racchi, M., Benussi, L., Curti, D., Binetti, G., Bianchetti, A., . . . Govoni, S. (1997). Effect of energy shortage and oxidative stress on amyloid precursor protein metabolism in COS cells. *Neurosci Lett, 231*(2), 113-117.

Georgieff, M. K. (2011). Long-term brain and behavioral consequences of early iron deficiency. *Nutr Rev, 69 Suppl 1*, S43-48. doi: 10.1111/j.1753-4887.2011.00432.x

Gibson, G. E., Sheu, K. F., Blass, J. P., Baker, A., Carlson, K. C., Harding, B., & Perrino, P. (1988). Reduced activities of thiamine-dependent enzymes in the brains and peripheral tissues of patients with Alzheimer's disease. *Arch Neurol, 45*(8), 836-840.

Giles, R. E., Blanc, H., Cann, H. M., & Wallace, D. C. (1980). Maternal inheritance of human mitochondrial DNA. *Proc Natl Acad Sci U S A, 77*(11), 6715-6719.

Goodman, L. (1953). Alzheimer's disease; a clinico-pathologic analysis of twenty-three cases with a theory on pathogenesis. *J Nerv Ment Dis, 118*(2), 97-130.

Gotz, M. E., Double, K., Gerlach, M., Youdim, M. B. H., & Riederer, P. (2004). The relevance of iron in the pathogenesis of Parkinson's disease. *Redox-Active Metals in Neurological Disorders, 1012*, 193-208. doi: DOI 10.1196/annals.1306.017

Greenbaum, C. J., Buckingham, B., Chase, H. P., Krischer, J., & Diabetes Prevention Trial, T. D. S. G. (2011). Metabolic tests to determine risk for type 1 diabetes in clinical trials. *Diabetes Metab Res Rev, 27*(6), 584-589. doi: 10.1002/dmrr.1205

Grivennikova, V. G., & Vinogradov, A. D. (2006). Generation of superoxide by the mitochondrial Complex I. *Biochim Biophys Acta, 1757*(5-6), 553-561. doi: 10.1016/j.bbabio.2006.03.013

Guan, X. M., Hess, J. F., Yu, H., Hey, P. J., & vanderPloeg, L. H. T. (1997). Differential expression of mRNA for leptin receptor isoforms in the rat brain. *Mol Cell Endocrinol, 133*(1), 1-7. doi: Doi 10.1016/S0303-7207(97)00138-X

Guo, B., Yu, Y., & Leibold, E. A. (1994). Iron regulates cytoplasmic levels of a novel iron-responsive element-binding protein without aconitase activity. *J Biol Chem, 269*(39), 24252-24260.

Guo, Y., Xu, M., Deng, B., Frontera, J. R., Kover, K. L., Aires, D., . . . Zhu, H. (2012). Beta-Cell Injury in Ncb5or-null Mice is Exacerbated by Consumption of a High-Fat Diet. *Eur J Lipid Sci Technol, 114*(3), 233-243. doi: 10.1002/ejlt.201100309

Haass, C., Lemere, C. A., Capell, A., Citron, M., Seubert, P., Schenk, D., . . . Selkoe, D. J. (1995). The Swedish mutation causes early-onset Alzheimer's disease by beta-secretase cleavage within the secretory pathway. *Nat Med, 1*(12), 1291-1296.

Haines, D. E., Dietrichs, E., Mihailoff, G. A., & McDonald, E. F. (1997). The cerebellar-hypothalamic axis: basic circuits and clinical observations. *Int Rev Neurobiol, 41*, 83-107.

Harris, M. E., Hensley, K., Butterfield, D. A., Leedle, R. A., & Carney, J. M. (1995). Direct evidence of oxidative injury produced by the Alzheimer's beta-amyloid peptide (1-40) in cultured hippocampal neurons. *Exp Neurol, 131*(2), 193-202.

Hebert, L. E., Scherr, P. A., Bienias, J. L., Bennett, D. A., & Evans, D. A. (2003). Alzheimer disease in the US population - Prevalence estimates using the 2000 census. *Archives of Neurology, 60*(8), 1119-1122. doi: DOI 10.1001/archneur.60.8.1119

Hoche, F., Guell, X., Sherman, J. C., Vangel, M. G., & Schmahmann, J. D. (2015). Cerebellar Contribution to Social Cognition. *Cerebellum*. doi: 10.1007/s12311-015-0746-9

Holscher, C. (2013). Central effects of GLP-1: new opportunities for treatments of neurodegenerative diseases. *J Endocrinol*. doi: 10.1530/JOE-13-0221

Hoppener, J. W., Ahren, B., & Lips, C. J. (2000). Islet amyloid and type 2 diabetes mellitus. *N Engl J Med, 343*(6), 411-419. doi: 10.1056/NEJM200008103430607

Horowitz, M. P., & Greenamyre, J. T. (2010). Mitochondrial Iron Metabolism and Its Role in Neurodegeneration. *Journal of Alzheimers Disease, 20*, S551-S568. doi: Doi 10.3233/Jad-2010-100354

Hsu, L. J., Sagara, Y., Arroyo, A., Rockenstein, E., Sisk, A., Mallory, M., . . . Masliah, E. (2000). alpha-synuclein promotes mitochondrial deficit and oxidative stress. *Am J Pathol, 157*(2), 401-410.

Hu, G., Jousilahti, P., Bidel, S., Antikainen, R., & Tuomilehto, J. (2007). Type 2 diabetes and the risk of Parkinson's disease. *Diabetes Care, 30*(4), 842-847. doi: 10.2337/dc06-2011

Huang, X. D., Atwood, C. S., Hartshorn, M. A., Multhaup, G., Goldstein, L. E., Scarpa, R. C., . . . Bush, A. I. (1999). The A beta peptide of Alzheimer's disease directly produces hydrogen peroxide through metal ion reduction. *Biochemistry, 38*(24), 7609-7616. doi: Doi 10.1021/Bi990438f

Huang, Z., Ohno, N., Terada, N., Saitoh, Y., Chen, J., & Ohno, S. (2013). Immunohistochemical detection of angiotensin II receptors in mouse cerebellum and adrenal gland using "in vivo cryotechnique". *Histochem Cell Biol, 140*(4), 477-490. doi: 10.1007/s00418-013-1084-y

Hutton, M., & Hardy, J. (1997). The presenilins and Alzheimer's disease. *Hum Mol Genet, 6*(10), 1639-1646.

Insel, B. J., Schaefer, C. A., McKeague, I. W., Susser, E. S., & Brown, A. S. (2008). Maternal iron deficiency and the risk of schizophrenia in offspring. *Arch Gen Psychiatry, 65*(10), 1136-1144. doi: 10.1001/archpsyc.65.10.1136

Ishii, K., Sasaki, M., Kitagaki, H., Yamaji, S., Sakamoto, S., Matsuda, K., & Mori, E. (1997). Reduction of cerebellar glucose metabolism in advanced Alzheimer's disease. *J Nucl Med, 38*(6), 925-928.

Iwai, K., Klausner, R. D., & Rouault, T. A. (1995). Requirements for iron-regulated degradation of the RNA binding protein, iron regulatory protein 2. *EMBO J, 14*(21), 5350-5357.

Janson, J., Laedtke, T., Parisi, J. E., O'Brien, P., Petersen, R. C., & Butler, P. C. (2004). Increased risk of type 2 diabetes in Alzheimer disease. *Diabetes, 53*(2), 474-481. doi: DOI 10.2337/diabetes.53.2.474

Janus, C., Pearson, J., McLaurin, J., Mathews, P. M., Jiang, Y., Schmidt, S. D., . . . Westaway, D. (2000). A beta peptide immunization reduces behavioural impairment and plaques in a model of Alzheimer's disease. *Nature, 408*(6815), 979-982. doi: 10.1038/35050110

Jhun, B. S., Lee, H., Jin, Z. G., & Yoon, Y. (2013). Glucose stimulation induces dynamic change of mitochondrial morphology to promote insulin secretion in the insulinoma cell line INS-1E. *PLoS One, 8*(4), e60810. doi: 10.1371/journal.pone.0060810

Jiang, R., Ma, J., Ascherio, A., Stampfer, M. J., Willett, W. C., & Hu, F. B. (2004). Dietary iron intake and blood donations in relation to risk of type 2 diabetes in men: a prospective cohort study. *American Journal of Clinical Nutrition, 79*(1), 70-75.

Jitrapakdee, S., Wutthisathapornchai, A., Wallace, J. C., & MacDonald, M. J. (2010). Regulation of insulin secretion: role of mitochondrial signalling. *Diabetologia, 53*(6), 1019-1032. doi: DOI 10.1007/s00125-010-1685-0

Johnstone, D., & Milward, E. A. (2010). Molecular genetic approaches to understanding the roles and regulation of iron in brain health and disease. *Journal of Neurochemistry, 113*(6), 1387-1402. doi: 10.1111/j.1471-4159.2010.06697.x

Jolivalt, C. G., Calcutt, N. A., & Masliah, E. (2012). Similar Pattern of Peripheral Neuropathy in Mouse Models of Type 1 Diabetes and Alzheimer's Disease. *Neuroscience, 202*, 405-412. doi: DOI 10.1016/j.neuroscience.2011.11.032

Jolivalt, C. G., Hurford, R., Lee, C. A., Dumaop, W., Rockenstein, E., & Masliah, E. (2010). Type 1 diabetes exaggerates features of Alzheimer's disease in APP transgenic mice. *Exp Neurol, 223*(2), 422-431. doi: 10.1016/j.expneurol.2009.11.005

Joseph-Mathurin, N., Dorieux, O., Trouche, S. G., Boutajangout, A., Kraska, A., Fontes, P., . . . Dhenain, M. (2013). Amyloid beta immunization worsens iron deposits in the choroid

plexus and cerebral microbleeds. *Neurobiol Aging, 34*(11), 2613-2622. doi: 10.1016/j.neurobiolaging.2013.05.013

Kalman, F. S., Lizak, B., Nagy, S. K., Meszaros, T., Zambo, V., Mandl, J., . . . Kereszturi, E. (2013). Natural mutations lead to enhanced proteasomal degradation of human Ncb5or, a novel flavoheme reductase. *Biochimie, 95*(7), 1403-1410. doi: 10.1016/j.biochi.2013.03.004

Kan, M., Guo, G., Singh, B., Singh, V., & Zochodne, D. W. (2012). Glucagon-like peptide 1, insulin, sensory neurons, and diabetic neuropathy. *J Neuropathol Exp Neurol, 71*(6), 494-510. doi: 10.1097/NEN.0b013e3182580673

Keller, U., Szinnai, G., Bilz, S., & Berneis, K. (2003). Effects of changes in hydration on protein, glucose and lipid metabolism in man: impact on health. *Eur J Clin Nutr, 57 Suppl 2*, S69-74. doi: 10.1038/sj.ejcn.1601904

Khan, S. M., Cassarino, D. S., Abramova, N. N., Keeney, P. M., Borland, M. K., Trimmer, P. A., . . . Bennett, J. P., Jr. (2000). Alzheimer's disease cybrids replicate beta-amyloid abnormalities through cell death pathways. *Ann Neurol, 48*(2), 148-155.

Kibbey, R. G., Pongratz, R. L., Romanelli, A. J., Wollheim, C. B., Cline, G. W., & Shulman, G. I. (2007). Mitochondrial GTP regulates glucose-stimulated insulin secretion. *Cell Metab, 5*(4), 253-264. doi: 10.1016/j.cmet.2007.02.008

Kim, E., Napierala, M., & Dent, S. Y. R. (2011). Hyperexpansion of GAA repeats affects post-initiation steps of FXN transcription in Friedreich's ataxia. *Nucleic Acids Research, 39*(19), 8366-8377. doi: Doi 10.1093/Nar/Gkr542

Kim, J., & Wessling-Resnick, M. (2014). Iron and mechanisms of emotional behavior. *J Nutr Biochem, 25*(11), 1101-1107. doi: 10.1016/j.jnutbio.2014.07.003

Kim, J. Y., Lee, E. Y., Sohn, H. J., Kim, D. W., Cho, S. S., & Seo, J. H. (2014). Sequential accumulation of iron in glial cells during chicken cerebellar development. *Acta Histochemica, 116*(4), 570-576. doi: 10.1016/j.acthis.2013.11.003

Kimmel, R. A., Turnbull, D. H., Blanquet, V., Wurst, W., Loomis, C. A., & Joyner, A. L. (2000). Two lineage boundaries coordinate vertebrate apical ectodermal ridge formation. *Genes Dev, 14*(11), 1377-1389.

Kish, S. J., Bergeron, C., Rajput, A., Dozic, S., Mastrogiacomo, F., Chang, L. J., . . . Nobrega, J. N. (1992). Brain cytochrome oxidase in Alzheimer's disease. *J Neurochem, 59*(2), 776-779.

Koirala, S., & Corfas, G. (2010). Identification of novel glial genes by single-cell transcriptional profiling of Bergmann glial cells from mouse cerebellum. *PLoS One, 5*(2), e9198. doi: 10.1371/journal.pone.0009198

Konofal, E., Cortese, S., Marchand, M., Mouren, M. C., Arnulf, I., & Lecendreux, M. (2007). Impact of restless legs syndrome and iron deficiency on attention-deficit/hyperactivity disorder in children. *Sleep Med, 8*(7-8), 711-715. doi: 10.1016/j.sleep.2007.04.022

Konofal, E., Lecendreux, M., Arnulf, I., & Mouren, M. C. (2004). Iron deficiency in children with attention-deficit/hyperactivity disorder. *Arch Pediatr Adolesc Med, 158*(12), 1113-1115. doi: 10.1001/archpedi.158.12.1113

Konofal, E., Lecendreux, M., Deron, J., Marchand, M., Cortese, S., Zaim, M., . . . Arnulf, I. (2008). Effects of iron supplementation on attention deficit hyperactivity disorder in children. *Pediatr Neurol, 38*(1), 20-26. doi: 10.1016/j.pediatrneurol.2007.08.014

Korenaga, K., Korenaga, M., Teramoto, F., Suzuki, T., Nishina, S., Sasaki, K., . . . Hino, K. (2013). Clinical usefulness of non-protein respiratory quotient measurement in non-alcoholic fatty liver disease. *Hepatol Res, 43*(12), 1284-1294. doi: 10.1111/hepr.12095

Koutnikova, H., Campuzano, V., Foury, F., Dolle, P., Cazzalini, O., & Koenig, M. (1997). Studies of human, mouse and yeast homologues indicate a mitochondrial function for frataxin. *Nature Genetics, 16*(4), 345-351. doi: Doi 10.1038/Ng0897-345

Lacalle-Aurioles, M., Aleman-Gomez, Y., Guzman-De-Villoria, J. A., Cruz-Orduna, I., Olazaran, J., Mateos-Perez, J. M., . . . Desco, M. (2013). Is the Cerebellum the Optimal Reference Region for Intensity Normalization of Perfusion MR Studies in Early Alzheimer's Disease? *PLoS One, 8*(12). doi: ARTN e81548 10.1371/journal.pone.0081548

Langerhans, P. (1869). Beitrage zur mikroscopischen anatomie der bauchspeichel druse. *Inaugural-dissertation.*

Larade, K., & Bunn, H. F. (2006). Promoter characterization and transcriptional regulation of Ncb5or, a novel reductase necessary for pancreatic beta-cell maintenance. *Biochim Biophys Acta, 1759*(5), 257-262. doi: 10.1016/j.bbaexp.2006.05.002

Larade, K., Jiang, Z., Zhang, Y., Wang, W., Bonner-Weir, S., Zhu, H., & Bunn, H. F. (2008). Loss of Ncb5or results in impaired fatty acid desaturation, lipoatrophy, and diabetes. *J Biol Chem, 283*(43), 29285-29291. doi: 10.1074/jbc.M804645200

LaVaute, T., Smith, S., Cooperman, S., Iwai, K., Land, W., Meyron-Holtz, E., . . . Rouault, T. A. (2001). Targeted deletion of the gene encoding iron regulatory protein-2 causes misregulation of iron metabolism and neurodegenerative disease in mice. *Nat Genet, 27*(2), 209-214. doi: 10.1038/84859

Lee, E., Eom, J. E., Kim, H. L., Baek, K. H., Jun, K. Y., Kim, H. J., . . . Kwon, Y. (2013). Effect of conjugated linoleic acid, mu-calpain inhibitor, on pathogenesis of Alzheimer's disease. *Biochimica Et Biophysica Acta-Molecular and Cell Biology of Lipids, 1831*(4), 709-718. doi: DOI 10.1016/j.bbalip.2012.12.003

Lemaire-Vieille, C., Bailly, Y., Erlich, P., Loeuillet, C., Brocard, J., Haeberle, A. M., . . . Cesbron, J. Y. (2013). Ataxia with cerebellar lesions in mice expressing chimeric PrP-Dpl protein. *J Neurosci, 33*(4), 1391-1399. doi: 10.1523/JNEUROSCI.2231-12.2013

Lenkei, Z., Palkovits, M., Corvol, P., & Llorens-Cortes, C. (1997). Expression of angiotensin type-1 (AT1) and type-2 (AT2) receptor mRNAs in the adult rat brain: a functional neuroanatomical review. *Front Neuroendocrinol, 18*(4), 383-439. doi: 10.1006/frne.1997.0155

Lewis, G. F., Carpentier, A., Adeli, K., & Giacca, A. (2002). Disordered fat storage and mobilization in the pathogenesis of insulin resistance and type 2 diabetes. *Endocr Rev, 23*(2), 201-229.

Li, X. L., Chen, T., Wong, Y. S., Xu, G., Fan, R. R., Zhao, H. L., & Chan, J. C. (2011). Involvement of mitochondrial dysfunction in human islet amyloid polypeptide-induced apoptosis in INS-1E pancreatic beta cells: An effect attenuated by phycocyanin. *Int J Biochem Cell Biol, 43*(4), 525-534. doi: 10.1016/j.biocel.2010.12.008

Liang, W. S., Reiman, E. M., Valla, J., Dunckley, T., Beach, T. G., Grover, A., . . . Stephan, D. A. (2008). Alzheimer's disease is associated with reduced expression of energy in posterior cingulate metabolism genes neurons. *Proceedings of the National Academy of Sciences of the United States of America, 105*(11), 4441-4446. doi: DOI 10.1073/pnas.0709259105

Liu, C. C., Kanekiyo, T., Xu, H., & Bu, G. (2013). Apolipoprotein E and Alzheimer disease: risk, mechanisms and therapy. *Nat Rev Neurol, 9*(2), 106-118. doi: 10.1038/nrneurol.2012.263

Lopez, M., Varela, L., Vazquez, M. J., Rodriguez-Cuenca, S., Gonzalez, C. R., Velagapudi, V. R., . . . Vidal-Puig, A. (2010). Hypothalamic AMPK and fatty acid metabolism mediate thyroid regulation of energy balance. *Nat Med, 16*(9), 1001-1008. doi: 10.1038/nm.2207

Lozoff, B. (2011). Early Iron Deficiency Has Brain and Behavior Effects Consistent with Dopaminergic Dysfunction. *Journal of Nutrition, 141*(4), 740s-746s. doi: 10.3945/jn.110131169

Maccarinelli, F., Pagani, A., Cozzi, A., Codazzi, F., Di Giacomo, G., Capoccia, S., . . . Levi, S. (2015). A novel neuroferritinopathy mouse model (FTL 498InsTC) shows progressive brain iron dysregulation, morphological signs of early neurodegeneration and motor coordination deficits. *Neurobiol Dis, 81*, 119-133. doi: 10.1016/j.nbd.2014.10.023

Maechler, P. (2013). Mitochondrial function and insulin secretion. *Mol Cell Endocrinol*. doi: 10.1016/j.mce.2013.06.019

Makris, A., Piperopoulos, A., & Karmaniolou, I. (2013). Multiple sclerosis: basic knowledge and new insights in perioperative management. *J Anesth*. doi: 10.1007/s00540-013-1697-2

Mangialasche, F., Solomon, A., Winblad, B., Mecocci, P., & Kivipelto, M. (2010). Alzheimer's disease: clinical trials and drug development. *Lancet Neurol, 9*(7), 702-716. doi: 10.1016/S1474-4422(10)70119-8

Marien, P., van Dun, K., & Verhoeven, J. (2015). Cerebellum and apraxia. *Cerebellum, 14*(1), 39-42. doi: 10.1007/s12311-014-0620-1

Martin, F. C., Le, A. T., & Handforth, A. (2005). Harmaline-induced tremor as a potential preclinical screening method for essential tremor medications. *Movement Disorders, 20*(3), 298-305. doi: 10.1002/mds.20331

Martin, S. D., & McGee, S. L. (2013). The role of mitochondria in the aetiology of insulin resistance and type 2 diabetes. *Biochim Biophys Acta*. doi: 10.1016/j.bbagen.2013.09.019

Mendler, M. H., Turlin, B., Moirand, R., Jouanolle, A. M., Sapey, T., Guyader, D., . . . Deugnier, Y. (1999). Insulin resistance-associated hepatic iron overload. *Gastroenterology, 117*(5), 1155-1163. doi: Doi 10.1016/S0016-5085(99)70401-4

Mendoza, J., Pevet, P., Felder-Schmittbuhl, M. P., Bailly, Y., & Challet, E. (2010). The cerebellum harbors a circadian oscillator involved in food anticipation. *J Neurosci, 30*(5), 1894-1904. doi: 10.1523/JNEUROSCI.5855-09.2010

Minoshima, S., Foster, N. L., & Kuhl, D. E. (1994). Posterior cingulate cortex in Alzheimer's disease. *Lancet, 344*(8926), 895.

Miyajima, H., Kono, S., Takahashi, Y., Sugimoto, M., Sakamoto, M., & Sakai, N. (2001). Cerebellar ataxia associated with heteroallelic ceruloplasmin gene mutation. *Neurology, 57*(12), 2205-2210.

Moos, T., & Mollgard, K. (1993). A sensitive post-DAB enhancement technique for demonstration of iron in the central nervous system. *Histochemistry, 99*(6), 471-475.

Morgan, D., Diamond, D. M., Gottschall, P. E., Ugen, K. E., Dickey, C., Hardy, J., . . . Arendash, G. W. (2000). A beta peptide vaccination prevents memory loss in an animal model of Alzheimer's disease. *Nature, 408*(6815), 982-985. doi: 10.1038/35050116

Mori, S., Matsui, T., Kuze, B., Asanome, M., Nakajima, K., & Matsuyama, K. (1998). Cerebellar-induced locomotion: reticulospinal control of spinal rhythm generating mechanism in cats. *Ann N Y Acad Sci, 860*, 94-105.

Mosconi, L., Berti, V., Swerdlow, R. H., Pupi, A., Duara, R., & de Leon, M. (2010). Maternal transmission of Alzheimer's disease: prodromal metabolic phenotype and the search for genes. *Hum Genomics, 4*(3), 170-193.

Mueller, C., Schrag, M., Crofton, A., Stolte, J., Muckenthaler, M. U., Magaki, S., & Kirsch, W. (2012). Altered serum iron and copper homeostasis predicts cognitive decline in mild cognitive impairment. *J Alzheimers Dis, 29*(2), 341-350. doi: 10.3233/JAD-2011-111841

Mutisya, E. M., Bowling, A. C., & Beal, M. F. (1994). Cortical Cytochrome-Oxidase Activity Is Reduced in Alzheimers-Disease. *Journal of Neurochemistry, 63*(6), 2179-2184.

Nakaya, Y., Ohnaka, M., Sakamoto, S., Niwa, Y., Okada, K., Nomura, M., . . . Kusonoki, M. (1998). Respiratory quotient in patients with non-insulin-dependent diabetes mellitus treated with insulin and oral hypoglycemic agents. *Ann Nutr Metab, 42*(6), 333-340. doi: 12753

Nelson, C., Erikson, K., Pinero, D. J., & Beard, J. L. (1997). In vivo dopamine metabolism is altered in iron-deficient anemic rats. *Journal of Nutrition, 127*(12), 2282-2288.

Newberg, A., Cotter, A., Udeshi, M., Brinkman, F., Glosser, G., Alavi, A., & Clark, C. (2003). Brain metabolism in the cerebellum and visual cortex correlates with neuropsychological testing in patients with Alzheimer's disease. *Nuclear Medicine Communications, 24*(7), 785-790. doi: 10.1097/01.mnm.0000080249.50447.99

Nguyenlegros, J., Bizot, J., Bolesse, M., & Pulicani, J. P. (1980). Diaminobenzidine Black as a New Histochemical-Demonstration of Exogenous Iron. *Histochemistry, 66*(3), 239-244. doi: Doi 10.1007/Bf00495737

Ohno, M. (2003). The dopaminergic system in attention deficit/hyperactivity disorder. *Congenit Anom (Kyoto), 43*(2), 114-122.

Oldreive, C. E., Harvey, J., & Doherty, G. H. (2008). Neurotrophic effects of leptin on cerebellar Purkinje but not granule neurons in vitro. *Neurosci Lett, 438*(1), 17-21. doi: 10.1016/j.neulet.2008.04.045

Olney, D. K., Pollitt, E., Kariger, P. K., Khalfan, S. S., Ali, N. S., Tielsch, J. M., . . . Stoltzfus, R. J. (2007). Young Zanzibari children with iron deficiency, iron deficiency anemia, stunting, or malaria have lower motor activity scores and spend less time in locomotion. *J Nutr, 137*(12), 2756-2762.

Opie, E. L. (1901). The Relation Oe Diabetes Mellitus to Lesions of the Pancreas. Hyaline Degeneration of the Islands Oe Langerhans. *J Exp Med, 5*(5), 527-540.

Oski, F. A., Honig, A. S., Helu, B., & Howanitz, P. (1983). Effect of iron therapy on behavior performance in nonanemic, iron-deficient infants. *Pediatrics, 71*(6), 877-880.

Parker, W. D., Jr., Filley, C. M., & Parks, J. K. (1990). Cytochrome oxidase deficiency in Alzheimer's disease. *Neurology, 40*(8), 1302-1303.

Parsons, L. M., Denton, D., Egan, G., McKinley, M., Shade, R., Lancaster, J., & Fox, P. T. (2000). Neuroimaging evidence implicating cerebellum in support of sensory/cognitive processes associated with thirst. *Proc Natl Acad Sci U S A, 97*(5), 2332-2336. doi: 10.1073/pnas.040555497

Pearse, A. G., & Polak, J. M. (1971). Neural crest origin of the endocrine polypeptide (APUD) cells of the gastrointestinal tract and pancreas. *Gut, 12*(10), 783-788.

Percinel, I., Yazici, K. U., & Ustundag, B. (2015). Iron Deficiency Parameters in Children and Adolescents with Attention-Deficit/Hyperactivity Disorder. *Child Psychiatry Hum Dev*. doi: 10.1007/s10578-015-0562-y

Perdomini, M., Hick, A., Puccio, H., & Pook, M. A. (2013). Animal and cellular models of Friedreich ataxia. *Journal of Neurochemistry, 126*, 65-79. doi: Doi 10.1111/Jnc.12219

Perry, E. K., Perry, R. H., Tomlinson, B. E., Blessed, G., & Gibson, P. H. (1980). Coenzyme A-acetylating enzymes in Alzheimer's disease: possible cholinergic 'compartment' of pyruvate dehydrogenase. *Neurosci Lett, 18*(1), 105-110.

Pimplikar, S. W. (2009). Reassessing the amyloid cascade hypothesis of Alzheimer's disease. *Int J Biochem Cell Biol, 41*(6), 1261-1268. doi: 10.1016/j.biocel.2008.12.015

Polling, S., Hill, A. F., & Hatters, D. M. (2012). Polyglutamine aggregation in Huntington and related diseases. *Adv Exp Med Biol, 769*, 125-140.

Ponka, P. (2004). Hereditary causes of disturbed iron homeostasis in the central nervous system. *Ann N Y Acad Sci, 1012*, 267-281.

Prevention, C. f. D. C. a. (2011). National diabetes fact sheet: national estimates and general information on diabetes and prediabetes in the United States, 2011.

Pro, J. D., Smith, C. H., & Sumi, S. M. (1980). Presenile Alzheimer disease: amyloid plaques in the cerebellum. *Neurology, 30*(8), 820-825.

Protter, D., Lang, C., & Cooper, A. A. (2012). alphaSynuclein and Mitochondrial Dysfunction: A Pathogenic Partnership in Parkinson's Disease? *Parkinsons Dis, 2012*, 829207. doi: 10.1155/2012/829207

Provini, F., & Chiaro, G. (2015). Neuroimaging in Restless Legs Syndrome. *Sleep Med Clin, 10*(3), 215-226, xi. doi: 10.1016/j.jsmc.2015.05.006

Puccio, H., Simon, D., Cossee, M., Criqui-Filipe, P., Tiziano, F., Melki, J., . . . Koenig, M. (2001). Mouse models for Friedreich ataxia exhibit cardiomyopathy, sensory nerve defect and Fe-S enzyme deficiency followed by intramitochondrial iron deposits. *Nat Genet, 27*(2), 181-186. doi: 10.1038/84818

Qu, S., Le, W. D., Zhang, X., Xie, W. J., Zhang, A. J., & Ondo, W. G. (2007). Locomotion is increased in A11-lesioned mice with iron deprivation: A possible animal model for restless legs syndrome. *Journal of Neuropathology and Experimental Neurology, 66*(5), 383-388. doi: DOI 10.1097/nen.0b013e3180517b5f

Quinlan, C. L., Perevoshchikova, I. V., Hey-Mogensen, M., Orr, A. L., & Brand, M. D. (2013). Sites of reactive oxygen species generation by mitochondria oxidizing different substrates. *Redox Biol, 1*(1), 304-312. doi: 10.1016/j.redox.2013.04.005

Rasouli, J., Lekhraj, R., Ozbalik, M., Lalezari, P., & Casper, D. (2011). Brain-Spleen Inflammatory Coupling: A Literature Review. *Einstein J Biol Med, 27*(2), 74-77.

Reetz, A., Solimena, M., Matteoli, M., Folli, F., Takei, K., & De Camilli, P. (1991). GABA and pancreatic beta-cells: colocalization of glutamic acid decarboxylase (GAD) and GABA with synaptic-like microvesicles suggests their role in GABA storage and secretion. *EMBO J, 10*(5), 1275-1284.

Reiman, E. M., Caselli, R. J., Chen, K., Alexander, G. E., Bandy, D., & Frost, J. (2001). Declining brain activity in cognitively normal apolipoprotein E epsilon 4 heterozygotes: A foundation for using positron emission tomography to efficiently test treatments to

prevent Alzheimer's disease. *Proc Natl Acad Sci U S A, 98*(6), 3334-3339. doi: 10.1073/pnas.061509598

Reiman, E. M., Caselli, R. J., Yun, L. S., Chen, K., Bandy, D., Minoshima, S., . . . Osborne, D. (1996). Preclinical evidence of Alzheimer's disease in persons homozygous for the epsilon 4 allele for apolipoprotein E. *N Engl J Med, 334*(12), 752-758. doi: 10.1056/NEJM199603213341202

Reiman, E. M., Chen, K. W., Alexander, G. E., Caselli, R. J., Bandy, D., Osborne, D., . . . Hardy, J. (2004). Functional brain abnormalities in young adults at genetic risk for late-onset Alzheimer's dementia. *Proceedings of the National Academy of Sciences of the United States of America, 101*(1), 284-289. doi: DOI 10.1073/pnas.2635903100

Rinne, J. O., Brooks, D. J., Rossor, M. N., Fox, N. C., Bullock, R., Klunk, W. E., . . . Grundman, M. (2010). 11C-PiB PET assessment of change in fibrillar amyloid-beta load in patients with Alzheimer's disease treated with bapineuzumab: a phase 2, double-blind, placebo-controlled, ascending-dose study. *Lancet Neurol, 9*(4), 363-372. doi: 10.1016/S1474-4422(10)70043-0

Ristow, M. (2004). Neurodegenerative disorders associated with diabetes mellitus. *J Mol Med (Berl), 82*(8), 510-529. doi: 10.1007/s00109-004-0552-1

Ristow, M., Mulder, H., Pomplun, D., Schulz, T. J., Muller-Schmehl, K., Krause, A., . . . Pfeiffer, A. F. (2003). Frataxin deficiency in pancreatic islets causes diabetes due to loss of beta cell mass. *J Clin Invest, 112*(4), 527-534. doi: 10.1172/JCI18107

Robertson, A. L., & Bottomley, S. P. (2012). Molecular pathways to polyglutamine aggregation. *Adv Exp Med Biol, 769*, 115-124.

Rodriguez-Diaz, R., Dando, R., Jacques-Silva, M. C., Fachado, A., Molina, J., Abdulreda, M. H., . . . Caicedo, A. (2011). Alpha cells secrete acetylcholine as a non-neuronal paracrine signal priming beta cell function in humans. *Nature Medicine, 17*(7), 888-U258. doi: Doi 10.1038/Nm.2371

Rogers, J. T., Bush, A. I., Cho, H. H., Smith, D. H., Thomson, A. M., Friedlich, A. L., . . . Cahill, C. M. (2008). Iron and the translation of the amyloid precursor protein (APP) and ferritin mRNAs: riboregulation against neural oxidative damage in Alzheimer's disease. *Biochem Soc Trans, 36*(Pt 6), 1282-1287. doi: 10.1042/BST0361282

Rogers, J. T., Randall, J. D., Cahill, C. M., Eder, P. S., Huang, X., Gunshin, H., . . . Gullans, S. R. (2002). An iron-responsive element type II in the 5'-untranslated region of the Alzheimer's amyloid precursor protein transcript. *J Biol Chem, 277*(47), 45518-45528. doi: 10.1074/jbc.M207435200

Rong, Y., Bao, W., Rong, S., Fang, M., Wang, D., Yao, P., . . . Liu, L. (2012). Hemochromatosis gene (HFE) polymorphisms and risk of type 2 diabetes mellitus: a meta-analysis. *Am J Epidemiol, 176*(6), 461-472. doi: 10.1093/aje/kws126

Rorsman, P., Berggren, P. O., Bokvist, K., Ericson, H., Mohler, H., Ostenson, C. G., & Smith, P. A. (1989). Glucose-inhibition of glucagon secretion involves activation of GABAA-receptor chloride channels. *Nature, 341*(6239), 233-236. doi: 10.1038/341233a0

Roschzttardtz, H., Conejero, G., Curie, C., & Mari, S. (2010). Straightforward histochemical staining of Fe by the adaptation of an old-school technique: identification of the endodermal vacuole as the site of Fe storage in Arabidopsis embryos. *Plant Signal Behav, 5*(1), 56-57.

Russo, A. J. (2009). Anti-metallothionein IgG and levels of metallothionein in autistic children with GI disease. *Drug Healthc Patient Saf, 1*, 1-8.

Sako, Y., & Grill, V. E. (1990). A 48-Hour Lipid Infusion in the Rat Time-Dependently Inhibits Glucose-Induced Insulin-Secretion and B-Cell Oxidation through a Process Likely Coupled to Fatty-Acid Oxidation. *Endocrinology, 127*(4), 1580-1589.

Salamone, J. D. (1992). Complex motor and sensorimotor functions of striatal and accumbens dopamine: involvement in instrumental behavior processes. *Psychopharmacology (Berl), 107*(2-3), 160-174.

Saleh, A., Chowdhury, S. K. R., Smith, D. R., Balakrishnan, S., Tessler, L., Martens, C., . . . Fernyhough, P. (2013). Ciliary neurotrophic factor activates NF-kappa B to enhance mitochondrial bioenergetics and prevent neuropathy in sensory neurons of streptozotocin-induced diabetic rodents. *Neuropharmacology, 65*, 65-73. doi: DOI 10.1016/j.neuropharm.2012.09.015

Saltiel, A. R., & Kahn, C. R. (2001). Insulin signalling and the regulation of glucose and lipid metabolism. *Nature, 414*(6865), 799-806. doi: 10.1038/414799a

Samaniego, F., Chin, J., Iwai, K., Rouault, T. A., & Klausner, R. D. (1994). Molecular characterization of a second iron-responsive element binding protein, iron regulatory protein 2. Structure, function, and post-translational regulation. *J Biol Chem, 269*(49), 30904-30910.

Santollo, J., & Daniels, D. (2015a). Control of fluid intake by estrogens in the female rat: role of the hypothalamus. *Front Syst Neurosci, 9*, 25. doi: 10.3389/fnsys.2015.00025

Santollo, J., & Daniels, D. (2015b). Multiple estrogen receptor subtypes influence ingestive behavior in female rodents. *Physiol Behav, 152*(Pt B), 431-437. doi: 10.1016/j.physbeh.2015.05.032

Schenk, D., Barbour, R., Dunn, W., Gordon, G., Grajeda, H., Guido, T., . . . Seubert, P. (1999). Immunization with amyloid-beta attenuates Alzheimer-disease-like pathology in the PDAPP mouse. *Nature, 400*(6740), 173-177. doi: 10.1038/22124

Schmahmann, J. D. (2001). The cerebrocerebellar system: anatomic substrates of the cerebellar contribution to cognition and emotion. *International Review of Psychiatry, 13*(4), 247-260. doi: Doi 10.1080/09540260120082092

Schmahmann, J. D., & Sherman, J. C. (1997). Cerebellar cognitive affective syndrome. *Int Rev Neurobiol, 41*, 433-440.

Schmahmann, J. D., & Sherman, J. C. (1998). The cerebellar cognitive affective syndrome. *Brain, 121 (Pt 4)*, 561-579.

Schmucker, S., Martelli, A., Colin, F., Page, A., Wattenhofer-Donze, M., Reutenauer, L., & Puccio, H. (2011). Mammalian Frataxin: An Essential Function for Cellular Viability through an Interaction with a Preformed ISCU/NFS1/ISD11 Iron-Sulfur Assembly Complex. *PLoS One, 6*(1). doi: ARTN e16199 DOI 10.1371/journal.pone.0016199

Schneider, S. A., Zorzi, G., & Nardocci, N. (2013). Pathophysiology and treatment of neurodegeneration with brain iron accumulation in the pediatric population. *Curr Treat Options Neurol, 15*(5), 652-667. doi: 10.1007/s11940-013-0254-5

Shulman, J. M., De Jager, P. L., & Feany, M. B. (2011). Parkinson's disease: genetics and pathogenesis. *Annu Rev Pathol, 6,* 193-222. doi: 10.1146/annurev-pathol-011110-130242

Sima, A. A., & Li, Z. G. (2006). Diabetes and Alzheimer's disease - is there a connection? *Rev Diabet Stud, 3*(4), 161-168. doi: 10.1900/RDS.2006.3.161

Simcox, J. A., & McClain, D. A. (2013). Iron and diabetes risk. *Cell Metab, 17*(3), 329-341. doi: 10.1016/j.cmet.2013.02.007

Singh, R., Barden, A., Mori, T., & Beilin, L. (2001). Advanced glycation end-products: a review. *Diabetologia, 44*(2), 129-146. doi: 10.1007/s001250051591

Slemmon, J. R., Hughes, C. M., Campbell, G. A., & Flood, D. G. (1994). Increased levels of hemoglobin-derived and other peptides in Alzheimer's disease cerebellum. *J Neurosci, 14*(4), 2225-2235.

Smith, M. A., Harris, P. L., Sayre, L. M., & Perry, G. (1997). Iron accumulation in Alzheimer disease is a source of redox-generated free radicals. *Proc Natl Acad Sci U S A, 94*(18), 9866-9868.

Smith, M. A., Harris, P. L. R., Sayre, L. M., & Perry, G. (1997). Iron accumulation in Alzheimer disease is a source of redox-generated free radicals. *Proceedings of the National Academy of Sciences of the United States of America, 94*(18), 9866-9868. doi: DOI 10.1073/pnas.94.18.9866

Smith, M. A., Hirai, K., Hsiao, K., Pappolla, M. A., Harris, P. L. R., Siedlak, S. L., . . . Perry, G. (1998). Amyloid-beta deposition in Alzheimer transgenic mice is associated with oxidative stress. *Journal of Neurochemistry, 70*(5), 2212-2215.

Solbach, K., Kraff, O., Minnerop, M., Beck, A., Schols, L., Gizewski, E. R., . . . Timmann, D. (2014). Cerebellar pathology in Friedreich's ataxia: atrophied dentate nuclei with normal iron content. *Neuroimage Clin, 6*, 93-99. doi: 10.1016/j.nicl.2014.08.018

Sorbi, S., Bird, E. D., & Blass, J. P. (1983). Decreased pyruvate dehydrogenase complex activity in Huntington and Alzheimer brain. *Ann Neurol, 13*(1), 72-78. doi: 10.1002/ana.410130116

Steen, E., Terry, B. M., Rivera, E. J., Cannon, J. L., Neely, T. R., Tavares, R., . . . de la Monte, S. M. (2005). Impaired insulin and insulin-like growth factor expression and signaling mechanisms in Alzheimer's disease--is this type 3 diabetes? *J Alzheimers Dis, 7*(1), 63-80.

Stroh, M., Swerdlow, R. H., & Zhu, H. (2014). Common defects of mitochondria and iron in neurodegeneration and diabetes (MIND): a paradigm worth exploring. *Biochem Pharmacol, 88*(4), 573-583. doi: 10.1016/j.bcp.2013.11.022

Swerdlow, R. H. (2007). Mitochondria in cybrids containing mtDNA from persons with mitochondriopathies. *J Neurosci Res, 85*(15), 3416-3428. doi: 10.1002/jnr.21167

Swerdlow, R. H. (2009). The neurodegenerative mitochondriopathies. *J Alzheimers Dis, 17*(4), 737-751. doi: 10.3233/JAD-2009-1095

Swerdlow, R. H. (2011a). Brain aging, Alzheimer's disease, and mitochondria. *Biochim Biophys Acta, 1812*(12), 1630-1639. doi: 10.1016/j.bbadis.2011.08.012

Swerdlow, R. H. (2011b). Role and Treatment of Mitochondrial DNA-Related Mitochondrial Dysfunction in Sporadic Neurodegenerative Diseases. *Current Pharmaceutical Design, 17*(31), 3356-3373.

Swerdlow, R. H. (2013). Bioenergetic Medicine. *Br J Pharmacol*. doi: 10.1111/bph.12394

Swerdlow, R. H., Burns, J. M., & Khan, S. M. (2010). The Alzheimer's disease mitochondrial cascade hypothesis. *J Alzheimers Dis, 20 Suppl 2*, S265-279. doi: 10.3233/JAD-2010-100339

Swerdlow, R. H., Burns, J. M., & Khan, S. M. (2013). The Alzheimer's Disease Mitochondrial Cascade Hypothesis: Progress and Perspectives. *Biochim Biophys Acta*. doi: 10.1016/j.bbadis.2013.09.010

Swerdlow, R. H., & Khan, S. M. (2004). A "mitochondrial cascade hypothesis" for sporadic Alzheimer's disease. *Med Hypotheses, 63*(1), 8-20. doi: 10.1016/j.mehy.2003.12.045

Swerdlow, R. H., & Khan, S. M. (2009). The Alzheimer's disease mitochondrial cascade hypothesis: an update. *Exp Neurol, 218*(2), 308-315. doi: 10.1016/j.expneurol.2009.01.011

Swerdlow, R. H., & Kish, S. J. (2002). Mitochondria in Alzheimer's disease. *Int Rev Neurobiol, 53*, 341-385.

Sysi-Aho, M., Ermolov, A., Gopalacharyulu, P. V., Tripathi, A., Seppanen-Laakso, T., Maukonen, J., . . . Oresic, M. (2011). Metabolic regulation in progression to autoimmune diabetes. *PLoS Comput Biol, 7*(10), e1002257. doi: 10.1371/journal.pcbi.1002257

Talbot, K., Wang, H. Y., Kazi, H., Han, L. Y., Bakshi, K. P., Stucky, A., . . . Arnold, S. E. (2012). Demonstrated brain insulin resistance in Alzheimer's disease patients is associated with IGF-1 resistance, IRS-1 dysregulation, and cognitive decline. *J Clin Invest, 122*(4), 1316-1338. doi: 10.1172/JCI59903

Tan, S., Sagara, Y., Liu, Y., Maher, P., & Schubert, D. (1998). The regulation of reactive oxygen species production during programmed cell death. *J Cell Biol, 141*(6), 1423-1432.

Thomann, P. A., Schlafer, C., Seidl, U., Santos, V. D., Essig, M., & Schroder, J. (2008). The cerebellum in mild cognitive impairment and Alzheimer's disease - a structural MRI study. *J Psychiatr Res, 42*(14), 1198-1202. doi: 10.1016/j.jpsychires.2007.12.002

Thomas-Reetz, A. C., & De Camilli, P. (1994). A role for synaptic vesicles in non-neuronal cells: clues from pancreatic beta cells and from chromaffin cells. *FASEB J, 8*(2), 209-216.

Thomas, D. G., Grant, S. L., & Aubuchon-Endsley, N. L. (2009). The role of iron in neurocognitive development. *Dev Neuropsychol, 34*(2), 196-222. doi: 10.1080/87565640802646767

Thomas, M. C., MacIsaac, R. J., Tsalamandris, C., & Jerums, G. (2004). Elevated iron indices in patients with diabetes. *Diabet Med, 21*(7), 798-802. doi: 10.1111/j.1464-5491.2004.01196.x

Thornton, S. N. (2011). Angiotensin inhibition and longevity: a question of hydration. *Pflugers Archiv-European Journal of Physiology, 461*(3), 317-324. doi: 10.1007/s00424-010-0911-4

Torrance, J. D., & Bothwell, T. H. (1968). A simple technique for measuring storage iron concentrations in formalinised liver samples. *S Afr J Med Sci, 33*(1), 9-11.

Trimmer, P. A., Swerdlow, R. H., Parks, J. K., Keeney, P., Bennett, J. P., Jr., Miller, S. W., . . . Parker, W. D., Jr. (2000). Abnormal mitochondrial morphology in sporadic Parkinson's and Alzheimer's disease cybrid cell lines. *Exp Neurol, 162*(1), 37-50. doi: 10.1006/exnr.2000.7333

Tsai, E. B., Sherry, N. A., Palmer, J. P., & Herold, K. C. (2006). The rise and fall of insulin secretion in type 1 diabetes mellitus. *Diabetologia, 49*(2), 261-270. doi: 10.1007/s00125-005-0100-8

Unger, E. L., Sterling, M. E., Jones, B. C., & Beard, J. L. (2008). Genetic variations in ventral midbrain iron influence diurnal locomotor activity and body temperature in BXD mice. *Faseb Journal, 22*.

Valla, J., Berndt, J. D., & Gonzalez-Lima, F. (2001). Energy hypometabolism in posterior cingulate cortex of Alzheimer's patients: superficial laminar cytochrome oxidase associated with disease duration. *J Neurosci, 21*(13), 4923-4930.

Valla, J., Yaari, R., Wolf, A. B., Kusne, Y., Beach, T. G., Roher, A. E., . . . Reiman, E. M. (2010). Reduced Posterior Cingulate Mitochondrial Activity in Expired Young Adult Carriers of the APOE epsilon 4 Allele, the Major Late-Onset Alzheimer's Susceptibility Gene. *Journal of Alzheimers Disease, 22*(1), 307-313. doi: Doi 10.3233/Jad-2010-100129

van den Ouweland, J. M., Lemkes, H. H., Trembath, R. C., Ross, R., Velho, G., Cohen, D., . . . Maassen, J. A. (1994). Maternally inherited diabetes and deafness is a distinct subtype of diabetes and associates with a single point mutation in the mitochondrial tRNA(Leu(UUR)) gene. *Diabetes, 43*(6), 746-751.

van Swieten, M. M. H., Pandit, R., Adan, R. A. H., & van der Plasse, G. (2014). The neuroanatomical function of leptin in the hypothalamus. *Journal of Chemical Neuroanatomy, 61-62*, 207-220. doi: 10.1016/j.jchemneu.2014.05.004

Vela, G., Stark, P., Socha, M., Sauer, A. K., Hagmeyer, S., & Grabrucker, A. M. (2015). Zinc in gut-brain interaction in autism and neurological disorders. *Neural Plast, 2015*, 972791. doi: 10.1155/2015/972791

Viggiano, D., & Sadile, A. G. (2000). Hypertrophic A10 dopamine neurones in a rat model of attention-deficit hyperactivity disorder (ADHD). *Neuroreport, 11*(17), 3677-3680.

Vlassenko, A. G., Mintun, M. A., Xiong, C. J., Sheline, Y. I., Goate, A. M., Benzinger, T. L. S., & Morris, J. C. (2011). Amyloid-beta plaque growth in cognitively normal adults: Longitudinal [11C]Pittsburgh compound B data. *Annals of Neurology, 70*(5), 857-861. doi: Doi 10.1002/Ana.22608

Wang, H. Y., Antinozzi, P. A., Hagenfeldt, K. A., Maechler, P., & Wollheim, C. B. (2000). Molecular targets of a human HNF1 alpha mutation responsible for pancreatic beta-cell dysfunction. *Embo Journal, 19*(16), 4257-4264. doi: DOI 10.1093/emboj/19.16.4257

Wang, H. Y., Maechler, P., Antinozzi, P. A., Hagenfeldt, K. A., & Wollheim, C. B. (2000). Hepatocyte nuclear factor 4 alpha regulates the expression of pancreatic beta-cell genes implicated in glucose metabolism and nutrient-induced insulin secretion. *Journal of Biological Chemistry, 275*(46), 35953-35959. doi: DOI 10.1074/jbc.M006612200

Wang, L., Xi, G., Keep, R. F., & Hua, Y. (2012). Iron enhances the neurotoxicity of amyloid beta. *Transl Stroke Res, 3*(1), 107-113. doi: 10.1007/s12975-011-0099-8

Wang, W. F., Guo, Y., Xu, M., Huang, H. H., Novikova, L., Larade, K., . . . Zhu, H. (2011). Development of diabetes in lean Ncb5or-null mice is associated with manifestations of endoplasmic reticulum and oxidative stress in beta cells. *Biochimica Et Biophysica Acta-Molecular Basis of Disease, 1812*(11), 1532-1541. doi: 10.1016/j.bbadis.2011.07.016

Wegiel, J., Wisniewski, H. M., Dziewiatkowski, J., Badmajew, E., Tarnawski, M., Reisberg, B., . . . Miller, D. C. (1999). Cerebellar atrophy in Alzheimer's disease-clinicopathological correlations. *Brain Research, 818*(1), 41-50.

Wen, Y. Q., Zhu, J. N., Zhang, Y. P., & Wang, J. J. (2004). Cerebellar interpositus nuclear inputs impinge on paraventricular neurons of the hypothalamus in rats. *Neurosci Lett, 370*(1), 25-29. doi: 10.1016/j.neulet.2004.07.072

Westermark, P. (1994). Amyloid and Polypeptide Hormones - What Is Their Interrelationship. *Amyloid-International Journal of Experimental and Clinical Investigation, 1*(1), 47-60. doi: Doi 10.3109/13506129409148624

Westermark, P., Wernstedt, C., Wilander, E., & Sletten, K. (1986). A Novel Peptide in the Calcitonin Gene Related Peptide Family as an Amyloid Fibril Protein in the Endocrine Pancreas. *Biochemical and Biophysical Research Communications, 140*(3), 827-831. doi: Doi 10.1016/0006-291x(86)90708-4

WHO. (2001). *Iron deficiency anaemia: assessment, prevention and control*. Retrieved from Available: http://www.who.int/nutrition/publications/micronutrients/anaemia_iron_deficiency/WHO_NHD_01.3/en/.

Xie, J., Zhu, H., Larade, K., Ladoux, A., Seguritan, A., Chu, M., . . . Bunn, H. F. (2004). Absence of a reductase, NCB5OR, causes insulin-deficient diabetes. *Proc Natl Acad Sci U S A, 101*(29), 10750-10755. doi: 10.1073/pnas.0404044101

Xiong, H., Zheng, C., Wang, J., Song, J., Zhao, G., Shen, H., & Deng, Y. (2013). The neuroprotection of liraglutide on Alzheimer-like learning and memory impairment by modulating the hyperphosphorylation of tau and neurofilament proteins and insulin signaling pathways in mice. *J Alzheimers Dis, 37*(3), 623-635. doi: 10.3233/JAD-130584

Xu, M., Wang, W., Frontera, J. R., Neely, M. C., Lu, J., Aires, D., . . . Zhu, H. (2011). Ncb5or deficiency increases fatty acid catabolism and oxidative stress. *J Biol Chem, 286*(13), 11141-11154. doi: 10.1074/jbc.M110.196543

Xue, B., Johnson, A. K., & Hay, M. (2013). Sex differences in angiotensin II- and aldosterone-induced hypertension: the central protective effects of estrogen. *Am J Physiol Regul Integr Comp Physiol, 305*(5), R459-463. doi: 10.1152/ajpregu.00222.2013

Yamamoto, A., Shin, R. W., Hasegawa, K., Naiki, H., Sato, H., Yoshimasu, F., & Kitamoto, T. (2002). Iron (III) induces aggregation of hyperphosphorylated tau and its reduction to iron (II) reverses the aggregation: implications in the formation of neurofibrillary tangles of Alzheimer's disease. *J Neurochem, 82*(5), 1137-1147.

Yoneda, S., Uno, S., Iwahashi, H., Fujita, Y., Yoshikawa, A., Kozawa, J., . . . Shimomura, I. (2013). Predominance of beta-cell neogenesis rather than replication in humans with an impaired glucose tolerance and newly diagnosed diabetes. *J Clin Endocrinol Metab, 98*(5), 2053-2061. doi: 10.1210/jc.2012-3832

Youdim, M. B., & Green, A. R. (1978). Iron deficiency and neurotransmitter synthesis and function. *Proc Nutr Soc, 37*(2), 173-179.

Zhang, L., Zhang, S., Maezawa, I., Trushin, S., Minhas, P., Pinto, M., . . . Trushina, E. (2015). Modulation of mitochondrial complex I activity averts cognitive decline in multiple animal models of familial Alzheimer's Disease. *EBioMedicine, 2*(4), 294-305. doi: 10.1016/j.ebiom.2015.03.009

Zhao, L. H., M.; Wang, C.; Xu, X.; Song, Y.; Jinnah, H.A.; Wodzinska, J; Iacovelli, J.; Wolkow, N.; Krajacic, P.; Weissberger, A.C.; Connelly, J.; Spino, M.; Lee, M.K.; Connor, J.; Giasson, B.; Leah Harris, Z.; Dunaief, J.L. (2015). Cp/Heph mutant mice have iron-induced neurodegeneration diminished by deferiprone. *J Neurochem, 135*(5), 958-974. doi: 10.1111/jnc.13292

Zhu, H., Larade, K., Jackson, T. A., Xie, J., Ladoux, A., Acker, H., . . . Bunn, H. F. (2004a). NCB5OR is a novel soluble NAD(P)H reductase localized in the endoplasmic reticulum. *J Biol Chem, 279*(29), 30316-30325.

Zhu, H., Qiu, H., Yoon, H. W., Huang, S., & Bunn, H. F. (1999). Identification of a cytochrome b-type NAD(P)H oxidoreductase ubiquitously expressed in human cells. *Proc Natl Acad Sci U S A, 96*(26), 14742-14747.

Zhu, H., Wang, W. F., & Wang, H. P. (2013). Impaired Iron Metabolism in Monogenic Ncb5or Diabetes. *Diabetes, 62*, A566-A566.

Zhu, J. N., & Wang, J. J. (2008). The cerebellum in feeding control: possible function and mechanism. *Cell Mol Neurobiol, 28*(4), 469-478. doi: 10.1007/s10571-007-9236-z

Zhu, J. N., Yung, W. H., Kwok-Chong Chow, B., Chan, Y. S., & Wang, J. J. (2006). The cerebellar-hypothalamic circuits: potential pathways underlying cerebellar involvement in somatic-visceral integration. *Brain Res Rev, 52*(1), 93-106. doi: 10.1016/j.brainresrev.2006.01.003

Zucca, F. A., Segura-Aguilar, J., Ferrari, E., Munoz, P., Paris, I., Sulzer, D., . . . Zecca, L. (2015). Interactions of iron, dopamine and neuromelanin pathways in brain aging and Parkinson's disease. *Progress in Neurobiology*. doi: 10.1016/j.pneurobio.2015.09.012

APPENDIX I: DEFINITIONS AND EQUATIONS

Average Respiratory Quotient: Mean respiratory quotient as calculated by

$RQ = CO_{2\ expelled} / O_{2\ consumed}$

Average vH_2O: Mean respiratory H_2O expulsion. Measured in milliliters per minute.

Average vO_2: Mean respiratory O_2 consumption. Measured in milliliters per minute.

Free Water: Water contents of the bladder.

Gait symmetry: (Right forelimb + left forelimb step frequency) / (Right hind limb + left hind limb step frequency). Presented as a real number.

Hydration Ratio: [(Total Water–Free Water) / Lean Mass]

LOD: A peak S/N:RMS less than 3.

LOQ: A peak signal to noise ratio root mean squared (S/N:RMS) of ten 10 or greater.

Max $\Delta A/\Delta T$: How quickly the limb is loaded during the initial period of stance; how rapidly does the animal decelerate. Measured in square centimeters per second.

Midline distance: Distance between the centroid of a paw at peak stance and a reference line drawn through the transverse midline of the animal. Measured in centimeters.

MPP = [(10 – 17 Hz) / (0 – 25 Hz)] x 100.

Paw drag: Area under the curve from time of full stance to the time the paw lifts off from the belt. Measured in square millimeters.

Paw overlap distance: Were paws to have been painted and paw prints made, ipsilateral fore and hind paws can become somewhat superimposed. This represents the distance between ipsilateral fore and hind paws if not superimposed. Measured in centimeters.

Pedestrian Activity: All non-wheel running locomotion as measured by beam breaks in the metabolic cage system.

RE = [(Theoretical value – Actual value) / Theoretical value] * 100. Presented as a percentage.

Resting Energy Expenditure: Mean value for 30 minute periods with lowest energy expenditure. Measured in kcal/hr.

Stance Width: The perpendicular distance between the centroids of either set of axial paws during peak stance. Measured in centimeters.

Step angle: The angle made between left and right hind paws as a function of stride length and stance width. Measured in degrees.

Swing duration: Time duration of the swing phase (no paw contact with belt). Measure in milliseconds.

Systemic Metabolism: Energy expenditure and substrate utilization measured by O_2 consumption and CO_2 production.

Total Energy Expenditure: Summed energy expenditure for entire cycle. Measured in kcal/hr.

Total Water: Free water and water content of lean tissue.

Wheel Running Activity: All wheel running locomotion as measured by the running wheel in the metabolic cage system. Measured in meters.

APPENDIX II: THE STRUGGLE

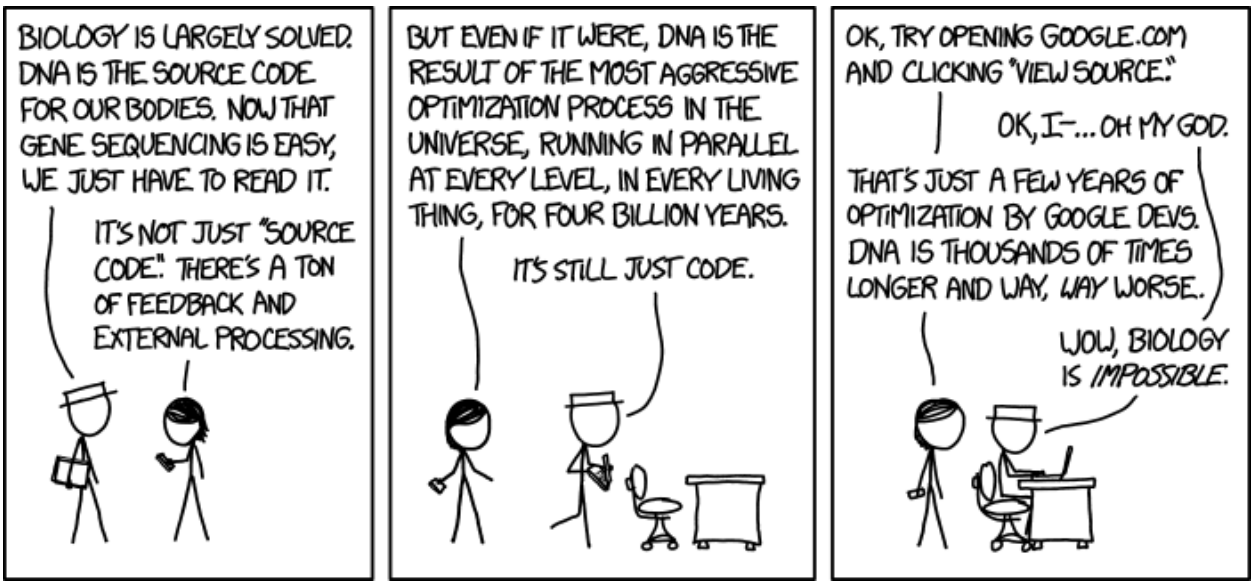

Creator: Randall Munroe www.xkcd.com

Creator: Randall Munroe www.xkcd.com